AN EXPERIMENTAL AND NUMERICAL STUDY ON CREEP BEHVAIOR OF SOIL NAIL WALLS IN HIGH PLASTICITY CLAYS

A Thesis

by

ABHIJITH CHANDRAKARAN KAMATH

Submitted to the Office of Graduate and Professional Studies of
Texas A&M University
in partial fulfillment of the requirements for the degree of

MASTER OF SCIENCE

Chair of Committee,	Marcelo Javier Sánchez Castilla
Committee Members,	Jean Louis Briaud
	Niall Slowey
Head of Department,	Robin Autenrieth

August 2016

Major Subject: Civil Engineering

ABSTRACT

The use of soil nails for earth retaining structures have increased tremendously. Since soil nail walls are now considered as permanent structures there is a need to study and characterize creep behavior of soil nail walls. FWHA restricts the construction of soil nail walls in high plasticity soils. This is because it is thought that clays with high plasticity fines show creep tendencies which will adversely affect the stability of the retaining wall in the long term. This thesis presents the results from laboratory testing on remolded high plasticity clays from Beaumont, Texas. Direct shear tests were conducted to understand the variation in strength with water content. Consolidated undrained tests were done to obtain undrained parameters of clay. Unconsolidated undrained and consolidated drained tests were also conducted to understand the drained behavior and variation of strength with depth. Creep tests on samples with two different saturations was conducted to understand the viscous behavior of clay under different saturation conditions. The deformation and stresses in nails of an actual soil nail wall constructed in Beaumont was monitored during construction and one year after construction. Numerical modelling of this wall using FLAC-3D was done with input parameters obtained from laboratory testing. A failure that occurred during construction because of over excavation was simulated. The creep behavior was modelled using Burger model. The stability of the retaining wall for a period of 75 years was predicted using this model. Field experience and results from numerical modelling and lab tests recommend that creep behavior of soil nail walls in high plasticity soils need not be necessarily considered in the design.

DEDICATION

To my parents, brother, sister

And

To my beloved wife, Anju

ACKNOWLEDGEMENTS

I would like to thank my committee chair, Dr. Sanchez, and my committee members, Dr. Briaud, Dr. Slowey for their guidance and support throughout the course of this research.

Thanks also go to my friends Dr. Mohsen, Dr. Gang and colleagues and the department faculty and staff for making my time at Texas A&M University a great experience. My duty would not be complete if I don't thank Dong Wang for his advice support and help during this study.

Finally, thanks to my mother and father for their encouragement and for their patience and love.

TABLE OF CONTENTS

Page

Page

LIST OF FIGURES

Page

Page

Page

Page

Page

Page

Page

Page

LIST OF TABLES

Page

CHAPTER I

INTRODUCTION

Soil nail walls are still one of the most sought of earth retaining structures due to their cost effectiveness. Soil nails are used as reinforcement not only in soils but also in soft rock and weathered soil like materials. The construction usually proceeds from top to bottom followed by applying shotcrete at the face in each excavation stage, so that the process is continuous. The nails are passive reinforcement placed after each excavation stage. In principle the aim will be to create a reinforced backfill which will behave similar to a gravity wall, Stocker and Riedinger (1990). The recommended depth of each excavation is 3ft-6ft. usually facing is put in place to obtain a pleasing look for the wall. After introduction the technique of soil nailing was widely used as in temporary structures after which they were replaced or additional measures were taken to withstand the soil mass. But recently it is being used and thought of as a permanent method of improving the soil mass.

If favorable conditions are available soil nail wall are preferred because of their ease of construction, speed of construction, flexibility and ability to be modified. The ability to make changes in the design even after construction starts or in between stages of construction makes soil nailing flexible and attractive. Soil nailing has also been used to stabilize landslides and the face of the wall is protected from erosion using geogrids.

Soil nail wall as a permanent structure will have to withstand the load for long time. Creep is the long term deformation due to sustained loading. Long term failure of

soil nail wall will happen when the load on the nails exceed the pullout capacity of the nail. A study on creep using modelling and lab tests was done as a part of this thesis.

Figure 1 Construction of soil nail wall, taken from RL. Wadsworth construction. Co.

1.1 History of soil nailing

By early 1960s the concept of using steel reinforcement as passive elements for stabilizing rock slopes had been used. The use of shotcrete can also be traced back to this time. The idea was to mobilize the shear strength of steel with small ground movement. In 1972 Versailles, France, used this concept of soil nailing as a part of road widening project. They were also able to report the pullout strength with grout curing time. The Bodenvernagelung project in West Germany was a 5 year project and it had used 7 walls,

instrumented nails and the results from the project were reported by Stocker et al (1979), Stocker (1990). The results from this test were later reported by Gassler (1990). He observed that there was only small bending moment that was developed in the walls.

In United States the first research on soil nailing was done by University of California Davis in 1976. They conducted the research for a hospital in Portland the area was about 2140m^2 and the longest wall was 76.3 meters and 11.3 meters deep. They installed inclinometers, strain gauges. They developed the Davis method from the inference they got from field observation and numerical modelling. A prominent study in this field came from France after a project named "CLOUTERRE" Schlosser (1992). Three walls were instrumented and loaded to failure and this study was key to french soil nail design manual. They concluded that the tension force in the nails was giving the reinforcement effect. An important observation was that the maximum force is observed at or near the failure zone. It was also reported that the deformation varied from .1% to .3% of the wall height.

Gassler and Gudehus (1981), reported that at least 20 soil nail projects were completed which proved that the technique was safe and cost effective. Juran and Elias (1987) reported an observed soil creep from strain data. The inclinometers showed very small to no change which the forces in the nail continued to increase and this was attributed to creep in residual soils. They hypothesized a cracking in the grout which was later confirmed by Thompson and Miller (1990). Another significance of this study was they were able to account for creep in concrete and its effect on stresses in nails. Figure 1 shows construction of a general soil nail wall.

1.2 Introduction to creep

Vyalov (1986) in his book Rheological fundamentals of soil mechanics was able to explain the general characteristics of creep in soils. He gave curves representing primary creep, secondary creep and tertiary creep. These curves will depended on the type of soil, the load level, water content and temperature. These curves are shown in Figure 2.

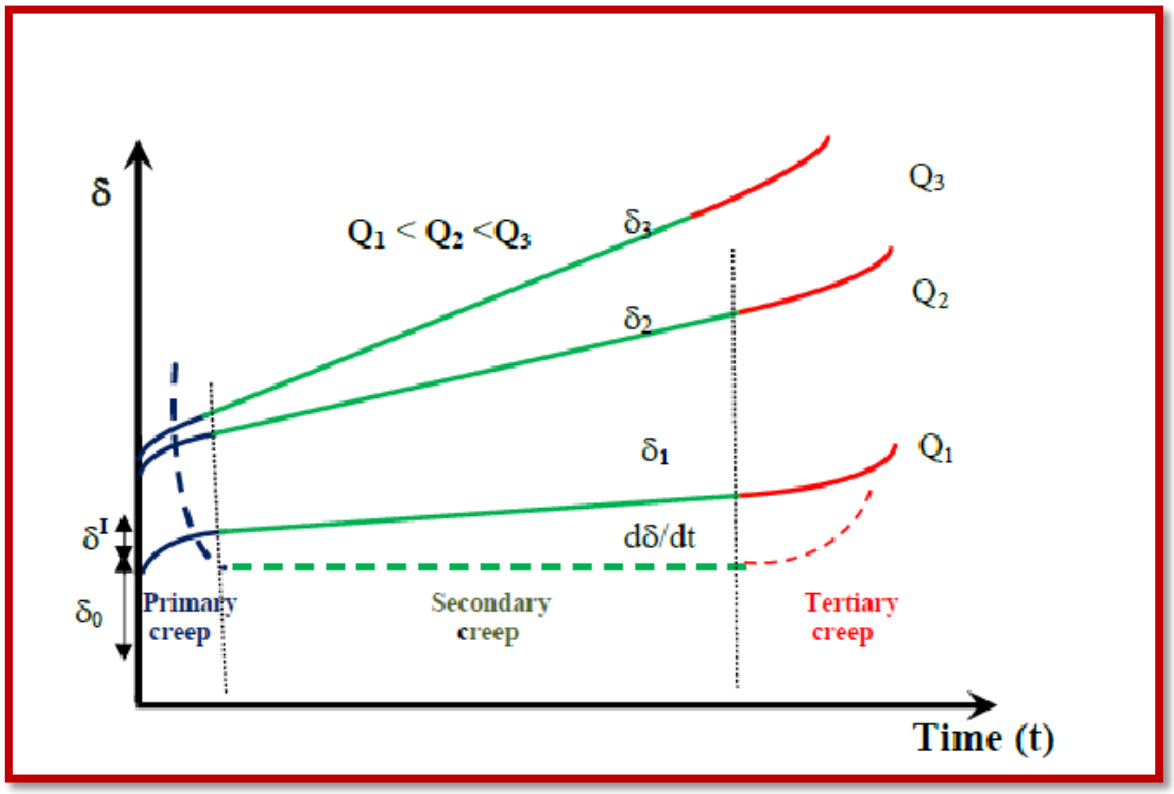

Figure 2 Creep curves in three stage of soil creep, Vyalov (1986).

Primary creep (blue line) will occur for a short duration of time. The rate of strain will decrease with time. Thus it can be seen that the rate has a high strain rate and will eventually decrease. The secondary creep starts after the primary creep (green line)

and will have a constant strain rate. The deformation rate remains constant for a longer time. After secondary creep, tertiary creep is observed. Here an increasing rate of deformation can be observed. At this stage strain rate increases gradually.

Another key observation can be made from the Figure 2. The load level has significant effect on the shape of the curve and the strain rates. This characteristic was attributed to the changes in fabric with creep. It was assumed that soil consists of clay particles, aggregates and voids Vyalov (1986). The fabric shows changes with load.

1.3 Research motivation

FHWA, Carlos et al (2003), states that soil nail wall is becoming common since it has proved to be cost effective. It also adds that there is a shift from the use of soil nail wall as temporary to permanent structure. From Table 1 it can be inferred that area of soil nail walls used in 2007-2008 in Texas was around 70,000ft2 while in 2011-2012 the area of wall constructed rose to 1467, 93 ft2 Galvan (2012). Thus soil nail walls has very high significance in Texas as more and more of these structures are being used.

Texas has large deposits of soils with high plasticity. These soils are prone to creep under sustained loading. There is a need to study the long term behavior of soil nail walls in these type of soils. GEC #7 does not recommend the use of soil nail walls in high plasticity soils. But from field experience it is noticed that many soil nail walls have been constructed in high plasticity clay and no reported failure has been noticed. So questions arise with respect to long term stability of soil nail walls in these soils. This thesis addresses this basic issue and to give recommendations and conclusions to practicing engineers.

There has not been many studies to characterize creep in soil nail walls. Though many researchers have attempted to study creep of soils in general (Havel 2004), Gustafsson and Tian (2011) no particular study on long term stability of soil nail walls have been done. In Texas A&M Kharanaghi (2015), Bi (2015) conducted a detailed study on creep in soil and soil nail composite systems. This study is an extension of their attempts to characterize creep in high plasticity soil nail walls. The excavation is undrained during construction stage, so ideally undrained modelling should be done for simulating the behavior of the wall during construction. Similarly it is also relevant to see how the effective stress varies during creep. Pore pressure measurements have to be done to understand this behavior.

Wall type	Area(Ft2)	
	2012	2007
MSE	3,196,417	2,000,000
Concrete block(no r/f)	47,791	150,000
Cantilever drilled shaft	72.286	100,000
Soil Nailed	146,793	70,000
Tied-back	161,827	20,000
Spread footing	505,019	10,000

Table 1 Different types of walls used in 2012 and 2008 in Texas after Galvan (2012).

GEC#7 places restrictions on constructions in high plasticity soils. It suggests that to minimize potential for long term deformation fine grained soils should be show plasticity. The potential for creep is shown by soils having plasticity index greater than 20 and liquid limit greater than 50. The tensile forces in nails increase by 15% in long term conditions due to creep. It is to be noted that this load is not used in design but is accounted in factor of safety. The post construction deformation in 6 months is about 15% of the movement at end of construction.

Thus it is very important to question if the creep has to be included in the design or whether any restrictions need to be placed while construction soil nail walls in soil with plastic fines.

1.4 Objective

1. To understand better the behavior of soil nail walls during construction including the development of load in each row of nails with successive excavation.

2. To compare the results from drained modelling conducted by Kharanaghi (2015) with undrained modelling ones done in this thesis in terms of horizontal deformation and load distribution in nails.

3. To gain a deeper insight into behavior of the high plasticity clay in Beaumont site under different conditions (Saturation, drainage etc.).

4. To determine the creep properties of the high plasticity clays from Beaumont site.

5. To model the creep of the soil nail wall at Beaumont and predict the horizontal deformation and load in nails for next 75 years, based on the creep properties and soil behavior observed at that site.

6. To analyze the stress distribution in the nails and draw conclusions on the rate of increase in the nail load.

1.5 Activities related to objective

To study creep behavior of soil nail walls it was important to identify relevant literature and the past research projects conducted on soil nail walls. It was also important to look at all relevant projects on study of creep in soils. All relevant papers on numerical modelling and experimental tests on nail walls were studied in terms of software used, model used, soil in which the nails were installed, laboratory tests done to characterize the soils. It was thus decided to combine numerical modelling with laboratory tests. The previous study at Texas A&M Kharanaghi (2015), Bi (2015) formed the base for this study.

1.5.1 Experimental plan

The geotechnical properties of the soil was found. Importance was given to find the Atterberg limits and soil classification. The soil strength under different conditions needed to be found to understand the behavior of soils in different water content in different depths. Direct shear test was employed to find the soil strength in fully saturated, dry and in situ saturation. Unconsolidated undrained tests can be conducted to find the strength variation with depth. The same test can be conducted on fully saturated soils to understand the strength variation in different depth with different water content.

Consolidated Undrained test is conducted to obtain strength parameters which can be used for modelling purposes. Three tests are conducted on the same soil to obtain cohesion and internal friction of the soil. Drained tests are conducted to understand the drained properties of the soil. In long-term the soil will drain and the drained properties help us to understand the behavior of the soil. Another important soil parameter required for the study is to find the creep parameter. This is obtained from Unconsolidated Undrained creep tests using different loads and saturation conditions.

1.5.2 Numerical modelling

Modelling using FLAC-3D is done to understand the wall behavior during construction and after construction for a year. Creep models were employed to predict the creep behavior of the nail. Comparison was done between observed deformation and loads in nails with values obtained from modelling. Further creep prediction was done using the numerical modelling. Load in the nails were compared to understand the increase in loads and to make recommendation on long term stability.

1.6 Organization of the text

Chapter 2 presents a short discussion on soil nailing, evaluation of soil conditions and its suitability for soil nailing, its advantages and disadvantages, construction methods, construction sequence and design methodologies. A short discussion on different creep models is also included.

Chapter 3 presents previous study done at Texas A&M on the Beaumont soil nail wall project.

Chapter 4 presents the laboratory results which include soil parameters, direct shear test results, UU test results, CU test results, CD test results, UU creep results. The procedure adopted is also included in this chapter

Chapter 5 is dedicated to the results from numerical modelling, creep predictions

Chapter 6 gives the conclusions and suggestions for future research

CHAPTER II

BACKGROUND

2.1 Soil nailing

2.1.1 Advantages

The advantages of soil nailing over conventional and other type of retaining structure are:

i. It requires minimum excavation and backfilling. Soil nailing can be done in-stiu and is environment friendly.
ii. Sufficient workspace is available.
iii. Temporary supporting works are not necessary.
iv. Machinery and equipment required are light weight.
v. Design flexibility and excavation shape.
vi. Flexibility in terms applicability to different slopes: natural// man made.
vii. Facing requirement is minimal.
viii. Can withstand unforeseen weak strata and ground water conditions.
ix. Cost effective.
x. Quick construction is possible.

2.1.2 Disadvantages

i. The space may become unusable due to presence of nails.
ii. There are chances for surface cracking and large lateral deformation when the temporary support is removed.
iii. Possibility of ground space loss in coarse grained soils.

iv. Not suitable for sands and soft clayey soils because of their inability to self-stand for required depth and chance of creeping.

v. Another observation is that there is less mobilized strength at lower parts of retaining wall.

vi. Specialized contractors required possibly experienced people.

vii. Permanent underground easements required.

viii. Large amount of underground water renders soil nailing impossible.

ix. Difficulties in construction if the site has utilities.

x. Since some deformation required to mobilize shear strength, it may not be recommended in situations where little to no movement is required.

2.2 Evaluation of ground conditions for soil nailing

Soil nails as reinforcement have been successfully used in many different locations, environmental conditions, soil formation, moisture conditions and loading. Although soil nail walls have not always been installed in favorable conditions, it has been generally adopted in soil condition, which largely influences the construction of the wall. It is also a well-known fact that total construction cost of soil nail walls can be brought down if constructed on favorable conditions. In this section a discussion of favorable and unfavorable conditions have been included.

2.2.1 Favorable conditions

Experience show that soil nailing can be effectively implemented at low cost under following conditions:

1. The excavated soil can stand without support for a height of 1-2 meters for 1-2 days.
2. Ground water table well below the lowest row of nails is considered ideal situation. The soil nail walls can be constructed under water table also, provided the soil is clay or silt which is relatively impermeable. But special care should be taken for long term pore pressure and the seepage conditions. Technical feasibility and implementation difficulties may make this type of retaining walls costly. Long term performance, creep needs to be monitored in such conditions.
3. Stability of drilled holes: Should be stable till the hole gets grouted and tendons are installed.

2.2.2 Feasibility of soil nail in different soil conditions

Soils with high organic content are considered unfavorable for soil nail walls. These soils can retain high water content and hence a lower strength is expected in natural state. The strength increases with consolidation. If fibers are present such soils show anisotropy and can provide acceptable strength in some directions but generally longer nails will have to be used in such conditions. Another situation where longer nails will have to be used is when the retained soil has collapsible soils or loess. Loess lose their strength when water migrates to the retained soil and a sudden drop in strength can be expected. Similarly collapsible soil show volume change behavior when they get

saturated. Aggressive soils also do not render a favorable condition for soil nails walls. They may corrode the nails, hence special attention should be given to treat the nails before placing in such conditions. But soil nails can be a cost effective method for short term retaining structures in aggressive soils. Soils which have no fines and are dry do not possess any cohesion and are not suitable since they cannot stand a vertical cut of 2 meters for couple of days. The ease of construction demands a soil which does not have rocks or particles of large diameter which may adversely affect the drilling operations. Weathered rocks with some weakness planes are considered favorable or unfavorable based on the orientation of weakness planes. Another factor to be considered is if the same drilling operation can be used throughout the formation. If blocks of instability exists in weathered rocks they need to be treated before the construction. The instabilities can be due to weakness along a plane or gouge in the joints, uplift and lateral hydrostatic pressures, and seepage forces. Treatment can be costly and may be difficult to perform. Soft Fine grained soils with expansive behavior or high plasticity are generally considered unfavorable for slope with nails. Creep deformations in long term and low bond strength at soil nail interface are the major concerns in such type of soils.

Hard and stiff fine grained soils with relatively high cohesion are considered to provide the necessary shear strength and bond strength. But it is recommended to ensure that such soils show low plasticity to avoid problems related to long term deformations. Unsaturated granular soils are considered good for nailing since they develop apparent cohesion through capillary forces. These soils should be always unsaturated so that the property is not lost. So care should be taken to prevent desiccation and water from

infiltrating to prevent it from getting saturated. Thus granular soils with fines can also be considered to have some cohesion and thus considered favorable.

2.2.3 Effect of ground water table

High water table including perched water table will affect the stability of drill holes. There is a chance that they may collapse before grouting. To avoid problems related to seepage and to stabilize the soil proper drainage should be provided. Granular soils with high water table are not recommended for soil nails. Corrosive groundwater may affect long term stability of the wall. If slope with nails is considered as a temporary structure, the water table may not affect the nails, else it requires to be treated. The deformation of the wall will be significantly larger in saturated condition than in dry or unsaturated soils.

2.3 Design of soil nail walls

A very short discussion of design of soil nail walls based on GEC#7 by Federal Highway Administration is included here. As in any design it involves to check the stability conditions and the serviceability conditions. Serviceability conditions involve safe and normal operation of the wall during its life time. Stability issues arise when the total stress is more than what the whole system or individual components could resist. Stability failure can occur through external failure, internal failure or facing failure.

2.3.1 External failure

External failure can occur by three modes, overturning, sliding, and bearing capacity failure. There are many limit state software's to check the external failure. GSLOPE, SNAIL etc. are some of the commonly used software's for estimating the factor of safety against failure. All these programs calculate the factor of safety and the length

of nails are increased if the factor of safety is less than recommended factor of safety. Figure 3 shows the three external failure states.

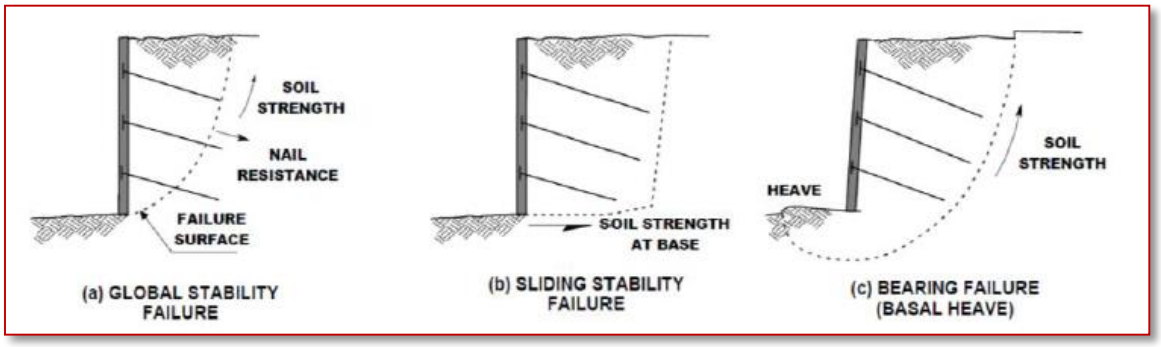

Figure 3 External failure modes: global stability failure, sliding stability failure, bearing failure, FWHA, Carlos et al (2003).

2.3.2 Internal failure

Nail pull out failure, bending and shear of nails, tensile failure of nails and slippage of bar-grout interface are the common methods of internal failure. Nail pullout failure occurs when the nail length is insufficient to resist the pull out force. This implies that the pullout capacity per u nit length of nail is not sufficient to resist that force. The bond between the grout and the nail is detrimental to the internal stability. The bond strength is derived mechanically from the protrusions on the nails. The bending and shear of soil nails are relatively less and disregarded, FWHA, Carlos et al (2003). Tension is the dominant force in soil nail force. The tension force is zero at the end increases to a maximum value T_{max} and then decreases to T_0 at the nail head. In soft soils T_{max} is dependent on pull out

capacity. The least of pullout capacity, tension capacity, facing capacity controls the $T_{max.}$ Figure 4 shows this load distribution in nails.

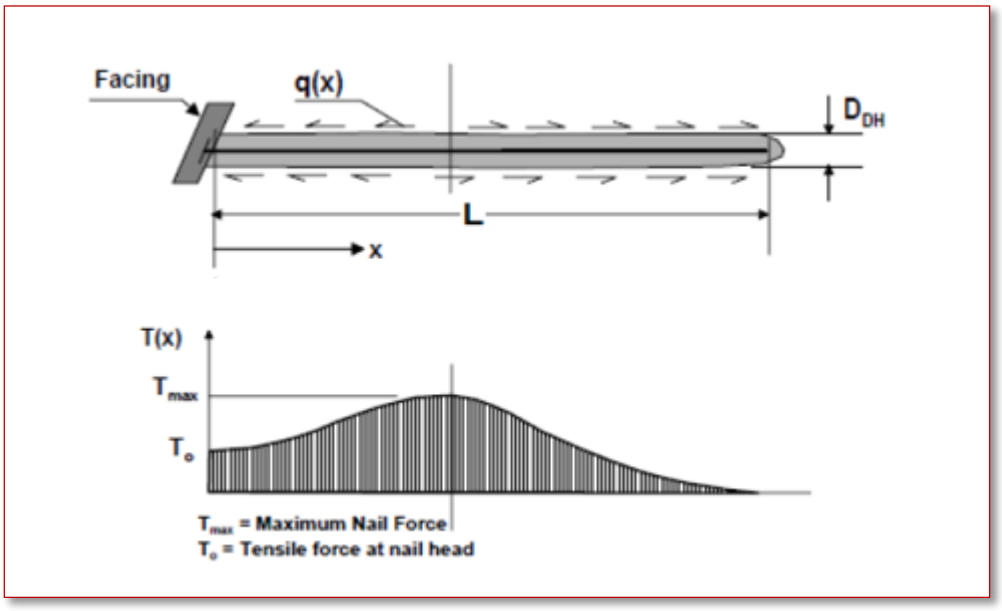

Figure 4 Load distribution in nails FWHA, Carlos et al (2003).

During construction of a soil nail wall there is a release of pressure with each excavation stage that is there will be a decrease in mean octahedral stress. Tavenas and Leroueil (1981) did a comprehensive study of creep and failure of slopes in clays. From their study it can be deduced that in soil nail walls where the excavations, which makes the soil over consolidated, and soil nail placing are relatively rapid the soil will act like a quasi-elastic material. If the soil under consideration is clay , has low permeability and the drainage path is long enough, then very less flow can be expected, given the excavation is

relatively fast. Development of negative pore pressure can be expected and the soil will show undrained characteristics. Temporary stability is achieved under this condition.

Skempton (1977) observed that a very long time as long as 50 years will be required for pore pressure equalization. The short term stability could be lost when the pore pressure increases and becomes positive. The failure may take years or decades to occur and will depend on the biological characteristics of the slope. One suggested method to estimate the instability is to measure the pore water pressure with suction probes and piezometers. The observed pore water pressure should be compared with predicted long term results. This analysis will give the expected time for failure.

The theoretical factor of safety during failure will be unity. If all the conditions prevailing in the field including the groundwater and boundary conditions are given the strength parameters during failure can be estimated using a limit equilibrium method. This analytical method, Janbu (1954) of estimating the parameters for a factor of safety of unity has the advantage that the error in estimating parameters is reduced but at the same time it does lack the advantages of effective stress analysis.

2.4 Creep models

Creep in soil nail walls is more complex than creep in soil and needs more in-depth study as soil nail walls are becoming common. Thought here has been no reported failure due to creep in soil nail walls, it is still a major concern in high plasticity soil which could deform significantly in long term GEC#7 (2003). It suggests that to reduce the potential of creep soil nail walls should be constructed in soil with plasticity index less than 15. Soft to very soft clays with low SPT value have low bond strength and may require long soil

nails. There is still no solid methods to determine soils with creep potential. Soils with high liquid limit greater than 50 and plasticity index are considered to have potential for creep. Lateral deflection and increase in nail stress results when the soil is subjected to constant effective stress. Generally post construction load on the nails increase upto 15 percent due to soil creep GEC#7 (2003). Though this is not accounted for directly, factor of safety includes this increase in stress. GEC #7 attributes the horizontal displacement of the wall to stress relaxation and creep. In this section various theories used to explain creep are discussed.

Rheological character is exhibited by most of the clays, especially soft soils with high plasticity. Soft soils show plastic flow rather than elastic deformation when they undergo long term loading. Study of rheological behavior outlines the relations between load, strain and time. To explain this behavior several theories have been proposed. Different people have grouped the theories in different ways. Two prominent studies were by Maslov (1968) and Feda (1992). Maslov gave his famous three term expression for shear strength in 1941,

$$\tau = \sigma tan\phi + \sum \mathrm{w} + cs$$

Where σ the normal stress is ϕ is the true angle of internal friction $\sum \mathrm{w}$ is the cohesiveness of water colloidal nature varying with W, cs is the structural cohesion inherent to the material.

Based on this he classified clayey soils into three:

1. Stiff clayey soils
2. Slightly plastic clayey soils

3. Plastic clayey soils

By 1930s he had formed the base for his two approaches namely phenomenological and physicomechanical. In phenomenological creep theory laboratory tests are to be conducted and a large number of parameters up to eight are to be found. The drawback of this idea is that it is unrealistic to perform lab tests on undisturbed soil sample with varying load, aging etc. The downside of Maslov's grouping was that at times the two groups started to be the same. Havel (2004) observed that after modification and substitution of parameters creep theories belonging to one group, it became same as the other. Feda (1992) also grouped the creep theories into micro and macro rheology.

2.4.1 Mechanical models

Since the behavior of real materials is very complex, they are modelled using simplified rheological models. The viscous behavior of materials is modelled using newton's laws. Newtonian fluid was a concept introduced by Newton . The ideal fluid i.e. a Newtonian fluid has a constant slope in shear stress vs strain rate. The rate of deformation is proportional to the applied stress in an ideal fluid. The relation between stresses, viscous strain is given by:

$$\sigma = \eta * \varepsilon/dt$$

Where ε is the strain, t is the time η the coefficient of viscosity. The piston, cylinder and viscous fluid model of Newton is shown in Figure 5.

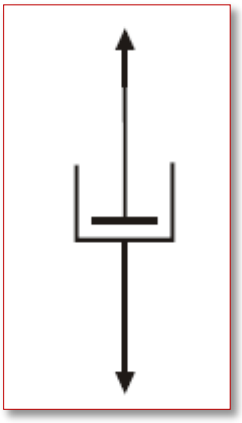

Figure 5 Newton's viscous model.

Similarly elastic behavior of a material is modelled using Hooke's law. According to Hooke's law stress is proportional to strain. The constant is called Young's modulus of elasticity. The model consist of an elastic spring in elastic medium. Figure 6 shows a spring elastic element.

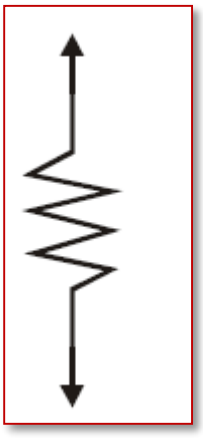

Figure 6 Linear elastic spring model.

The plastic behavior can be modeled using ideally plastic body called St. Venant body which is a frictional joint. When the force applied is less than the plastic flow limit no deformation is observed, but once it exceeds the flow limit it elongates plastically. This model is represented in Figure 7.

Figure 7 St venant viscous body.

The combination of these three basic elements can be used to define creep behavior of the soils. Maxwell model is a combination of spring element and dashpot element in series. The total strain will be equal to sum of strain in spring and dashpot. The strain in elastic element is instant but the viscous element will show delayed strain. The stress will be the same in both the elements. The Maxwell's model can be represented by the equation:

$$\sigma + {}^{\eta}/_{E}\,\dot{\sigma} = \eta\,\dot{\varepsilon}$$

On application of load the spring will react immediately and elongate viscous element will take time to react. Thus initial strain will be due to Hooke's element $=\sigma_0/E$. Similarly when the load is removed there will be an immediate elastic recovery, but the strain due to Newton's element will remain. Thus Maxwell's model can be used for creep prediction but it does not necessarily represent materials with decreasing strain rate. There is always a permanent strain associated with any load. Maxwell's body is shown in Figure 8. The initial strain due to Hooke's element can also be seen from the figure.

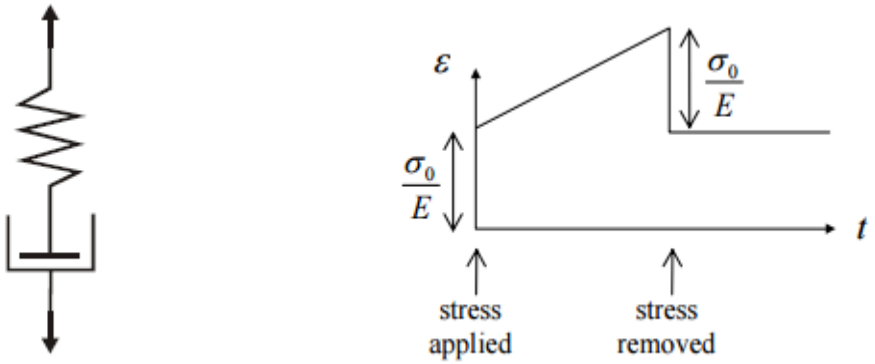

Figure 8 Maxwell's model (left), creep-recovery response of the Maxwell model (right).

Kelvin (Voigt) Model places the spring and dash pot element in parallel. With the assumption of no bending, the strain experienced by both the elements will be the same. This implies that both the elements deform at the same time. Unlike Maxwell model the strain immediately after the load will be zero. The Kelvin Model can be represented by the equation:

$$\sigma = E\varepsilon + \eta\, \dot{\varepsilon}$$

When load is applied the spring has the tendency to elongate but the dashpot takes time to react. In that case all the stress will be concentrated on the dashpot. Thus initially the curve will have a slope of σ_0 /n. With time the spring will start elongating and there will be a decrease in stress in dashpot. Finally it reaches limit where spring takes all the stress and the strain will be maximum. Thus the creep depends on the time for transfer of stress. Figure 9 shows the model and the response.

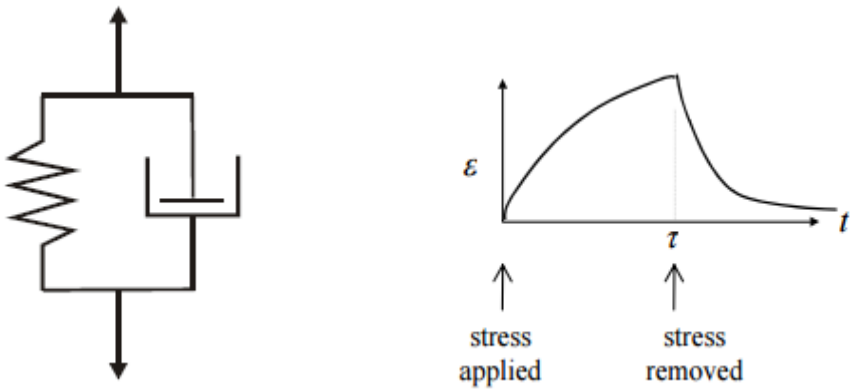

Figure 9 Kelvins model (left), creep-recovery response of Kelvin model (right).

Bingham model has the St. Venants body connected in parallel with Newtons viscous element. An important characteristic of this model is the yield point concept. This point differentiates the state of rest and motion. Thus a body will be at rest at low stress and flows like a viscous fluid in high stress. This model in not used for research purposes

mainly because eof the inability to define the yield point and is only used for quality control tests. Thus these mechanical models can be used only as a description of the laboratory behvaior of soils. Another point to be understood is that for different loading conditions different models could be used. Figure 10 shows the behavior of different models and the slope of the line is taken as the viscocity.

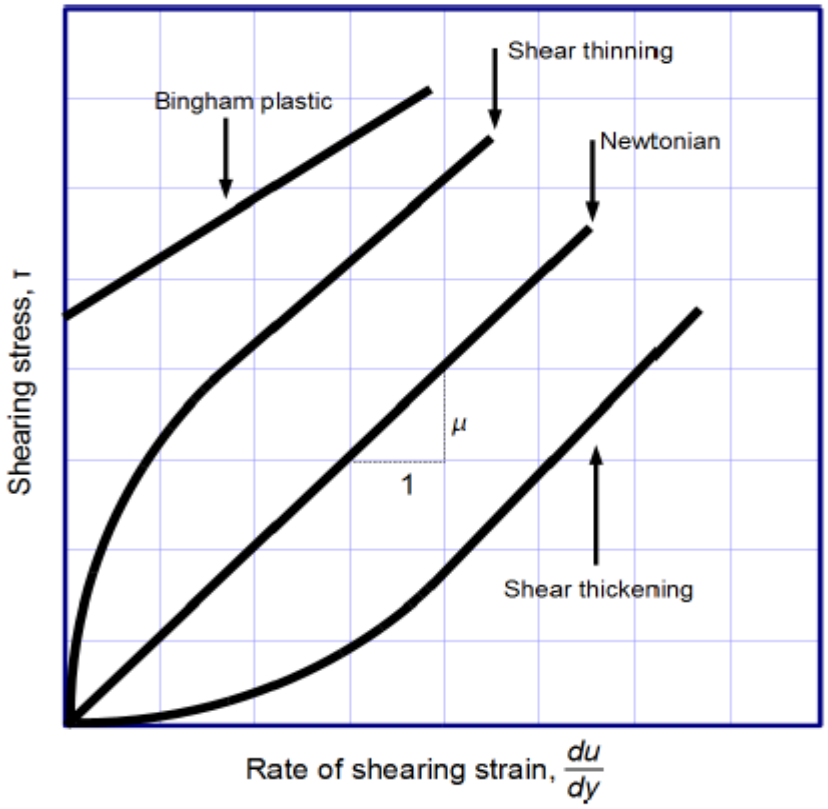

Figure 10 Behavior of different fluid models.

2.4.2 Experimental models

The concept of limiting compression curve on compression of granular soils was proposed by Pestana and Whittle (1998). It was similar to normal compression line explained in critical state soil mechanics. They proposed that all virgin compression curves of each granular soil would converge on to limiting compression curve at high effective stress. It was later extended to include time dependent creep behavior. A limiting compression curve regime was defined which consisted of parallel isochronous compression lines Pestana and Whittle (1998). The limiting compression curve represents a linear variation between logarithm of void ratio and logarithm of effective stress given by:

$$\log(e) = -\rho c \log(\sigma v / \sigma vz)$$

Where ρc=compressibility index and σ vz =reference effective stress, e is the void ratio.

Gasparre et al (2003) conducted detailed experimental study to understand the evolution of particle breakage and time depended behavior of soils. To study the time effect they performed creep tests under isotropic conditions. An effective stress was applied slowly and was let to creep was 1000 hours. Their key observations are as follows:
a. Strain rates increase with time and reach a constant after 50 hours in triaxial test. In an odeometer test creep strain do not start immediately if an instantaneous load is applied. They start after 425 hours and stabilize after 50 hours. This shows that creep strain has a limit with time (Figure 11).

b. An instantaneous load and letting the sample to creep for 100 hours shows more crushing than gradual loading for 100 hours. From this they observed that there is a load rate limit above which breakage is maximum. In other cases breakage will increase with duration.

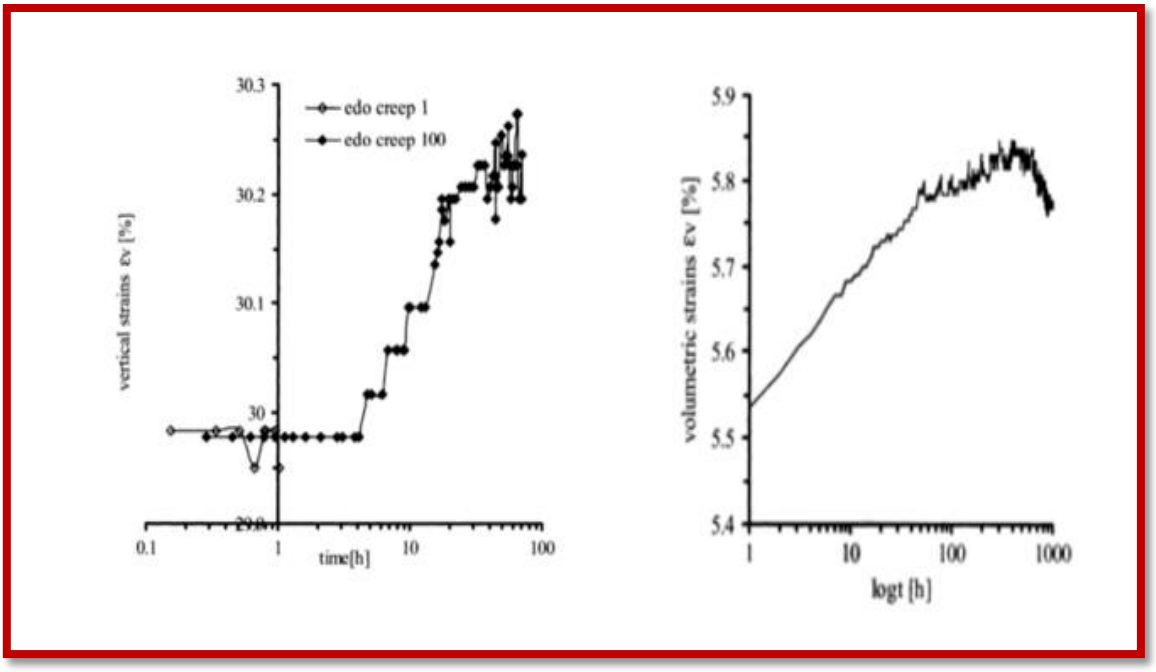

Figure 11 Variation of strain with time, Gasparre et al (2003).

Briaud and Garland (1985) analyzed two models , one which gives a straight line in a semi log plot and other which leads to a straight line in a log- log plot. From this they proposed the model:

$$\frac{s}{s_1} = \left(\frac{t}{t_1}\right)^n$$

Where the settlement s_1 is the value of settlement observed at time $t = 1\text{min}$ (after the beginning of a holding load); and n is the viscous exponent. Its value varies from 0.005~0.03 for sands and 0.02~0.1 for clays. They recommended to perform undrained creep tests and obtain the n value or to use the following equations to obtain a conservative value of n.

$$n = 0.44(Su / P_a)^{-0.22}$$

$$n = 0.028 + 0.00060w$$

$$n = 0.035 + 0.00066PI$$

$$n = 0.036 + 0.046LI$$

Where LI is liquidity index, PI is plasticity index, w is the water content and Su is the undrained shear strength.

Briaud and Gibbens (1999) did an analysis of dependency of creep deformation on time in their load test on spread footings in sand. The loading protocol adopted was to hold a particular load for 24 hours or 30 minutes and observe the creep settlement. Then the load is increased and held for another 24 hours. The load increment was 10% of estimated load capacity of the soil. They made a significant observation that most of the creep deformation occurred when the load was held constant. Another observation that load had a significant effect on the creep deformation. The Figure 12 and Figure 13 shows this property.

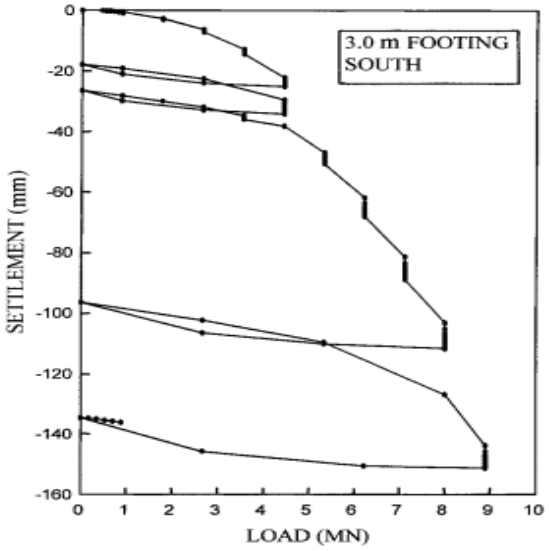

Figure 12 Load vs settlement curve, Briaud and Gibbens (1999).

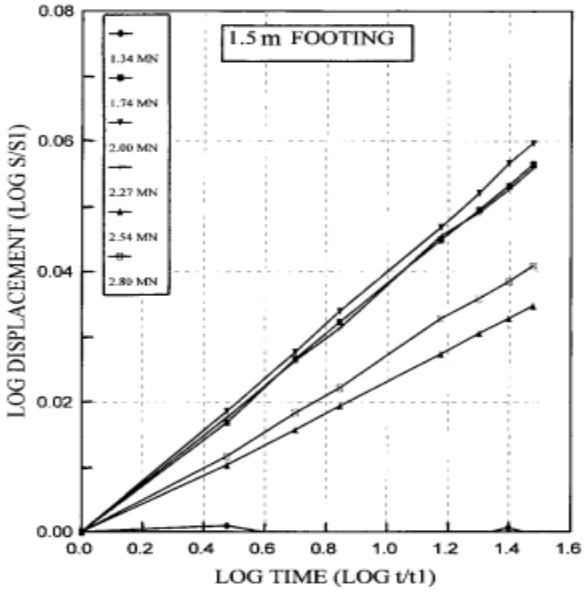

Figure 13 Creep deformation for 30 minute loading, Briaud and Gibbens (1999).

Hunter and Khalili (2000) proposed a creep failure criterion for over consolidated clays. Creep failure occurs at a strength less than the peak strength. The creep failure starts at the same strain for peak stress in a conventional strength test. They also added that the strength can be as low as critical state strength. The time for the failure is predicted based on the gained strength. The Figure 14 shows the failure prediction using accumulated strain.

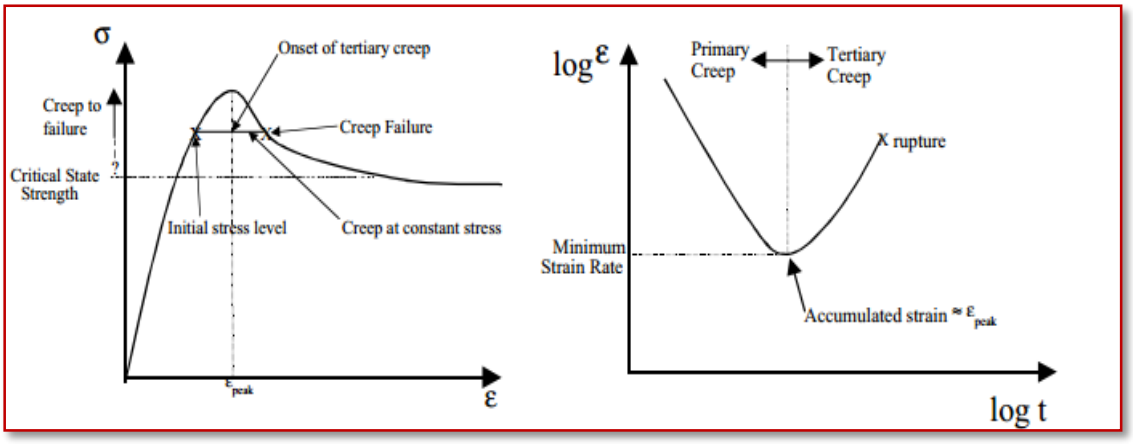

Figure 14 Failure of sample during creep tests (left), minimum strain rate for failure, Hunter and Khalili (2000).

One of the most recent studies on laboratory creep tests by Luo and Chen (2014) on soft soils involved triaxial creep test with different drainage conditions. They observed that failure time in undrained triaxial test is longer than shear creep test. The found that the axial strain and creep characteristics of the soil change with the drainage conditions. As expected the creep strain of drained triaxial test was more than undrained triaxial test. The creep curves from their drained and undrained tests are shown in Figure 15.

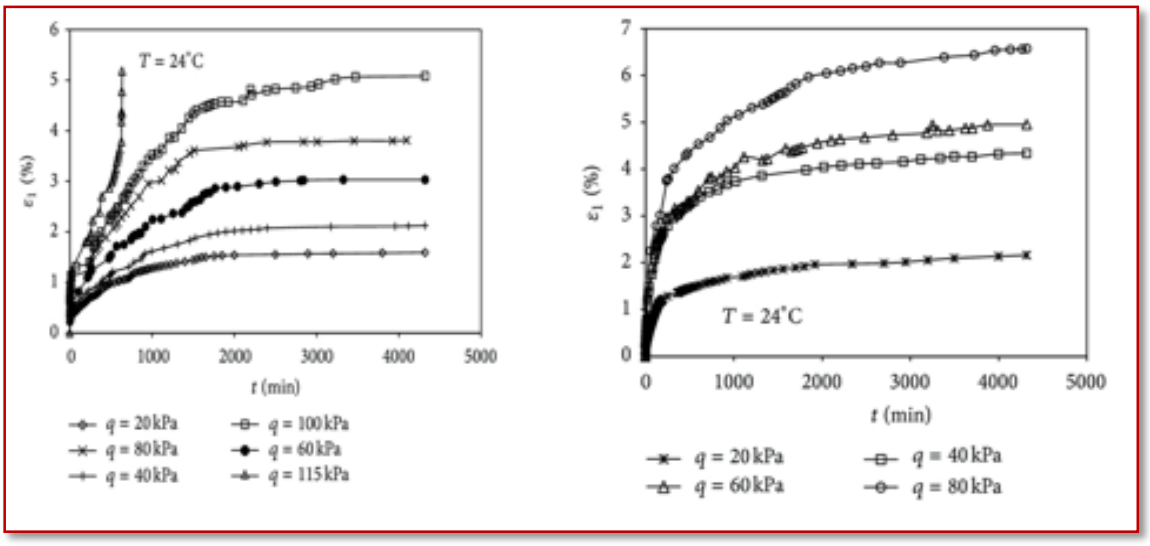

Figure 15 Time vs strain curves for creep tests, undrained creep test (left), drained creep test (right), Luo and Chen (2014).

Lai et al (2014) developed a model for predicting creep behavior of unsaturated soils. As in saturated soil a power function was proposed for strain-time relationship and a hyperbolic function for stress-strain relationship. Important observations were that axial strain is directly proportional to deviatoric stress and inversely proportional to matric suction. Figure 16 depicts this model.

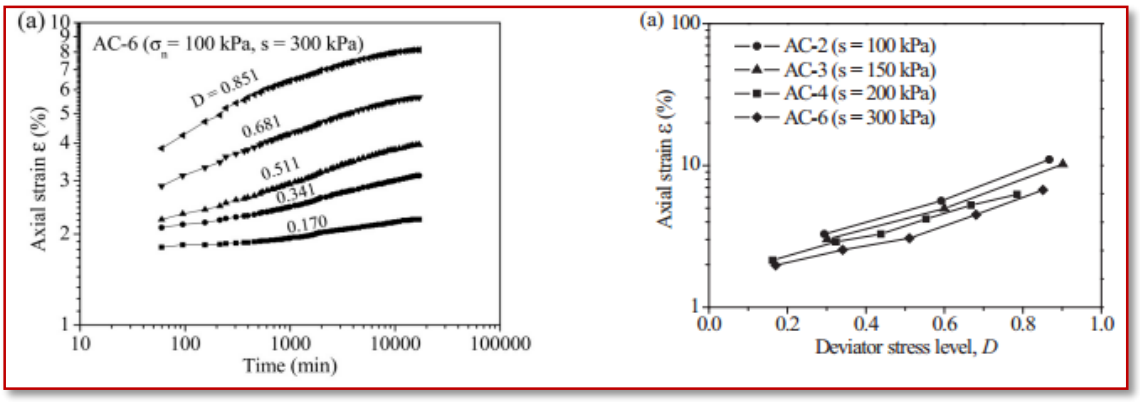

Figure 16 Strain time relation (left), stress strain relation (right), Lai et al (2014).

2.5 Previous study at Texas A&M

An emergency slope repair project using soil nails in Beaumont, Texas was studied to understand the creep behavior by Kharanaghi (2015), Bi (2015). This project was selected after carefully examining other 7 ongoing soil nail wall project in Texas (after visiting some and analyzing the suitability to study creep). This retaining wall is situated under the ramp of US 69 in the Beaumont district. The slope had failed at the edges of the bridge. Soil nail were used to stabilize this failure. This location was ideal because the soil had a very high plasticity index, thus provided the ideal soil conditions for creep study. The Figure 17 and Figure 18 shows the location of the project. Some key features of the wall were:

(i) Length = 453 ft.

(ii) Maximum height = 25 ft.

(iii) Minimum height = 3.75 ft.

(iv) Lowest point = 4+53.

(v) Highest point = 0+76.

Figure 17 Beaumont project site after Kharanaghi (2015).

Figure 18 Aerial view of the Beaumont project site after Kharanaghi (2015).

Figure 19 Failure at Beaumont site, before construction of soil nail wall.

The slope failure before construction can be seen from the Figure 19. It was decided to install 6 rows of soil nails to stabilize the slope near the bridge. Nail length varies with section. Elevation of the wall is shown in the Figure 20 .Thus the excavation was decided to be done in 6 stages. As a part of the research study Kharanaghi, graduate student in Texas A&M conducted the following activities as a part of his doctoral thesis:

(i) To measure horizontal displacements inclinometers were installed at positions 2+00 and 1+46 (Figure 20)

(ii) 6 Sacrificial nails were installed to study pullout strength

(iii) Two vibrating strain gauges were installed on each nail at 2ft and 15ft on the nail

(iv) Tilt meters were installed to observe the tilt in the wall

(v) Water content probes were installed to measure the variation in water content in different seasons.

Creep tests were conducted on the nails and the percentage of pullout capacity that creep failure occurred was found. It was observed that creep failure occurred at a load level more than 94% of pullout capacity. Load distribution in the nails were also found.

The cross section of the wall at 1+46 is given in the Figure 21. Two inclinometers were installed one at section 2+00 and other at section 1+46. During construction after the first stage, a failure occurred at section 2+00 due to over excavation. The failure resulted in bending of the casing which made further reading impossible. Additional casings were installed at section 2+00 and 1+46 after the failure and the reading were taken.

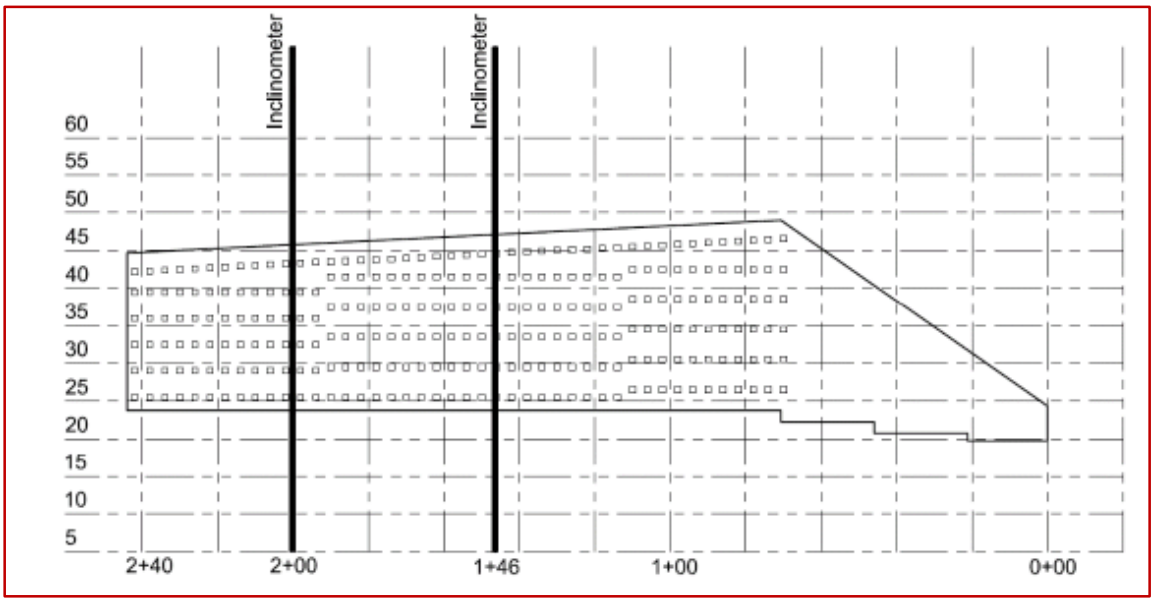

Figure 20 Location of inclinometers at Beaumont site.

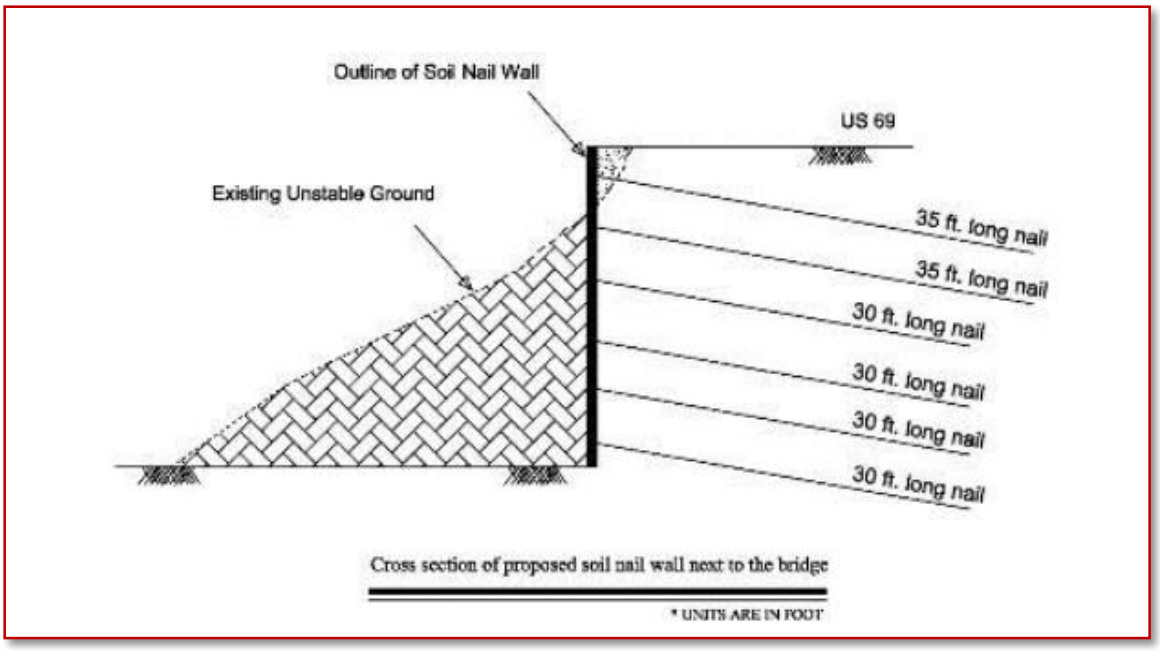

Figure 21 Nail position, cross section of the soil nail wall at Beaumont.

The Drained analysis was done using FLAC 3D on the cross section 1+46 by Kharanaghi (2015). The drained soil strength parameters were found from the correlation between plasticity index and the drained internal friction angle. The predicted horizontal deformation was found to be fitting well with the observed reading. But for the top 5 feet the deformation was under predicted. This is probably because during construction the excavation is in undrained conditions. This aspect is considered in this thesis. Undrained parameters are found from lab tests and these parameters are used in undrained wet analysis which will reflect the conditions in the field during construction.

To study creep the Burger model was adopted. The creep tests conducted in the lab were modelled using the Burger model. The relation between the n value and the viscosity parameters were developed using these simulations. The parameters that were found were ‘m shear’, ‘m vis’, ‘k shear’, ‘k vis’ these are spring and dashpot elements from Maxwell and Kelvin element. The results from this simulation are shown in the Figures 22, Figure 23, and Figure 24 below:

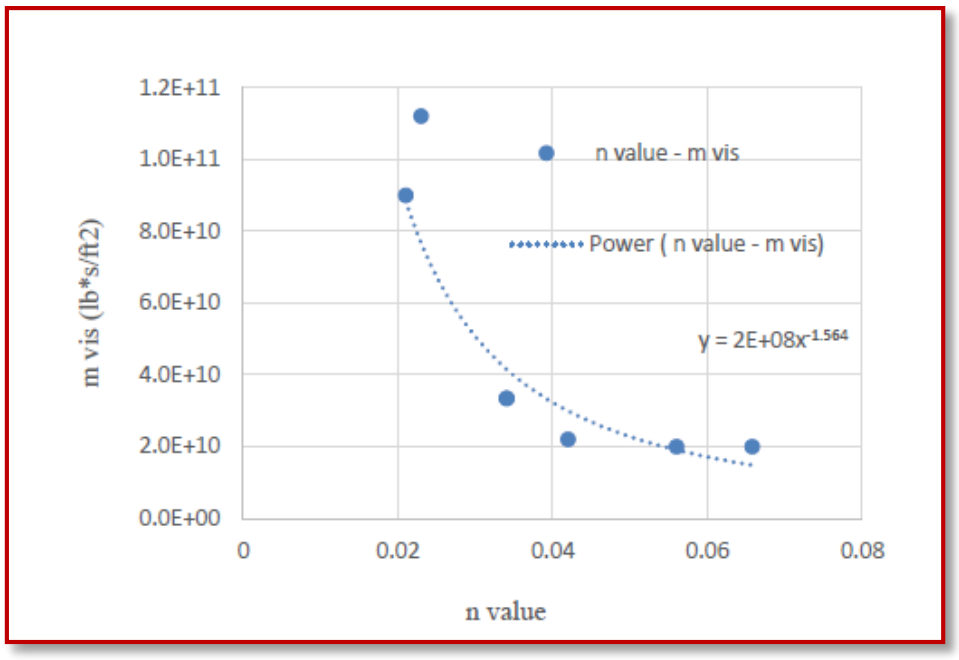

Figure 22 Relation between Maxwell's viscous parameters and 'n' value, after Kharanaghi (2015).

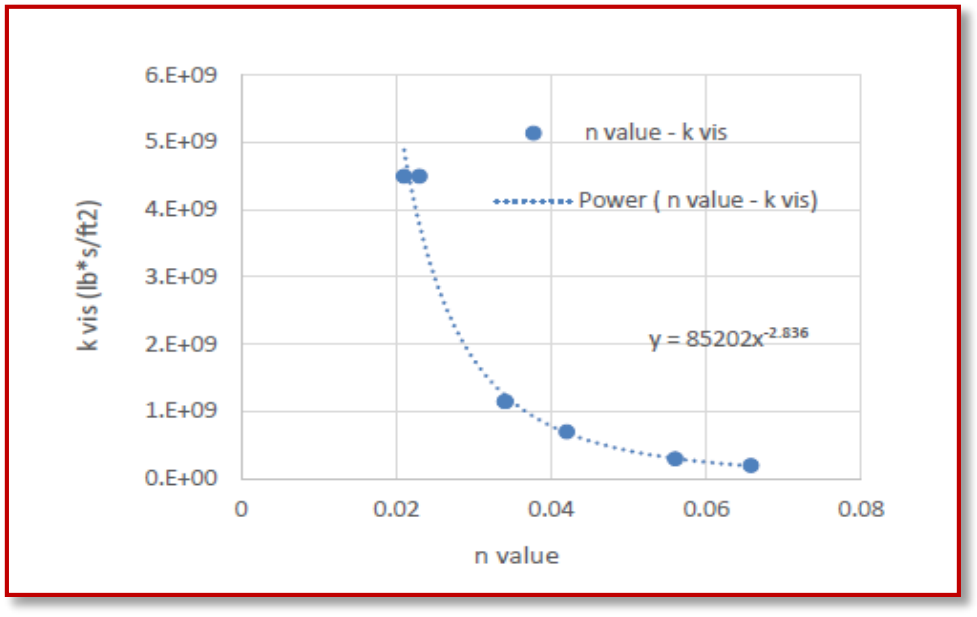

Figure 23 Relation between Kelvin viscous parameters and 'n' value, after Kharanaghi (2015).

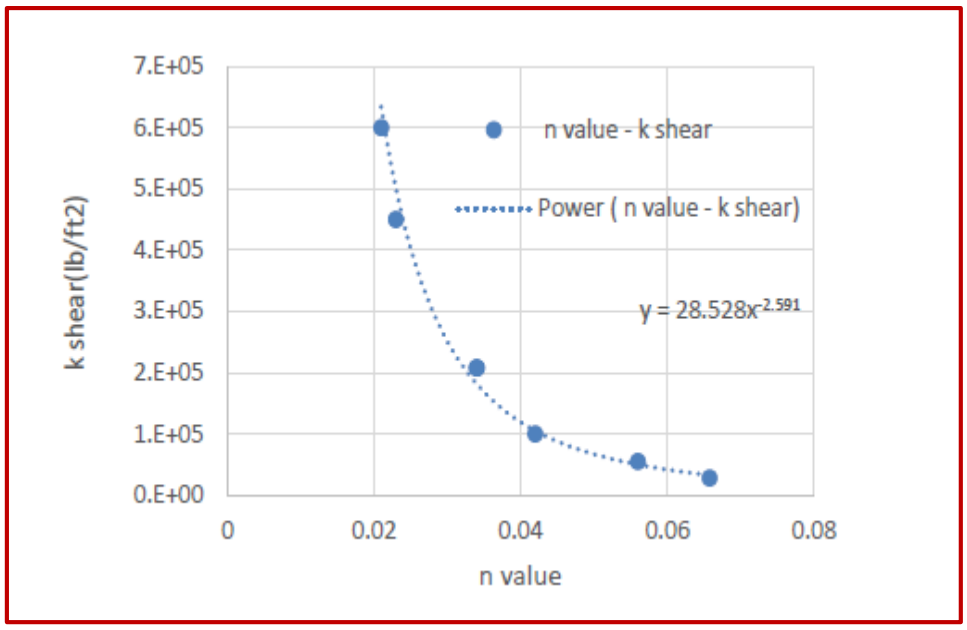

Figure 24 Relation between Kelvins shear parameters and 'n' value, after Kharanaghi (2015).

CHAPTER III

LABORATORY TESTING

This chapter presents all laboratory tests performed to characterize the soil from the Beaumont site. The important properties studied include Atterberg limits, shear strength parameters, variation of shear strength with depth, and creep behavior. The common geotechnical laboratory tests like direct shear, triaxial tests were conducted to assess the shear strength variation with different conditions. Triaxial undrained creep tests were conducted to assess the creep parameters which could be later used in modelling. A brief discussion of each test and their results are included here.

3.1 Soil properties

Basic soil properties like water content, unit weight, Atterberg limits and saturation on undisturbed samples were found by Bi (2015). In the laboratory experiment designed for this thesis it was decided to match insitu properties (Table 2) of soil after remolding. Table gives the geotechnical properties of the soil used in this thesis.

Depth (ft.)	Water content (%)	Liquid limit (%)	Plastic limit (%)	Unit weight (pcf)
4	33.8	77.8	23.7	121.6
12	25.5	91.9	24.3	118.5
22	21.8	65.1	16.8	127.9

Table 2 Soil properties of Beaumont field site from undisturbed samples (After Bi 2015).

3.2 Classification

An attempt to classify the soil according to new classification technique suggested by Jang and Santamarina (2015) was done. For this liquid limit was found by adding three different liquids namely, water, kerosene and saline water (water with 2M Nacl added). Drop cone penetrometer was used for this. Soil sample after mixing the required quantity of liquid is placed in a 5.5 cm diameter and 4 cm deep metal cylinder. The weight of the drop cone is 80gm and has an angle of 30 degrees. The cone is dropped for 5 seconds and the penetration is read from the dial gauge. A series of tests with increasing water contents were conducted. Figure 25 shows a typical drop cone penetrometer used in the laboratory. The water content at 20 mm penetration was taken as the liquid limit.

In this new proposed method of classification, fines are classified on the basis of the liquid limits from three different liquids. The sensitivity S_E is found from the ration of liquid limit from the tests. Sensitivity is given by:

$$SE = \sqrt{(\frac{LLDW}{LLbrine} - 1)^2 + (\frac{LLker}{LLbrine} - 1)^2}$$

Where LL_{DW} is the liquid limit from distilled water and LL_{brine} is the liquid limit from brine and LL_{ker} is the liquid limit found with kerosene.

Figure 25 Typical fall cone penetrometer, (After ELE International).

The classification chart is shown in the Figure 26. Total of 12 classes are defined based on electrical sensitivity and plasticity. Black dots belongs to different soils tested and classified based on this method. Results from liquid limit tests done with kerosene is shown in Table 3, with brine is shown in Table 4 and with water is shown in Table 5.

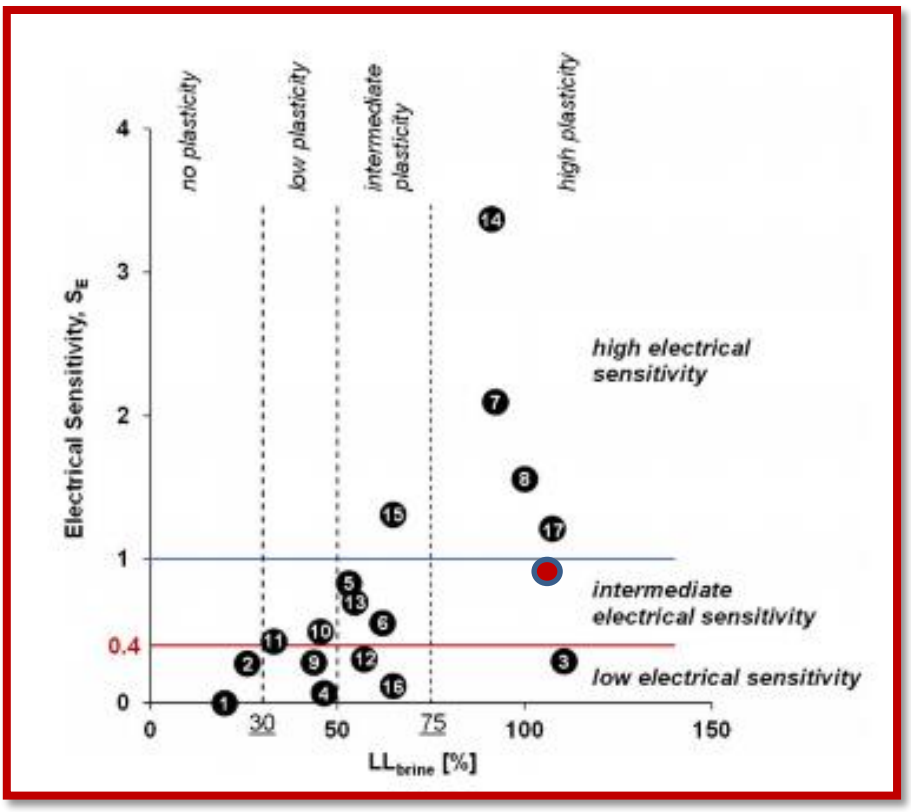

Figure 26 Classification chart of fine grains, Jang and Santamarina (2015).

Penetration (mm)	Kerosene (%)
150	31
200	32.93
252	36.16
280	37

Table 3 Results from cone penetrometer test for liquid limit using kerosene.

Penetration (mm)	Water content (%)
154	63.3
180	70
210	80.21
258	88.8

Table 4 Results from cone penetrometer test for liquid limit using water.

Penetration (mm)	Brine (%)
158	31.8
172	38.2
236	56.7
300	80

Table 5 Results from cone penetrometer test for liquid limit using brine solution.

A straight line was fit through he points and the liquid content at 20 mm penetration was considered as liquid limit. The plots of the liquid % vs Penetration is shown in Figure 27, Figure 28, and Figure 29.

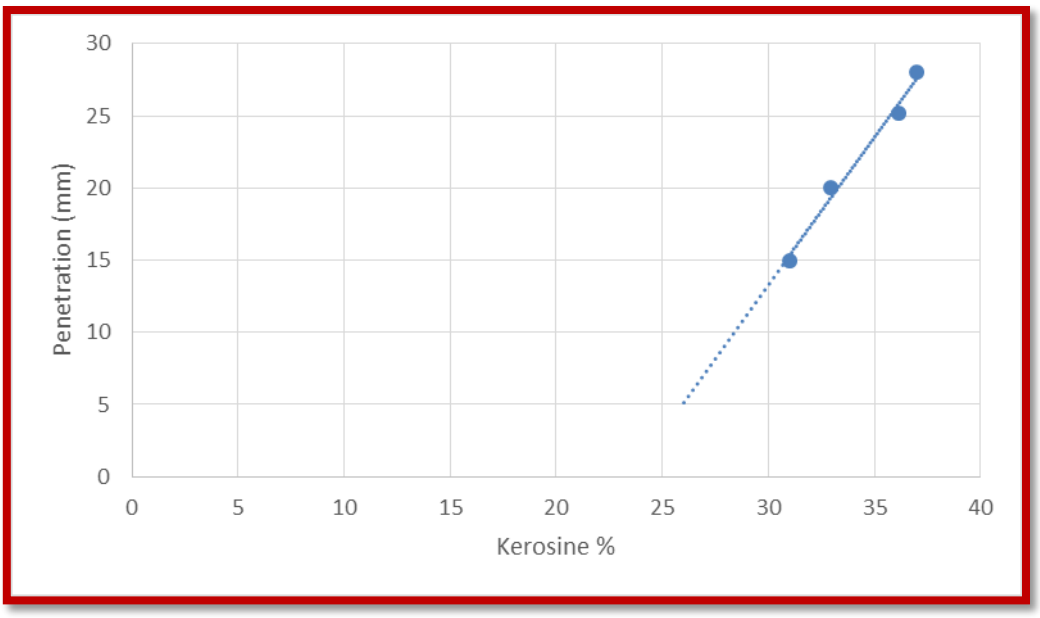

Figure 27 Penetration vs kerosene content.

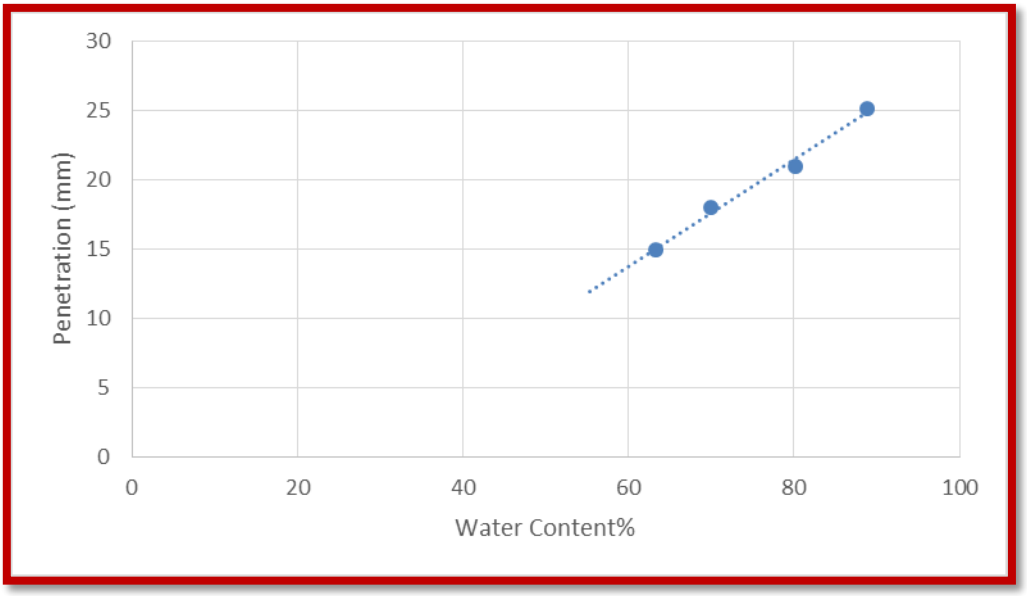

Figure 28 Penetration vs water content.

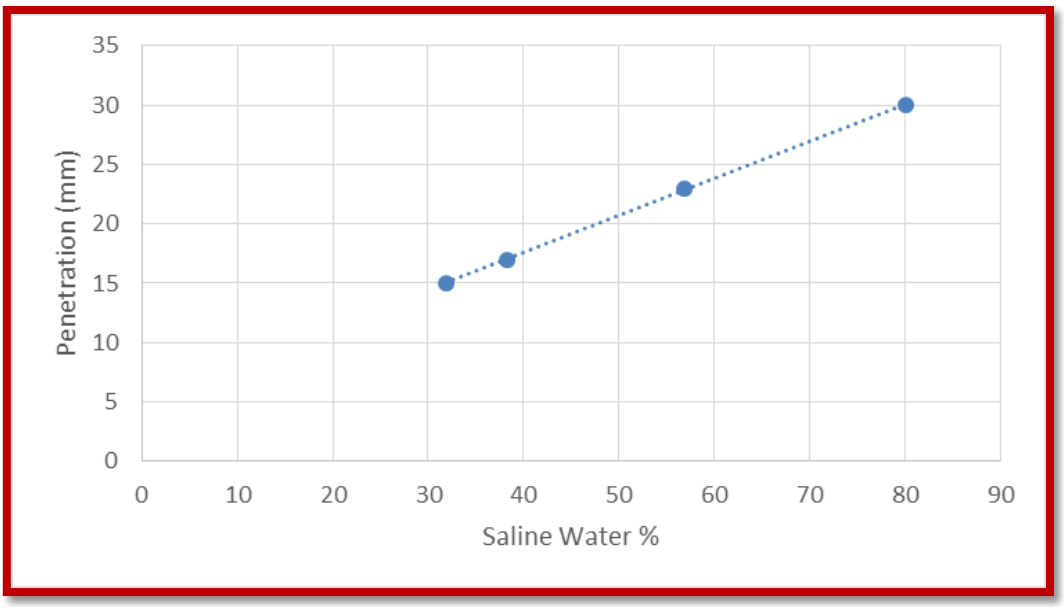

Figure 29 Penetration vs saline water content.

From the graphs the liquid limit corresponding to 20 mm penetration was found. Liquid limit when water was used was 77 and with saline water is 48 and with kerosene is 35. Sensitivity was calculated using the equation as 0.55. From the classification chart shown in Figure 26 the soil can be classified as fines with intermediate plasticity and intermediate sensitivity.

3.3 Direct shear test

Direct shear test was conducted to obtain shear strength at various saturation. The conventional direct shear apparatus was used for this. The tests were conducted at three different saturation and for three different normal stress. Shear strength was obtained for full saturated, insitu saturation and air dried sample. The strain rate for fully saturated and insitu saturation was kept low to ensure complete drainage of the sample and to ensure

that there will be no generation of pore pressure. All samples other than dry samples were consolidated under the normal stress. Vertical consolidation was monitored during the consolidation stage. On an average each sample took about five days for complete consolidation. For dry samples faster rate of shearing was adopted.

The apparatus consist of a box split into two halves. The normal force is applies to the specimen through a cap. A constant rate of strain is applied to the sample and let it to shear. The shear force i.e. the resisting force is recorded by the force transducer and shear stress calculated from the area of sheared cross-section. The failure occurs at a predefined plane at the intersection of two halves of the box. One of the main advantage is the time to failure. For clays it is generally observed that triaxial test take longer time than direct shear tests. Issues related to cavitation are also avoided in this test.

3.3.1 Sample preparation

Remolded samples were used for this test. Care was taken to remold the samples to ensure they represent the in situ conditions. The following steps were followed for sample preparation:

1. The soil passing through required sieves was collected and the required amount of sample was taken.
2. Water content of the dry soil was measured.
3. Additional water required to obtain the required water content was added by carefully spraying water on the dry soil.
4. The soil after mixing the water was stored in a zip lock and placed in the moisture room for 24 hours. This was done for uniform distribution of soil.

5. The sample of size 6.2 cm in diameter and 2.6 cm in height was cast. The sample was again placed in the moisture room.

All samples were prepared by the above procedure. To obtain dry samples:

1. The wet sample was placed for air drying
2. The sample dimensions were measured every 6-8 hours. The weight was also measured.
3. The sample was cut to required dimensions when there was no more change in dimensions/ change in weight.

Samples cracked as they dried and had to be remolded again. When a very slow strain rate was adopted for fully saturated soil, the equipment showed issues like excessive heating up.

3.3.2 Testing procedure

ASTM Standard D-3080 was followed for this test. A short description of the procedure is described below:

1. The porous stone was placed at top and bottom of the specimen to ensure two way drainage. The sample and porous stone was placed in the shear box and was then placed in shear bowl. The rigid cap was placed on top of the top porous tone. The alignments screws were tightened.
2. The shear force loading system was placed in such a way that no force was measured in the load measuring device. The apparatus is checked to ensure that it gives correct readings.

3. The shear bowl was filled with water till the brim. For our special case to ensure full saturation wet clothes were placed on top of the specimen o ensure that the specimen is not drying. For dry test water is not used. The Normal load required for normal stress was applied. The consolidation of the sample was recorded. After complete consolidation shear was started.
4. The alignment screws were removed. The plastic screws were give a small turn to avoid any friction between the two halves. The shear rate selected was applied and the time was noted. Force transducer was used to measure the shearing force. Shearing was continued till the shear resistance was constant. The sample was tested for dry, saturated for three normal forces.
5. The soil sample was collected from the center of the sample after testing, ie along the plane of failure.

To ensure full saturation during the test wet clothes were put on the top of the test apparatus and additional water was added as and when a decrease in water level was observed. At least 5 samples had to be disposed of due to excessive cracking observed in the sample when drying. A small alteration helped to resolve this issue. The sample was cast at a saturation lesser than in situ saturation.

3.3.3 Direct shear test results

The direct shear test results are given in the Table 6.

Moisture Condition	Applied Normal stress(Psi)	Shear stress(Psi)
Fully Saturated Water content=28.3%	6.67	4
	10.29	5.1
	14	7.6
In situ saturation Water content=25.5%	6.67	8
	10.29	10.3
	14	12.18
Dry Water content=3.6%	6.67	41
	10.29	42
	14	46

Table 6 Data of samples at failure.

Plots of direct shear test conducted on fully saturated samples are shown in Figure 30. Results from samples with insitu saturation are given in the Figure 31 and the results from fully dry tests are given in Figure 32. As the soil becomes dry the strength of the samples increases due to suction effect. It can be inferred that the strength increase and the soil will show less creep behavior with decrease in saturation.

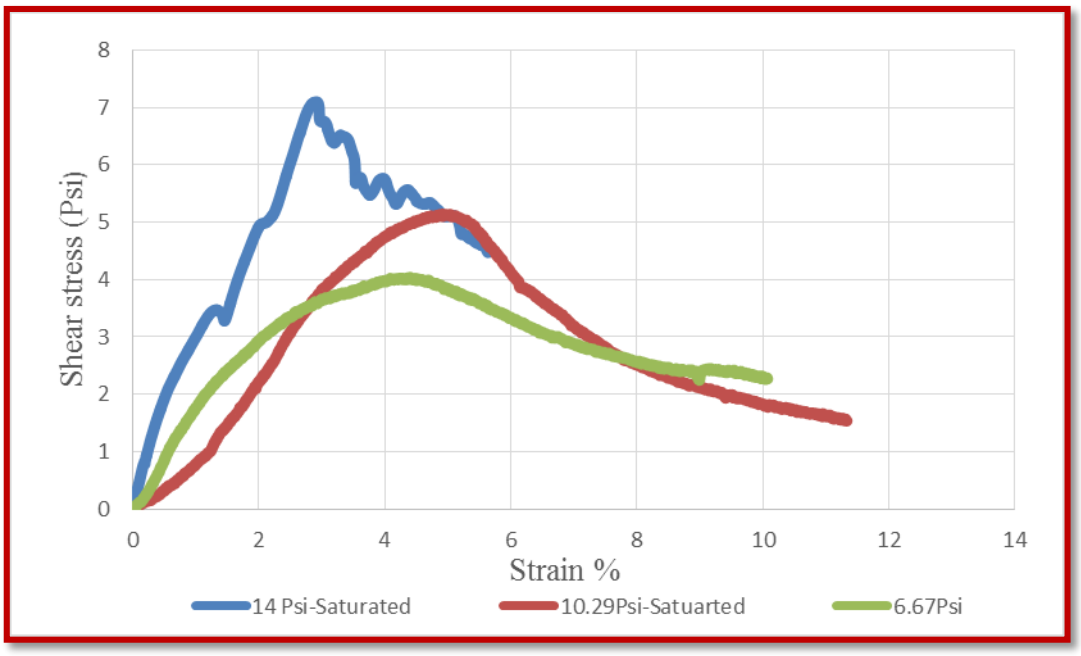

Figure 30 Direct shear test on fully saturated sample.

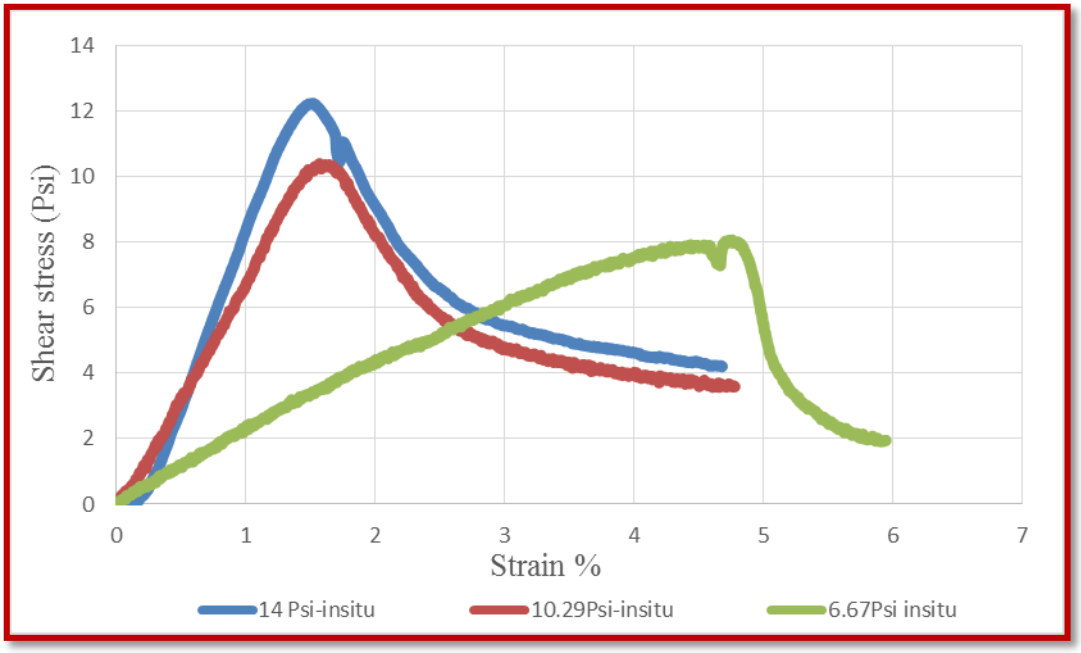

Figure 31 Direct shear test on sample with in situ saturation.

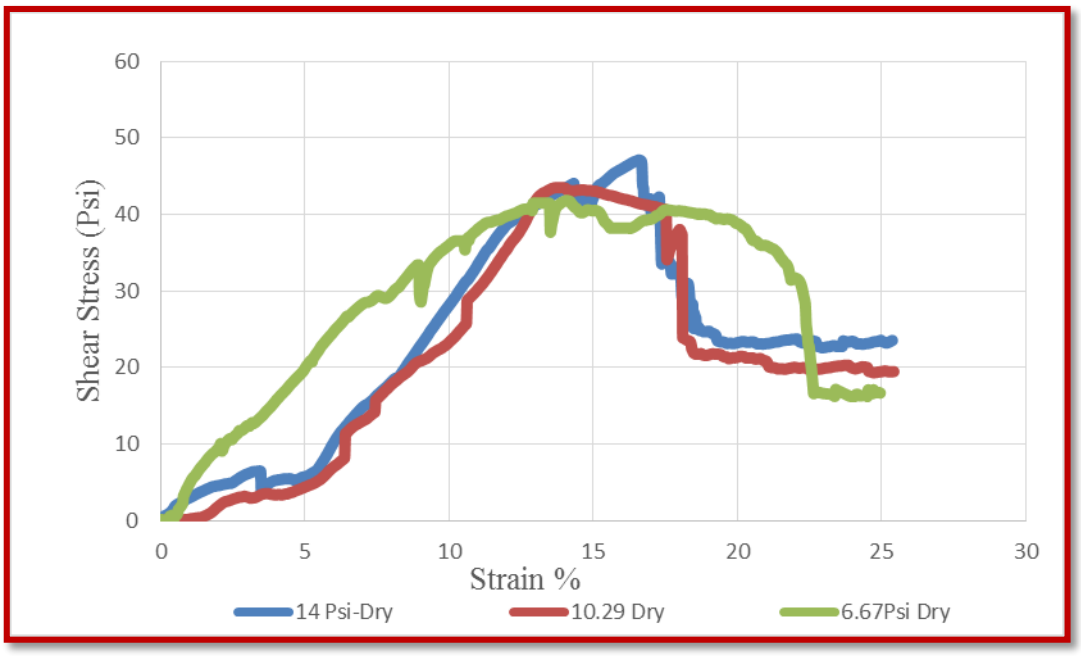

Figure 32 Direct shear on air dry sample.

3.4 Triaxial tests

Due to its versatile nature, it is one of the most common geotechnical lab test performed. Triaxial as the name implies comes from the nature of the test, where three different pressure are acting on the soil sample in three different directions. Unlike direct shear test there is no predefined failure plane and the soil fails along the weakest plane. Drainage conditions can be varied and controlled as drained or undrained in this test. ASTM D 4767 defines failure as the maximum stress or stress at 15% strain which ever happens first. Further, failure can be defined depending on the soil and the application of the results. Germaine and Ladd (1988) observed that triaxial test are used for the study of basic soil behavior, deformation, creep tests, stress history, cyclic loading.

The sample is encased in a non-permeable thin membrane, usually latex or rubber. Filter paper is placed above and below the sample. Two porous stone one on the top of the filter paper and one below the filter paper at the bottom are placed. This arrangement is then placed on the bottom platen. A cap with provision for loading the sample is kept at the top of the specimen. A transparent hollow cylinder is used to encase the membrane and the sample inside it. Load is applied by moving the piston downwards.

A confining stress can be applied in all perpendicular directions of the sample. This applied through a fluid usually water and the pressure is called minor principal stress. The deviator stress is the stress applied in vertical direction in addition to the minor principal stress. Combined deviator and the radial stress forms the major principal stress. This stress stage is shown in the Figure 33. When the deviatoric stress is applied the sample height decreases and bulges outwards. The water moved out of the sample is the change in volume of the sample. Three types of triaxial test can be conducted varying the drainage condition:

Unconsolidated-Undrained: No drainage is allowed in this test throughout the test. When confining stress is applied there will be no consolidation occurring during the test. The sample is kept fully saturated. Usually pore pressure are not measured and total stresses are reported. This is a fast test and sample takes less than an hour for failure.

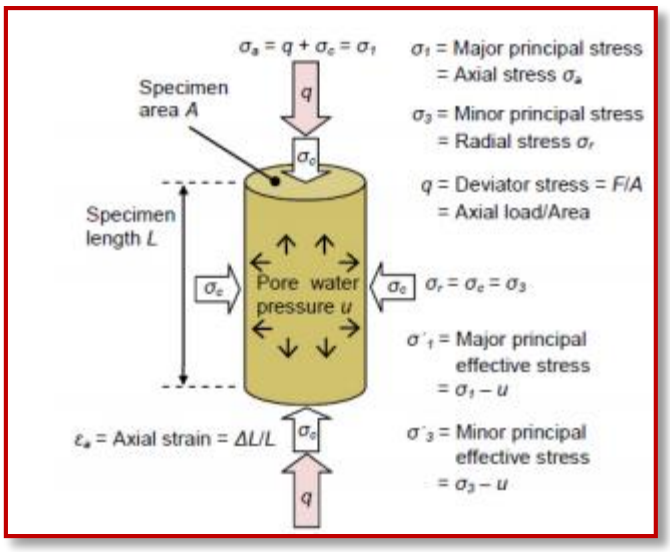

Figure 33 Principle of stress state in triaxial test after Dr. Sean Rees, GDS instruments.

Consolidated Undrained: Unlike the previous test the sample is set to consolidate after applying the confining pressure. Drainage is allowed during this stage of the test. The drainage valves are closed during the next stage of the test. The sample is loaded to shear and the pore water pressure if measured the stress can be expressed in effective stress analysis. Positive pore water pressure are measured when the sample expands and negative when sample contrasts.

Consolidated Drained: The sample is consolidated like the Cu test under the required confining stress. The difference lies in the drainage, the drainage valves are not closed during the shearing stage. The pore water pressure is not developed in the test. Care should be taken to apply stress in a very slow strain rate. Here total stress is equal to effective stress. Triaxial setup used in this study is shown in Figure 34.

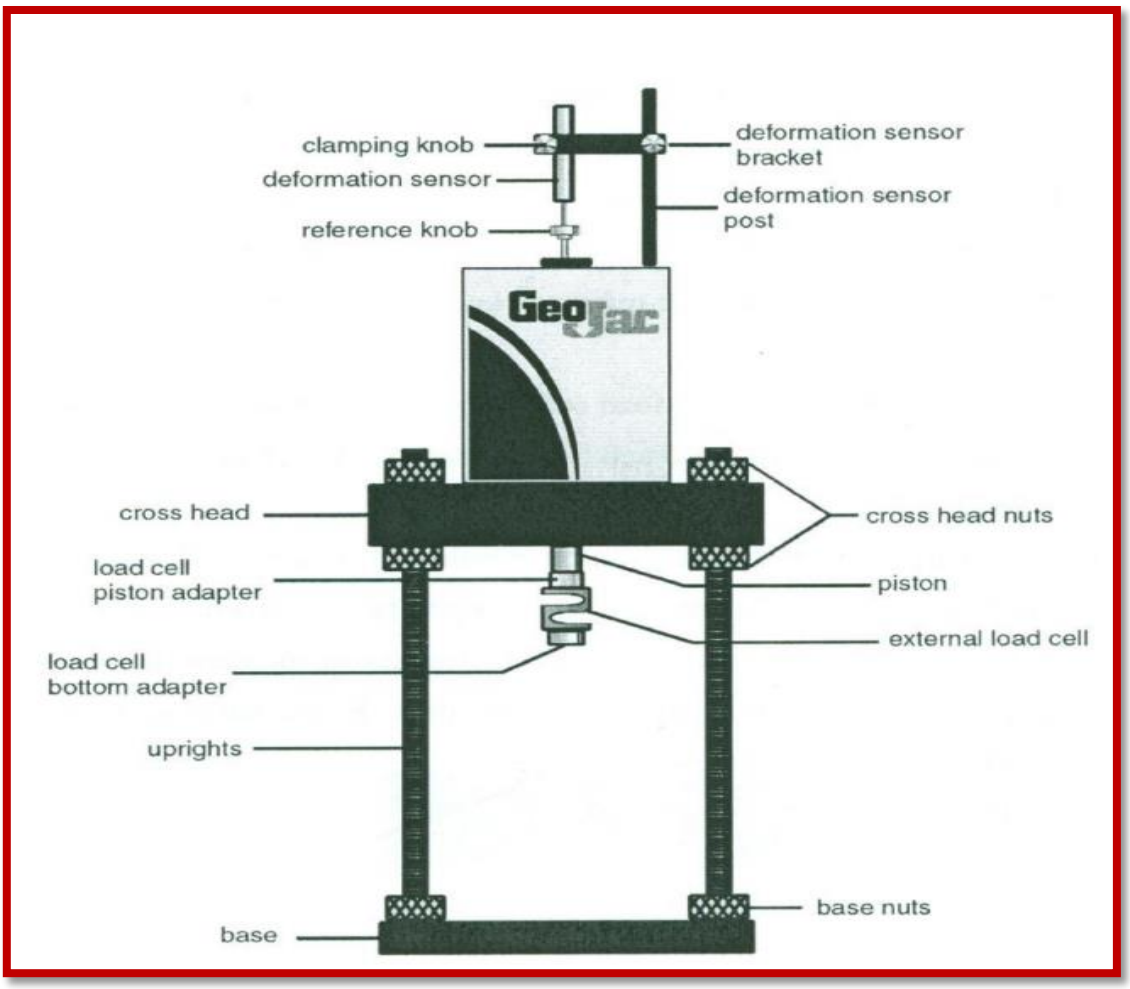

Figure 34 GEOTAC triaxial test equipment after Aubney and G. Biscontin.

3.4.1 Sample preparation

The sample is prepared like in the direct shear test. The average sample size of 3 inch height and 1.5 inch diameter is used. The sample is prepared in accordance with ASTM D 4767. The soil is mixed with calculated water to get the required saturation. The soil is kept in a zip lock and placed in the moisture room for 24 hours. The sample is cast in 7 layers. Corrugations are made after each layer for proper bonding between the layers.

After extruding the sample, it is placed in the moisture room for another 24 hours. The water content is measured using the remaining soil. Acre is taken to ensure that the sample represents the insitu sample in the best possible way.

3.4.2 Procedure

GEOTAC TruePath system was used to conduct all the triaxial tests. It consist of an external load cell to measure the load applied to the specimen. Pressure transducers are used for pore pressure and cell pressure measurement and monitoring. Automatic data acquisition system helps to record the data continuously at regular intervals. The software has a graphical interface, where monitoring can be done live when the test is run. A short description of the testing procedure is discussed here:

The sample is encased in the rubber membrane and the filter paper and porous stones are placed. The sample is installed on the top of the base platen. The valves are desired by flushing water through them back and forth. To ensure saturation water is let in through the sample bottom and drained through the top. Back saturation is also applied to ensure saturation. B- Value check is done to ensure the sample saturation.

Next is the consolidation phase. During the consolidation phase cell pressure is again increased to the required confining pressure to simulate the in situ behavior. The sample is left to consolidate. Consolidation can be checked by change in pore pressure. When the pore pressure is more or less constant, we can assume consolidation. The drainage conditions are applied as required for the test. After consolidation shearing is started. This involves applying load on the sample and measuring the resistance using the load transducer.

3.4.3 Errors

There are lot of sources of error in a triaxial test. The errors can occur from sample preparation to water content determination. Utmost care was taken during sample preparation stage that errors during this stage can be assumed to be nil. The pressure transducers are bound to show errors when there was very small pressure. Some points did show lot of variation. One CU test had to be repeated because leak was observed during the consolidation stage. It was observed after three days of consolidation. This test was repeated. From then on Vaseline was used to prevent any further leaks. After consolidation stage when the valve was closed pore pressure increase was observed. The sample was set to consolidate 12 hours after the consolidation to ensure that consolidation was proper. During creep tests it was required to change from strain control to stress control to maintain a constant load for 24 hours. During stress control the machine was not able to maintain the same stress for 24 hour period. Fluctuations in load was observed for some tests, (unsaturated tests on samples 22, and 12ft). An increase in stress from 5.8psi to 6.1 psi for a period of about one hour was observed for test on sample from 22ft and an increase of stress from 7.1 psi to 7.3 psi was observed for a total period of 1.5 hours on samples from depth 12ft.

3.4.4 Triaxial test results

The results from both saturated and unsaturated triaxial tests are given in Table 7. Figure 35 gives the total stress vs strain plot from saturated tests. Figure 36 shows increase in pore pressure with strain. Effective stress is plotted in figure 37.

Depth(ft)	Water content (%)	Saturation (%)	Normal stress(Psi)	Shear stress(Psi)
4	30.9	100	5	5.6
4	26.3	85	5	6.6
12	28.3	100	15	6.1
12	24	85	15	7.8
22	21.5	100	21	7.4
22	18	85	21	8.8

Table 7 Results from UU test**.**

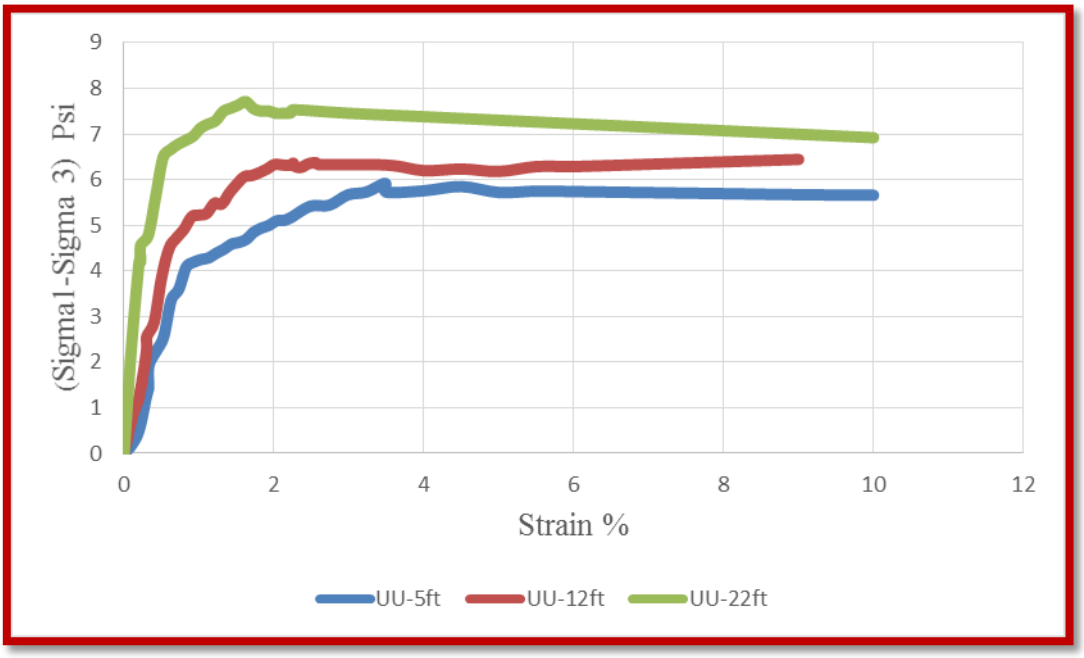

Figure 35 Saturated uu test strain vs total stress.

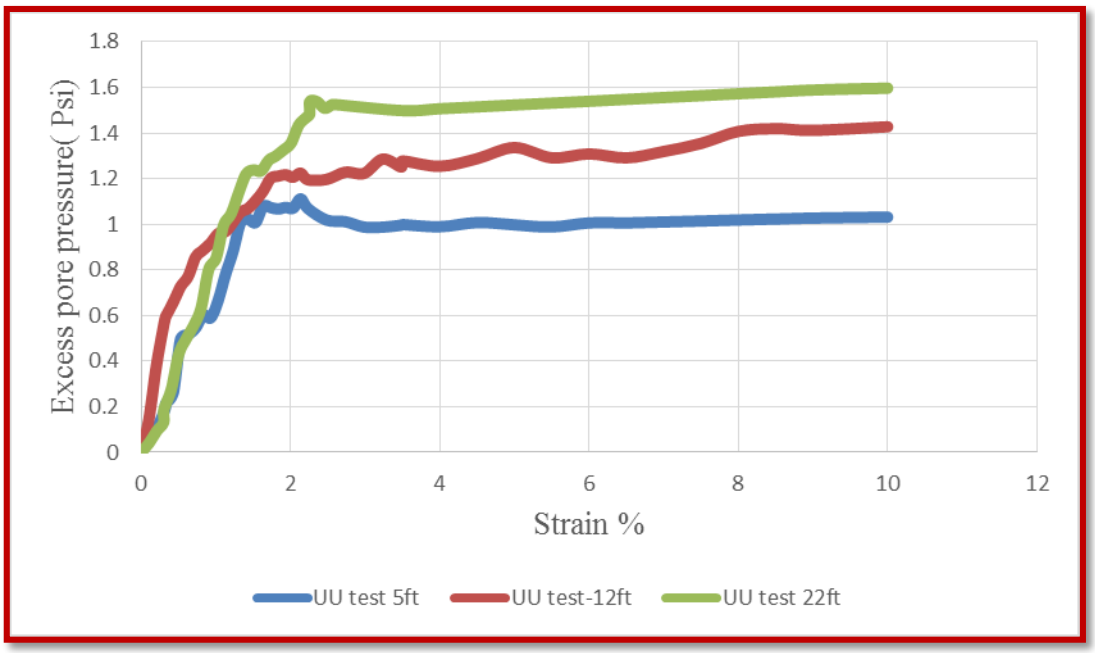

Figure 36 Saturated uu test strain vs excess pore pressure.

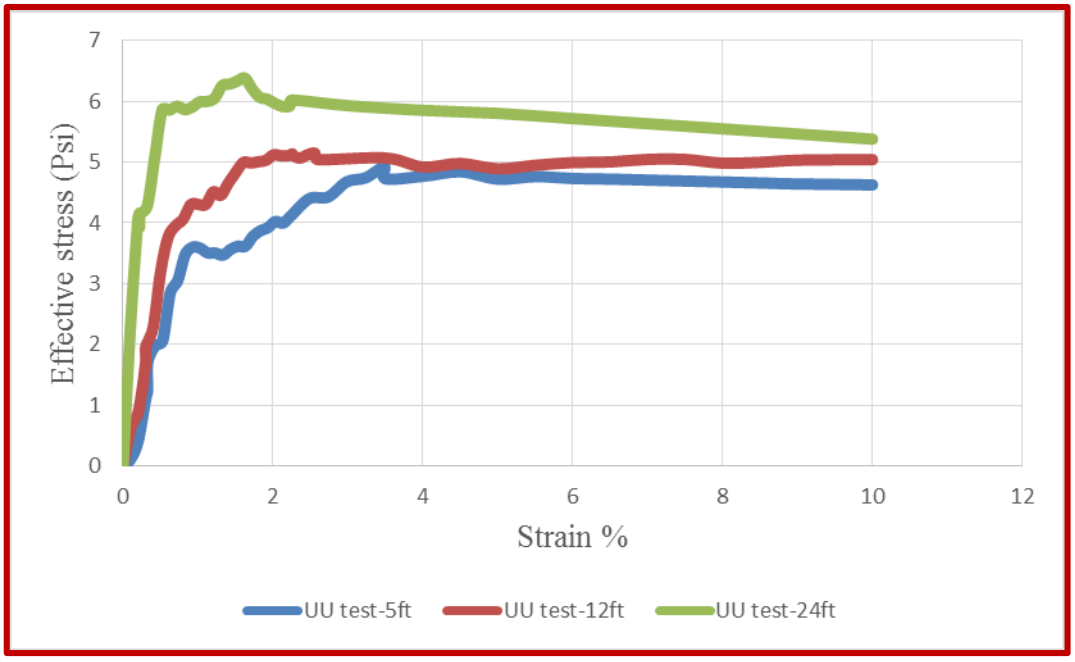

Figure 37 Saturated uu test strain vs effective stress.

Attempt was done to fit strain/stress vs strain to fit the hyperbola. Figure 38, Figure 39, Figure 40 below show that it fits well.

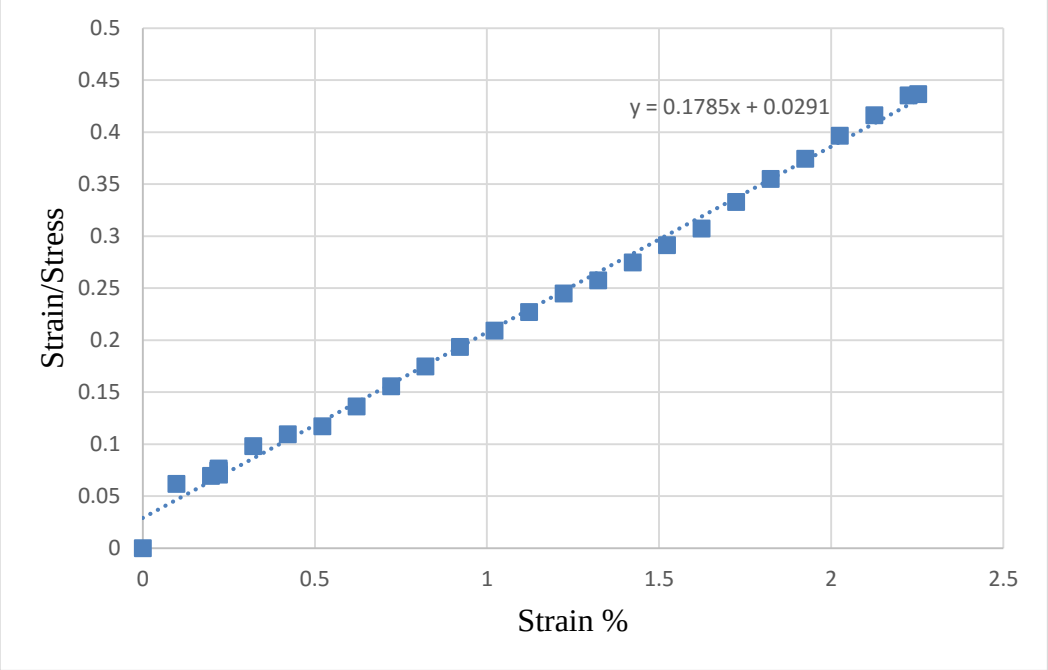

Figure 38 Strain/stress vs strain % of sample at depth 4ft.

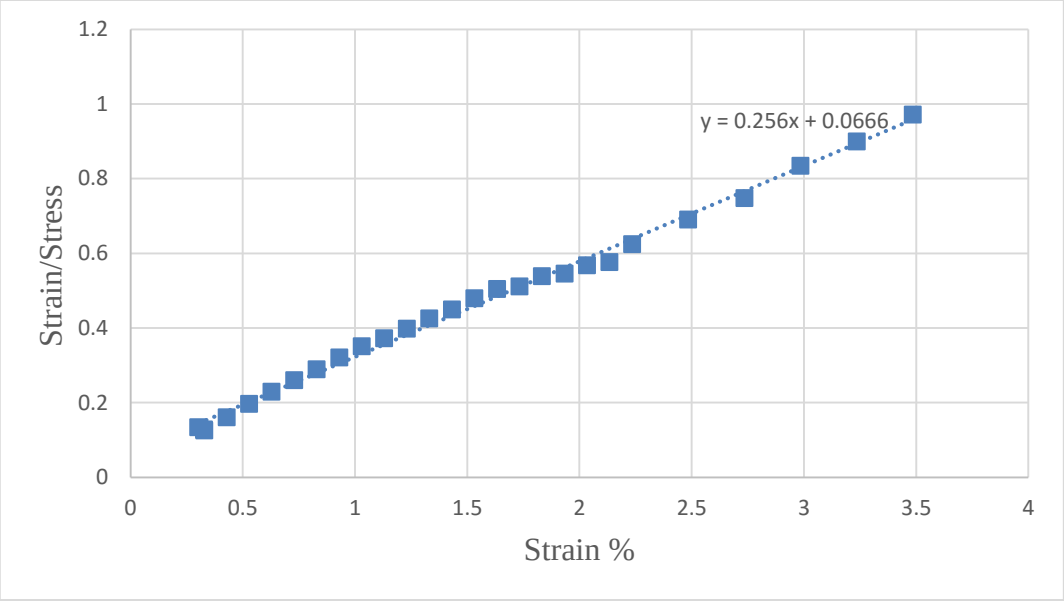

Figure 39 Strain/stress vs strain % sample at depth 12ft.

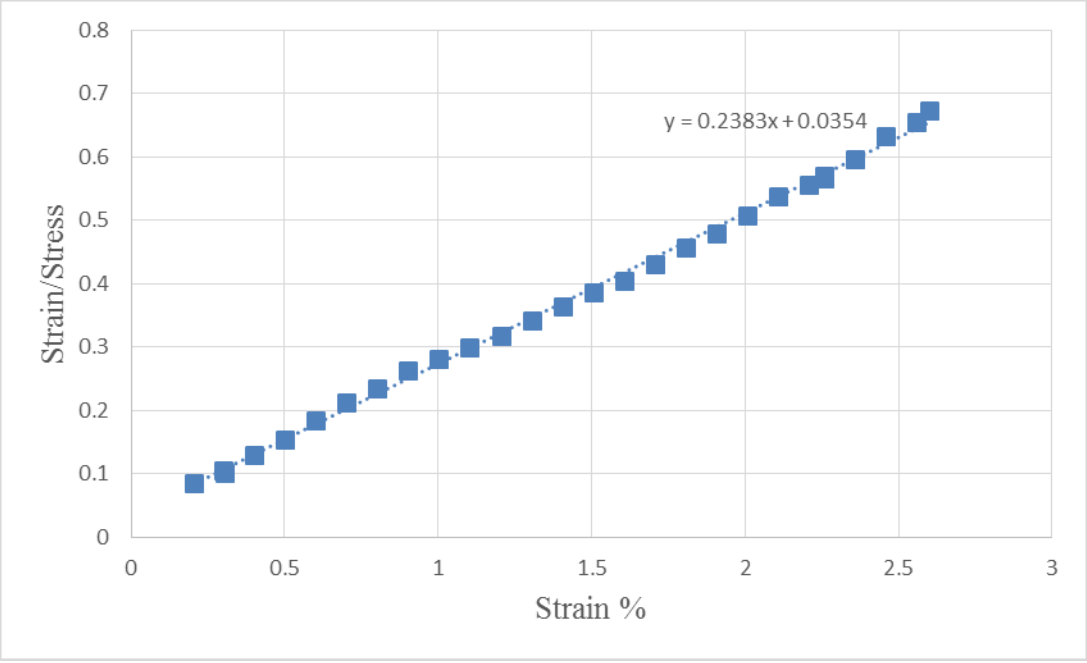

Figure 40 Strain/stress vs strain % sample at depth 22ft.

The unsaturated test results are shown in Figure 41. We can see that sample from 22ft shows the highest strength followed by samples from 12ft and 5 ft. Peak strains are observed after a strain of 5 %.

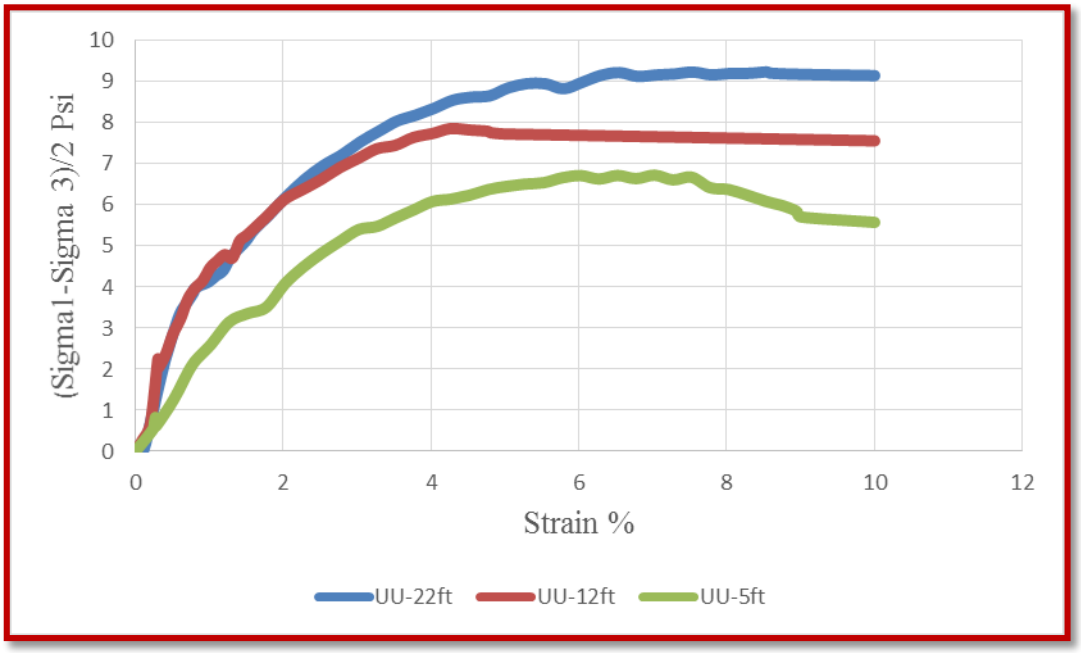

Figure 41 Unsaturated uu test strain vs total stress.

Attempt was done to fit strain/stress vs strain to fit the hyperbola. Figure 42, Figure 43, Figure 44 below show that it fits well.

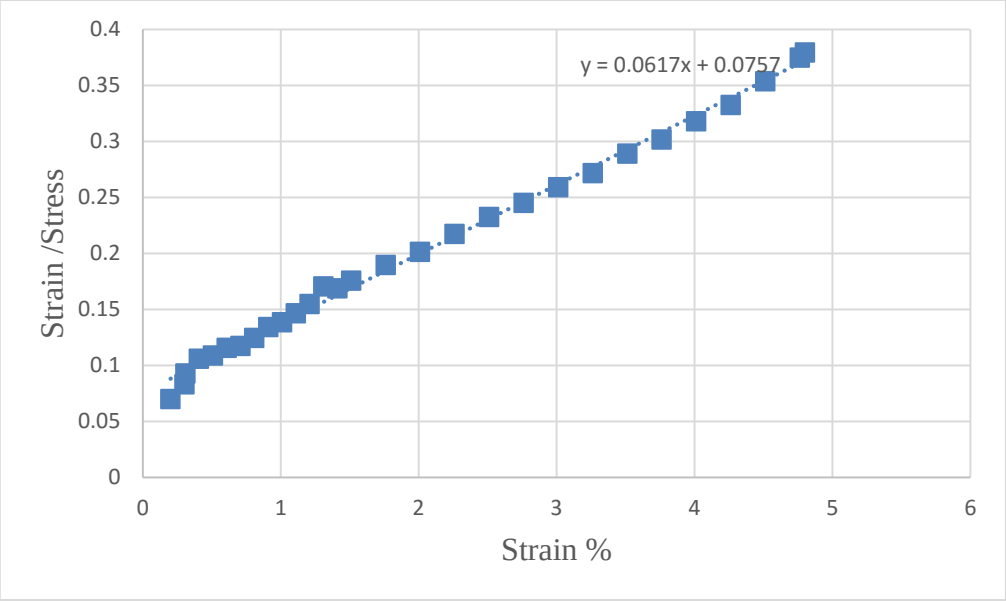

Figure 42 Strain/stress vs strain % sample at depth 4ft.

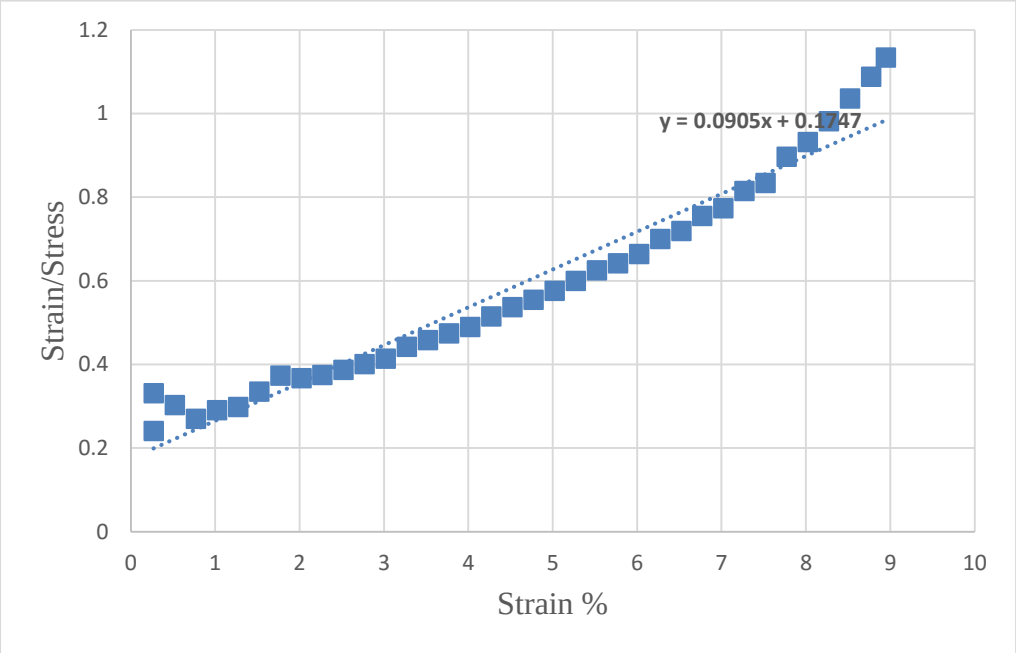

Figure 43 Strain/stress vs strain % sample at depth 12ft.

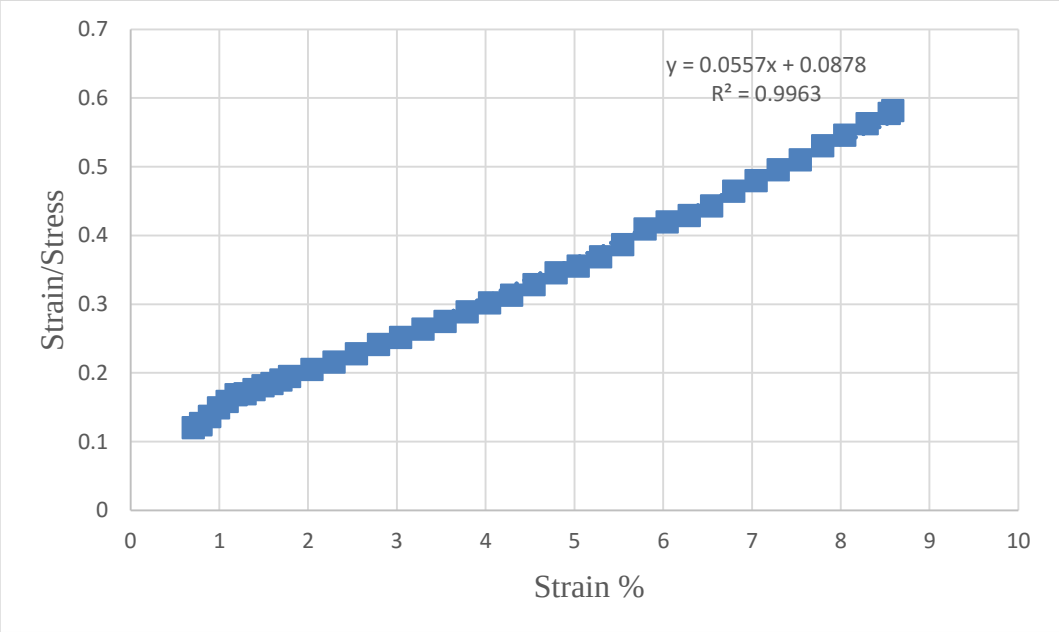

Figure 44 Strain/stress vs strain % sample at depth 22ft.

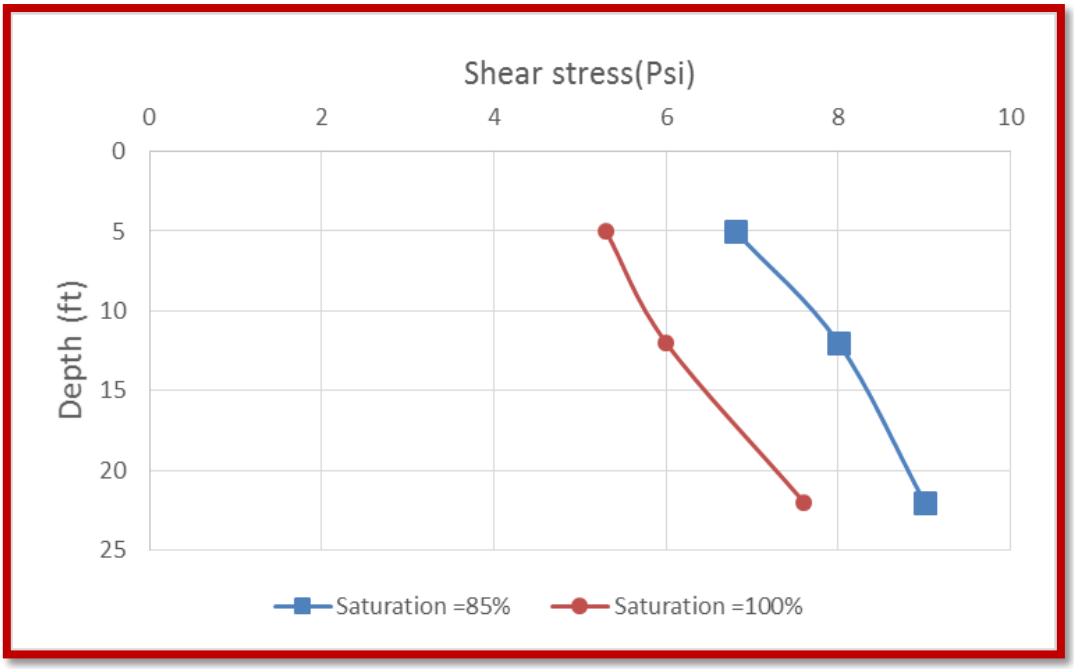

Figure 45 Shear Stress variation with depth.

The strength of the soil increases with depth. The soil at depth 22ft is more or less natural soil. The embankment depth is about 20-22ft. And as expected with less water content soil gains strength. The strength gain from saturated to unsaturated on an average is about 15%. The variation of strength is shown in Figure 45.

3.5 Consolidated undrained

Consolidated undrained tests are triaxial test in which drainage is allowed during consolidation phase and drainage valves are closed during shearing stage. The shearing rate is kept around 1% to develop pore pressure. After applying the confining pressure the sample is let to consolidate. The consolidation is continued for 10 days and the sample is considered consolidated when there is no more generation of pore pressure. Three tests are conducted with three different consolidation pressure. Figure 46 shows the effective stress plot for a confining pressure of 8 Psi. Figure 47 gives the effective deviatoric stress and confining stress for a confining stress of 12 Psi. Figure 48 gives effective deviatoric stress for confining stress of 16 Psi. The undrained strength parameters c and Φ are found by drawing the best fit line through the Mohr circle drawn from the tests. The values are shown in the Figure 49

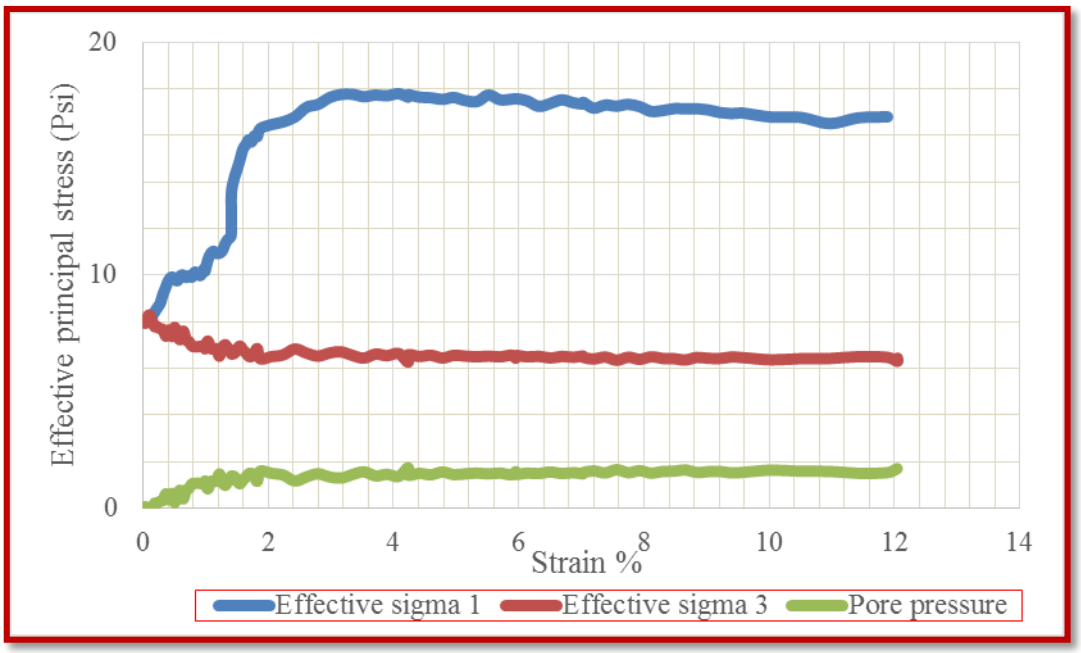

Figure 46 Consolidated undrained test with confining pressure 8 Psi.

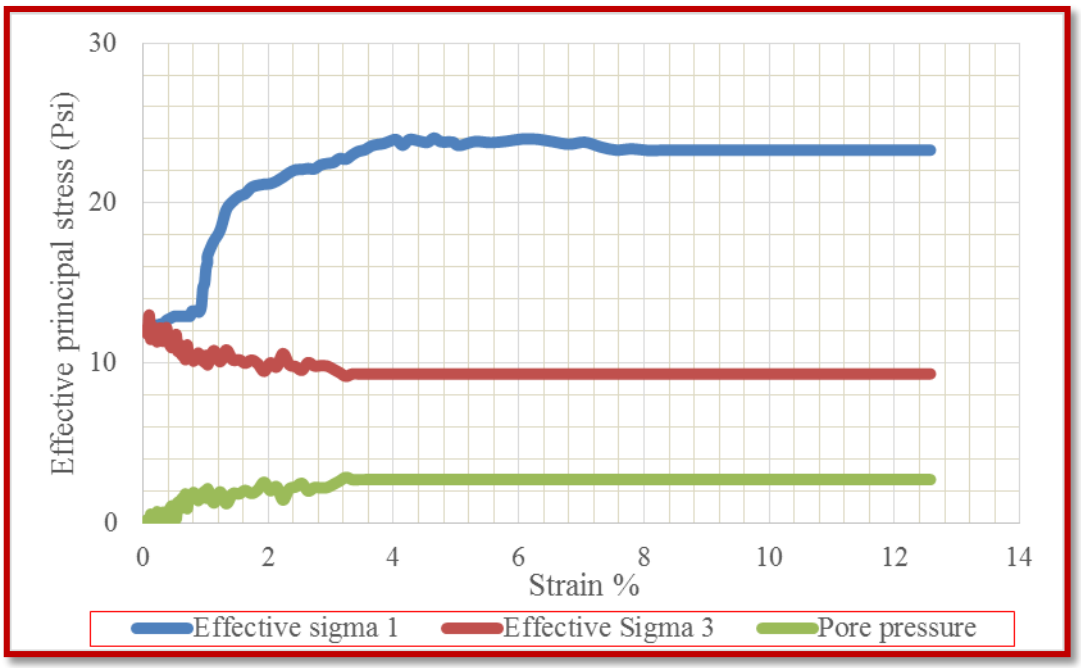

Figure 47 Consolidated undrained test with confining pressure 12 psi.

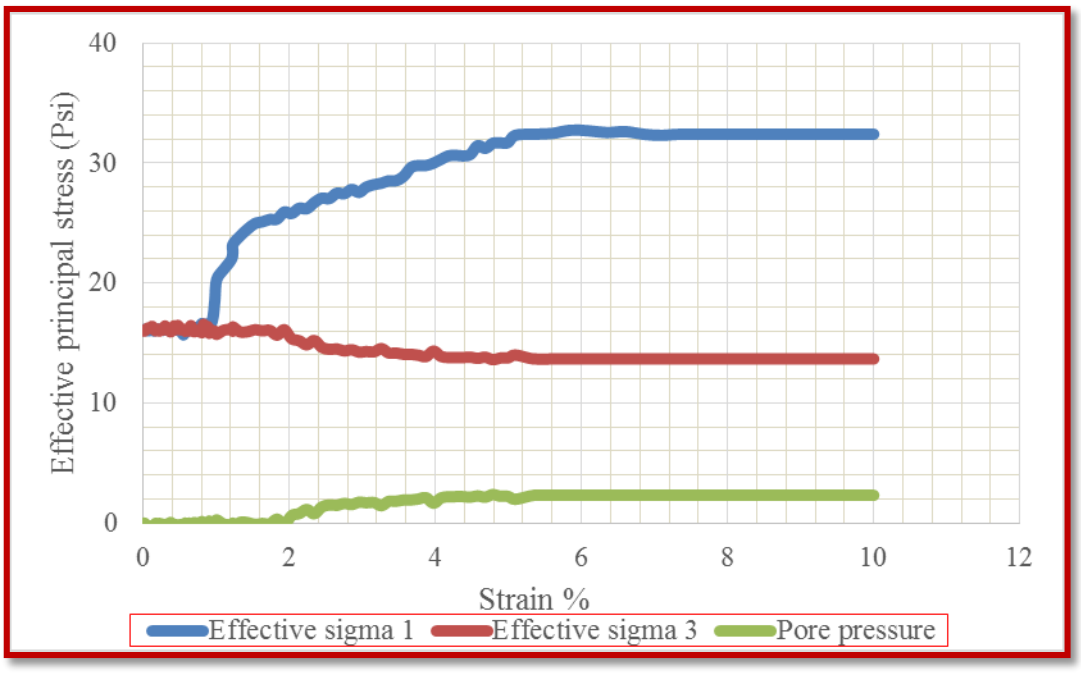

Figure 48 Consolidated undrained test with confining pressure 16 Psi.

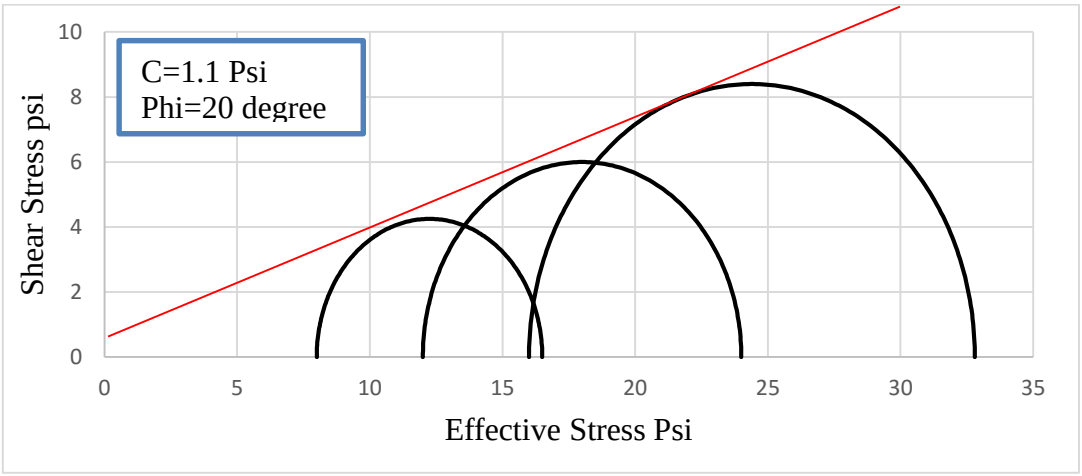

Figure 49 Mohr circle from consolidated undrained test.

The cohesion and friction angle obtained from the test were used in numerical modelling stage.

3.6 Consolidated drained

In consolidated undrained test the drainage valve is open during consolidation and is kept open during shearing. The shearing strain is kept very low to ensure there is no development of pore pressure. These tests were conducted on undisturbed soils collected from the site. Each test took more than three weeks to complete. The consolidation stage took about ten to fourteen days and the shearing took one week. The samples from depth 9ft (Figure 50) and 22ft (Figure 51) were subjected to drained tests.

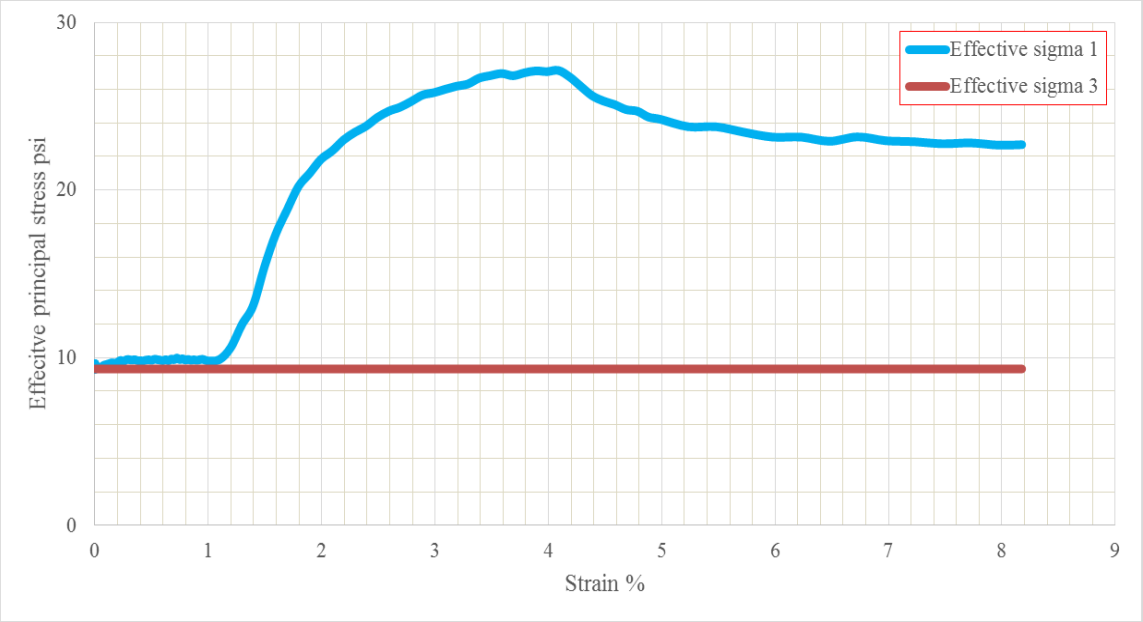

Figure 50 Consolidated drained test confining pressure 9 Psi.

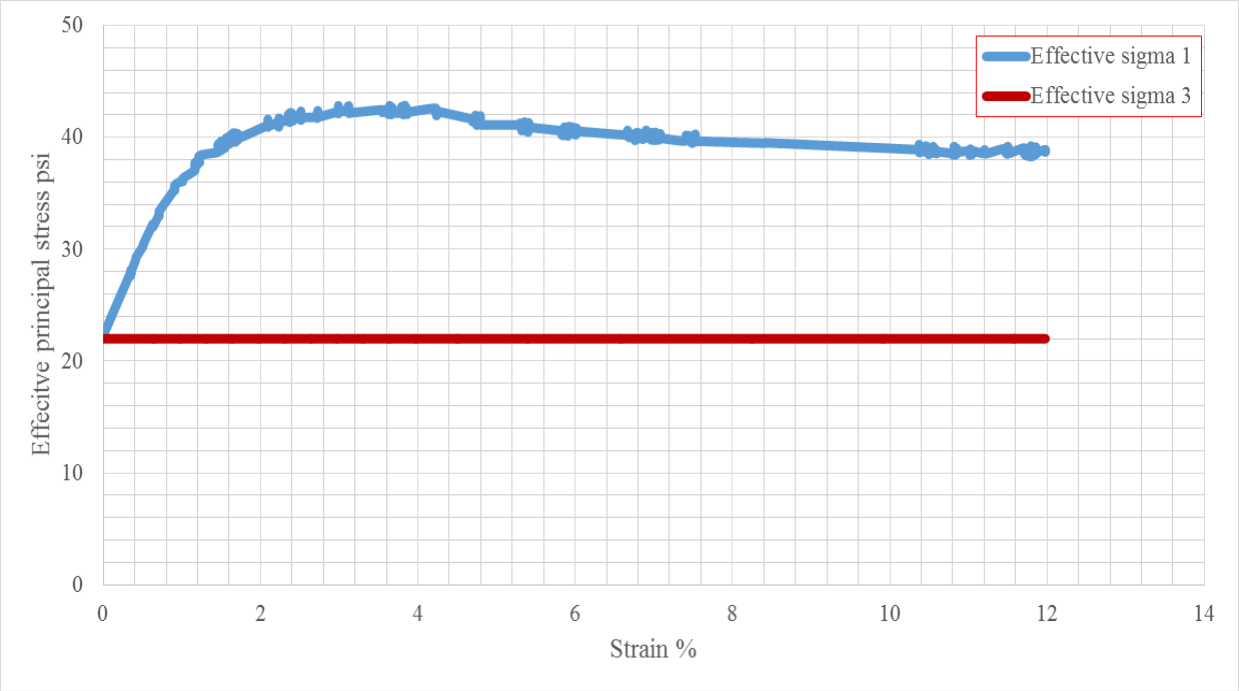

Figure 51 Consolidated drained test confining pressure 22 psi.

3.7 Unconsolidated undrained creep

UU creep tests are conducted to study the creep behavior of the soil. These tests are ideal because there is no drainage allowed and hence there will be no consolidation. The deformation will be due to creep only. Instead of letting the soil to fail in a undrained unconsolidated test, when the it reached a predefined load or stress it is held for a particular amount of time. After which the test is continued to another stress level and held for the same amount of time as before. This is continued till failure. Soil from three different depth were tested with two different saturation, fully saturated and 85% saturation. The loading protocol followed was to hold load at approximately 30% 50% and 90 % of peak load obtained from unconsolidated undrained tests. It is to be noted that the effect of

different holding loads may not be obvious because the increase in stress for each step is less than conventional 2.8 Psi. This is because the soil is soft clay with low shear strength. Unequal load increments is also justified on the basis that, once the basic creep behavior is deduced lower holding stress that is below 50% shows less creep.

3.7.1 Procedure

1. The sample preparation and setup is same as the unconsolidated undrained tests
2. The load is applied at constant strain to reach the first holding load. Then the procedure switches to stress controlled and the sample is let to creep.
3. After 24 hours or when the strain is constant the procedure switches to strain control and is loaded to next holding load.
4. This procedure is continued till failure.

3.7.2 Strain-time plots

Briaud and Garland (1985) proposed the rate effect model to predict the time-dependent behavior of soils. The mode can be expressed as follows:

$$\frac{s}{s_1} = \left(\frac{t}{t_1} \right)^n$$

Each test was monitored closely and if there is no more change at particular load the load was increased without waiting for 24 hours. Load time plots were obtained for each load. Following tests were conducted on remolded samples:

1. Sample from 4ft with full saturation
2. Sample from 12ft with full saturation
3. Sample from 22ft with full saturation

4. Sample from 4ft with 85% saturation
5. Sample from 12ft with 85% saturation
6. Sample from 22ft with 85% saturation

The loads in the test were selected on the basis of having at least one stress in the range of seating load, one in the working load and one below peak stress. In the log strain-log time curves, it can be seen that they all show similar trend for each test.

Difficulties were faced in holding the load at constant stress. Similarly the stress approximations from the unconsolidated undrained tests were not accurate. For example it was attempted to keep one load at range of 1.5-2 psi but for sample from depth at 22ft went up to 2.2 Psi. But still the aim was to have at least one stress in the three loading ranges. Bi (2015) had observed that the creep parameter was more or less the same for working load. The minimum increase in load to decrease the effect of previous holding load will be less than conventional tests because these soils have low strength and high plasticity.

Stress strain curve, increase of strain with time, log time vs log deformation plots of sample at depth 4ft with 85% saturation is shown in Figure 52, Figure 53 and Figure 54 respectively.

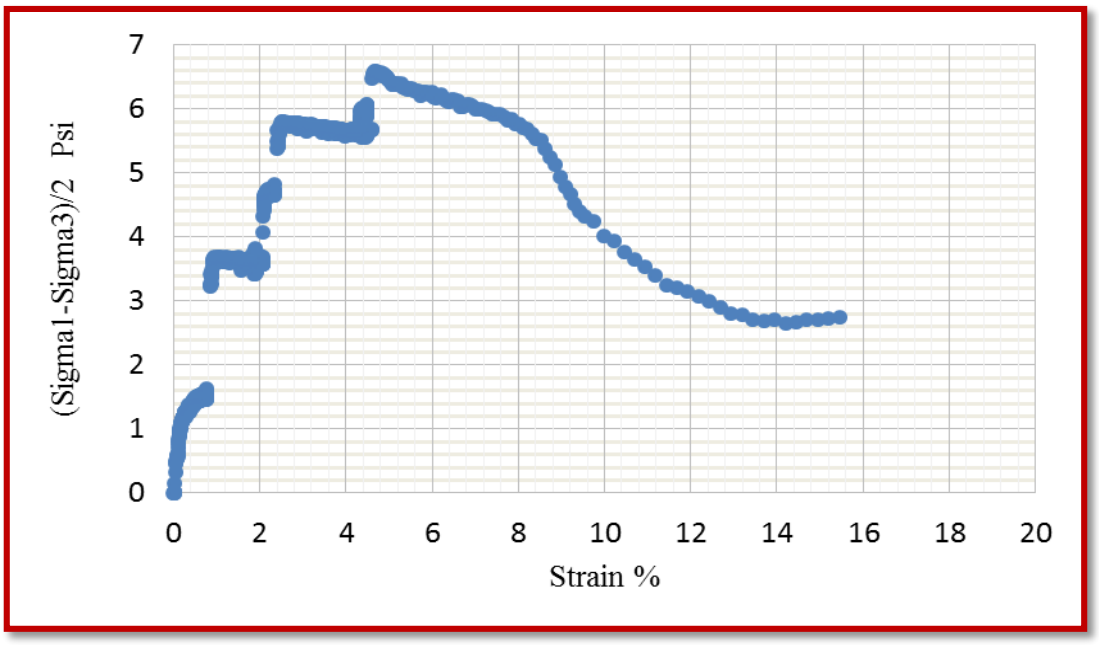

Figure 52 Total stress from triaxial uu creep test on the soil sample from the Beaumont project from a depth between 4ft.

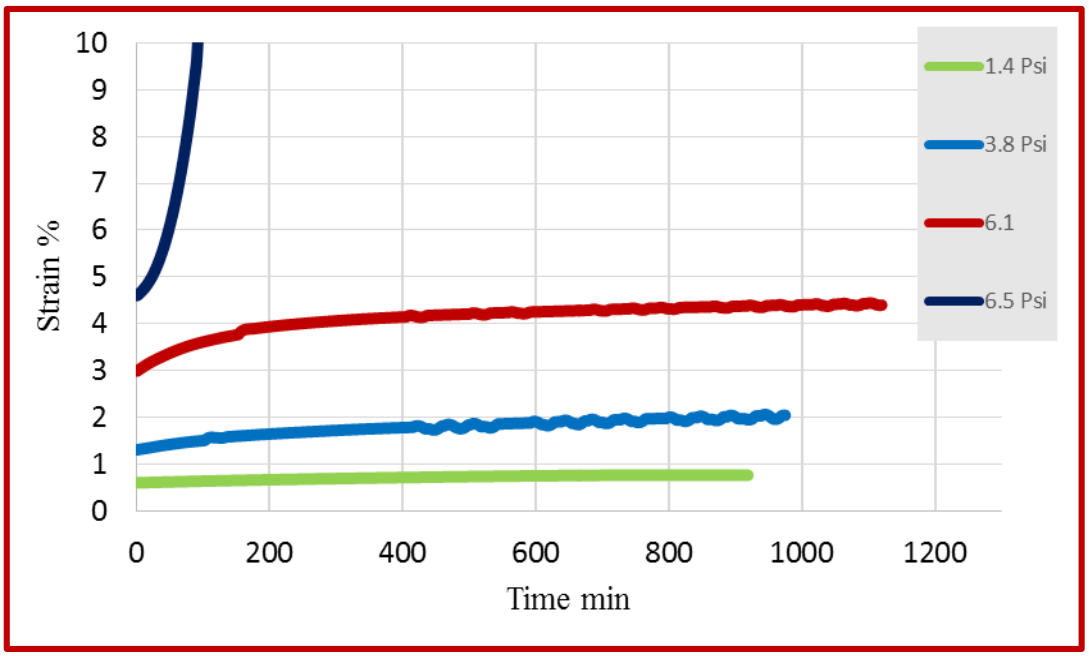

Figure 53 Strain-time curves from a triaxial uu creep test performed on the sample from Beaumont project at a depth between 4ft.

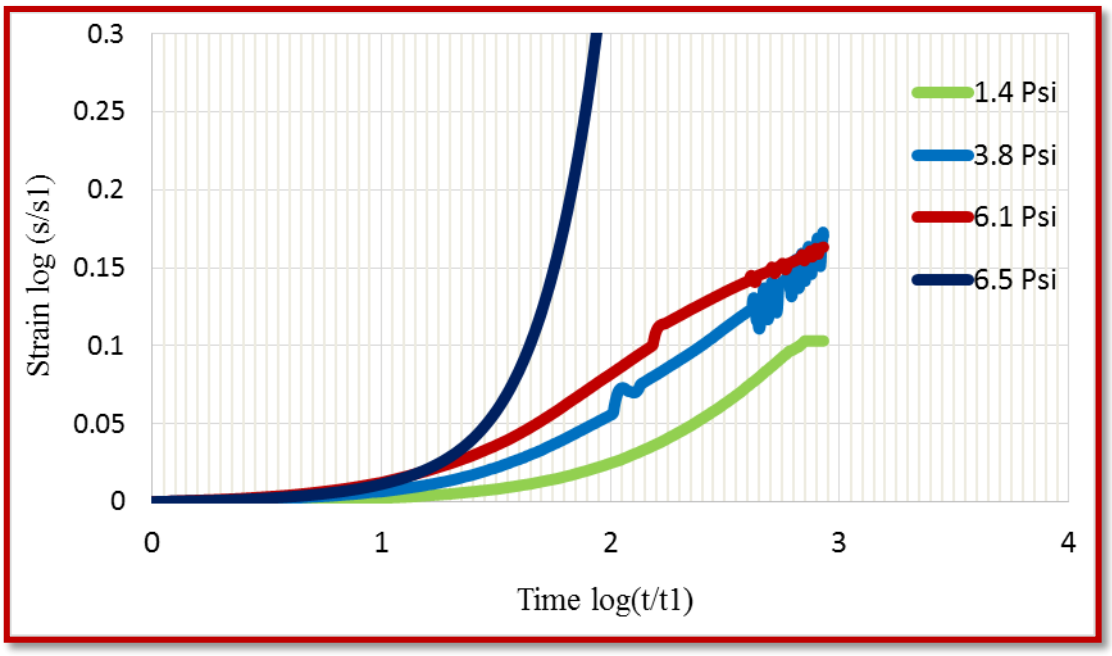

Figure 54 Strain–time curves for all the holding stress plotted in log-log scale on the soil samples from the Beaumont project from depth between 4ft.

Stress strain curve, increase of strain with time, log time vs log deformation plots of sample at depth 12ft with 85% saturation is shown in Figure 55, Figure 56 and Figure 57 respectively.

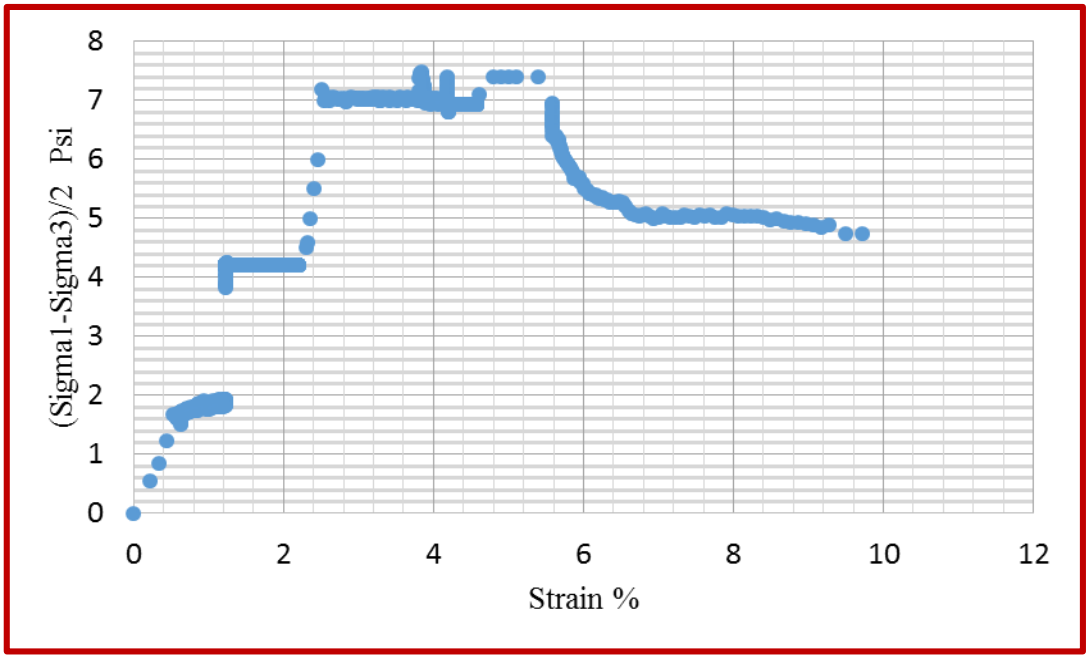

Figure 55 Total stress from triaxial uu creep test on the soil sample from the Beaumont project from a depth between 12ft.

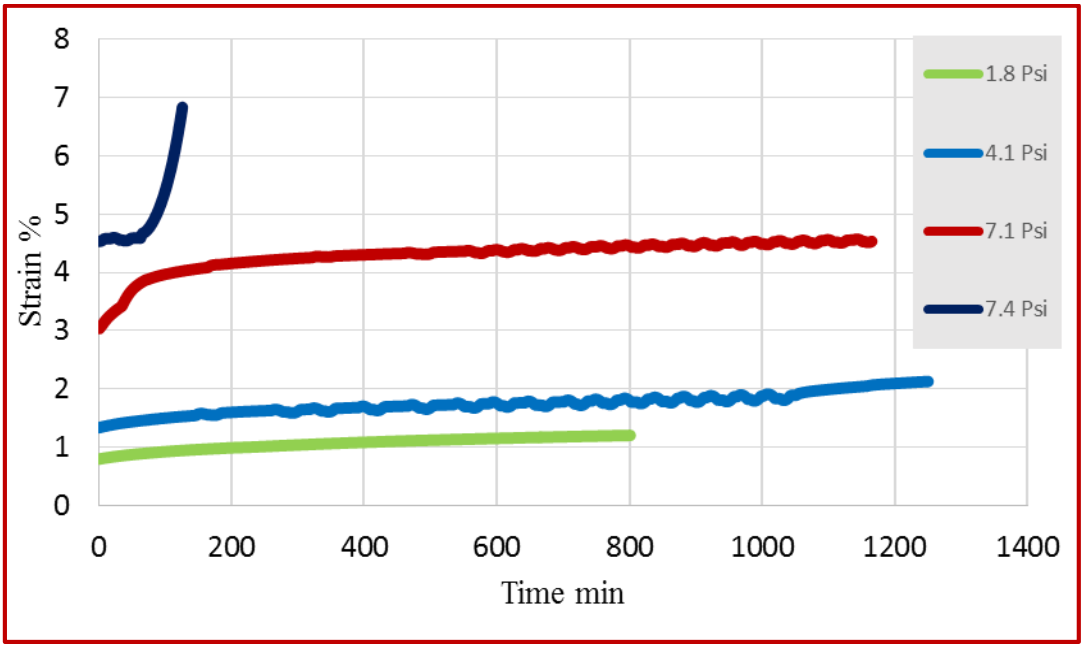

Figure 56 Strain-time curves from a triaxial uu creep test performed on the sample from Beaumont project at a depth between 12ft.

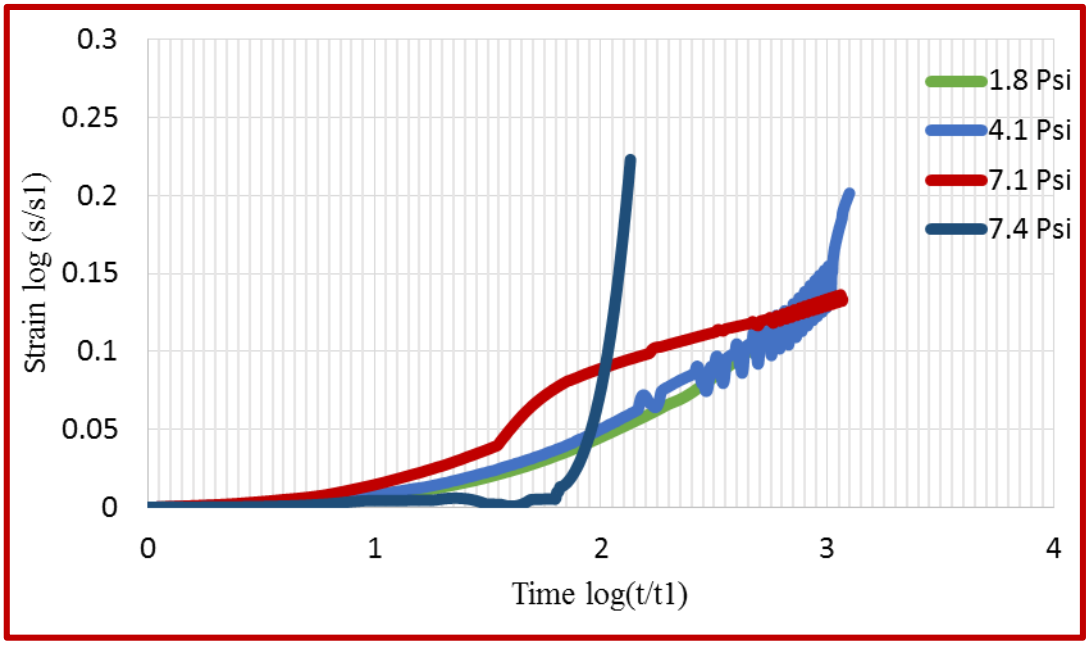

Figure 57 Strain–time curves for all the holding stress plotted in log-log scale on the soil.

Stress strain curve, increase of strain with time, log time vs log deformation plots of sample at depth 22ft with 85% saturation is shown in Figure 58, Figure 59 and Figure 60 respectively.

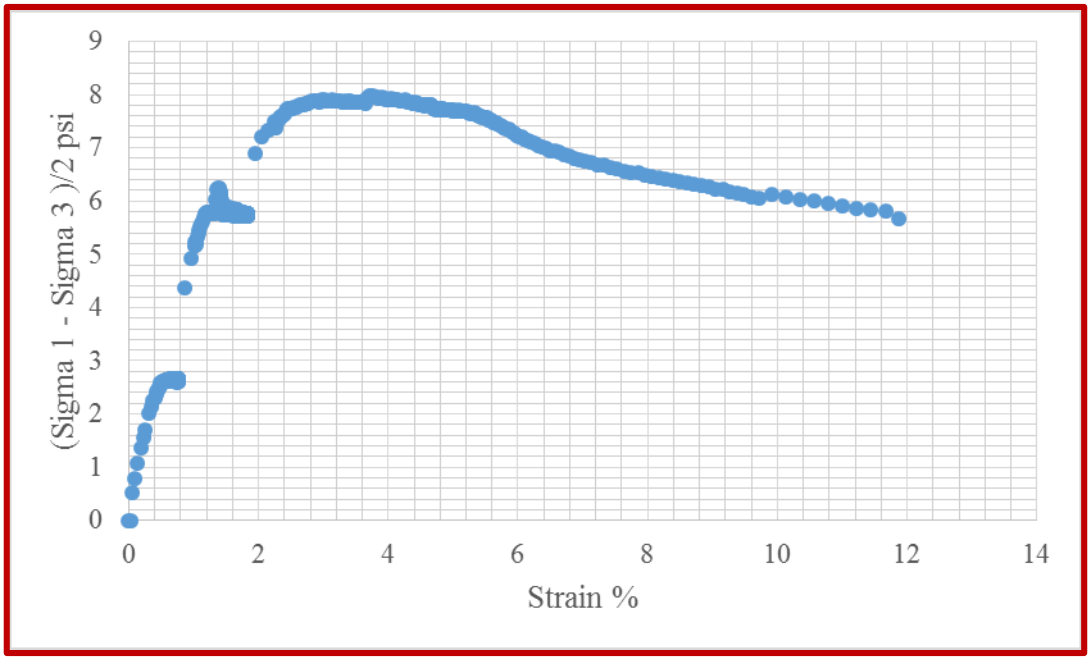

Figure 58 Total stress from triaxial uu creep test on the soil sample from the Beaumont project from a depth between 22 ft.

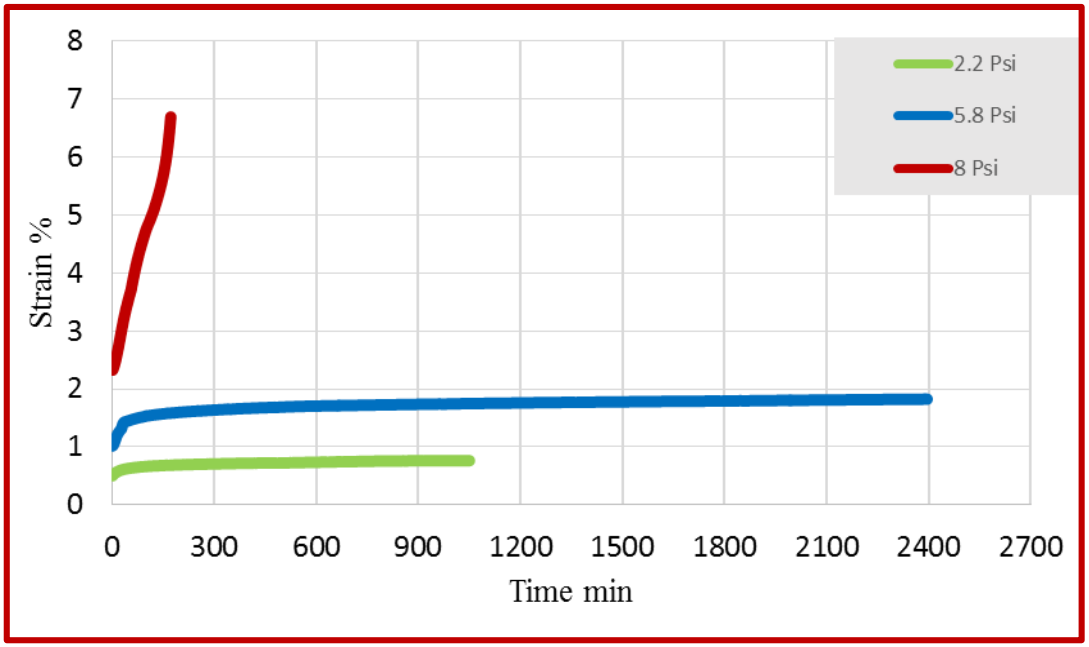

Figure 59 Strain-time curves from a triaxial uu creep test performed on the sample from Beaumont project at a depth between 22 ft.

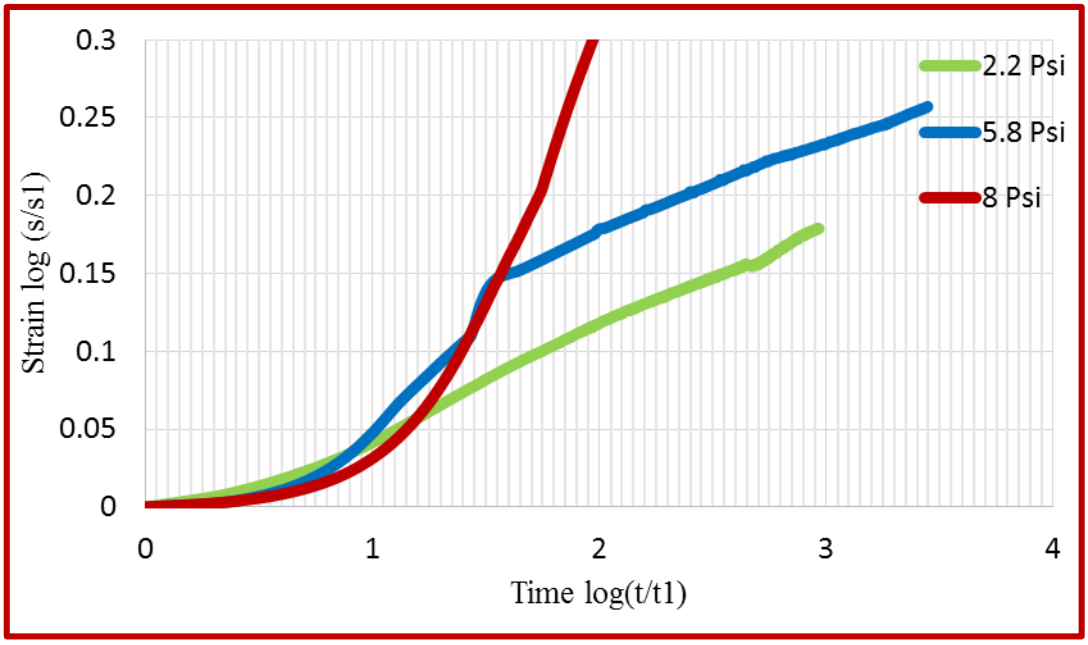

Figure 60 Strain–time curves for all the holding stress plotted in log-log scale on the soil samples from the Beaumont project from depth between 22 ft.

Stress strain curve, increase of strain with time, log time vs log deformation plots of sample at depth 4ft with full saturation is shown in Figure 61, Figure 62 and Figure 63 respectively.

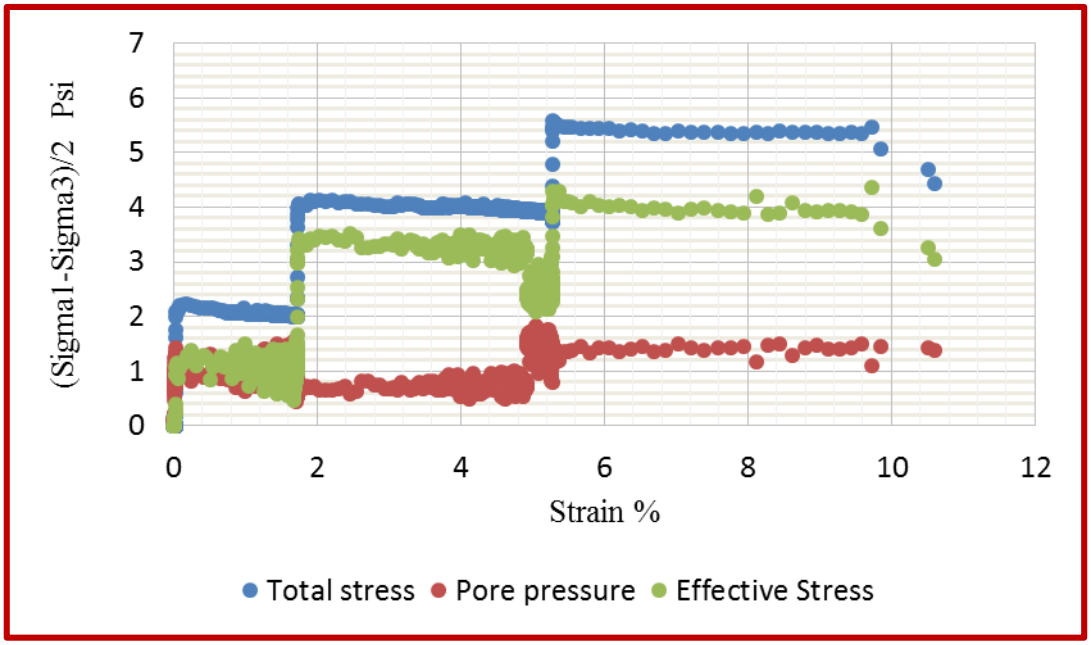

Figure 61 Total stress, effective stress, and pore-water pressure from triaxial UU creep test on the soil sample from the Beaumont project from a depth between 4ft.

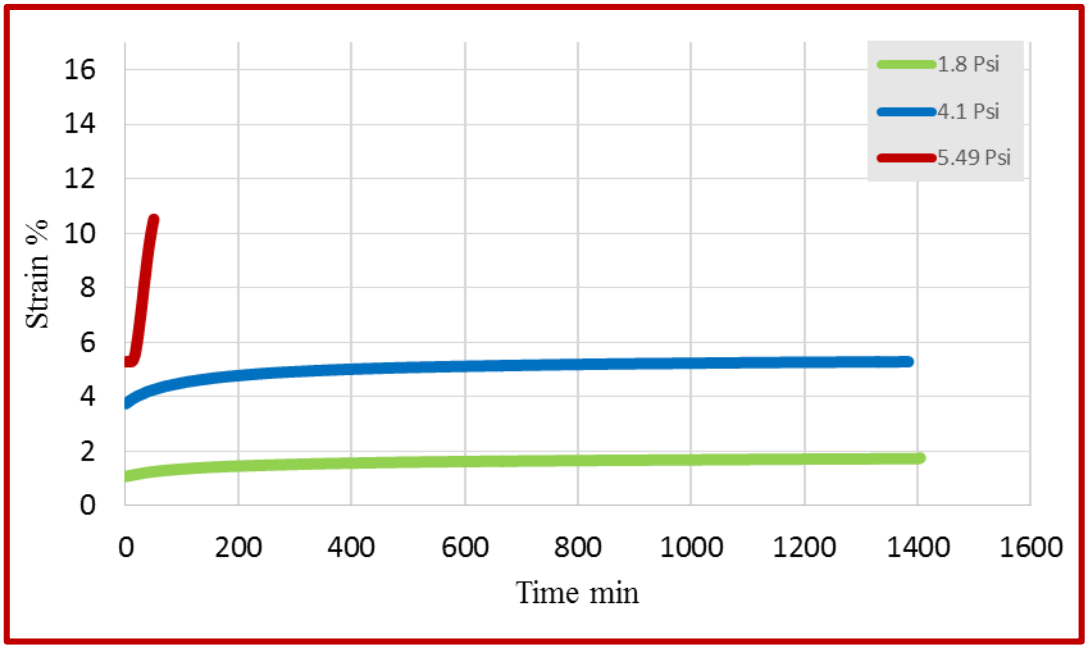

Figure 62 Strain-time curves from a triaxial UU creep test performed on the sample from Beaumont project at a depth between 4 ft.

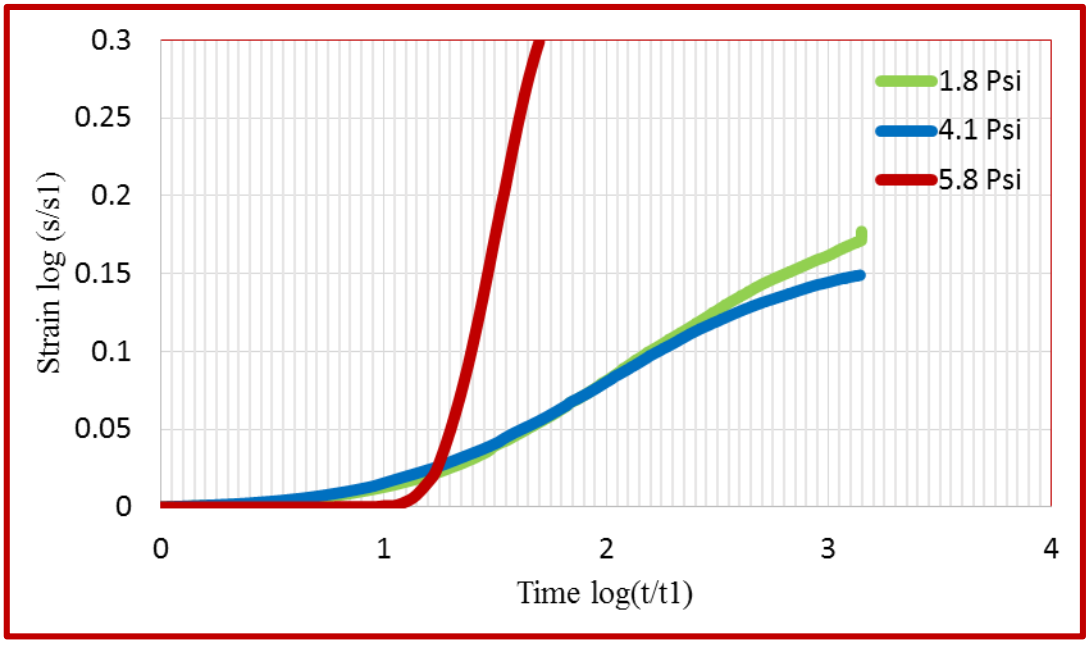

Figure 63 Strain–time curves for all the holding stress plotted in log-log scale on the soil samples from the Beaumont project from depth between 4 ft.

Stress strain curve, increase of strain with time, log time vs log deformation plots of sample at depth 12ft with full saturation is shown in Figure 64, Figure 65 and Figure 66 respectively.

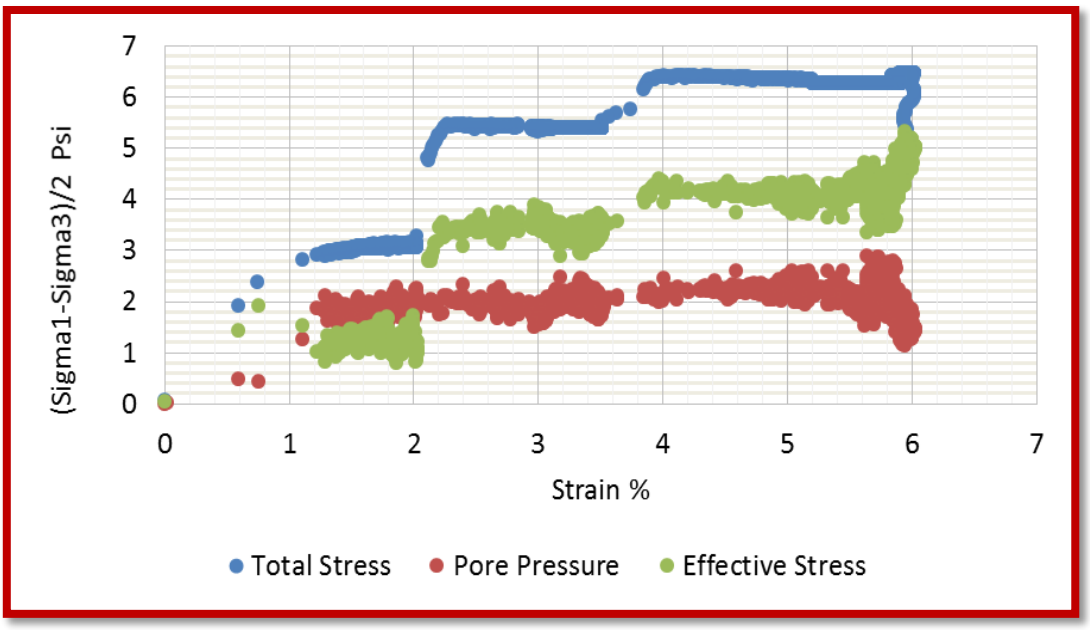

Figure 64 Total stress, effective stress, and pore-water pressure from triaxial uu creep test on the soil sample from the Beaumont project from a depth between 12 ft.

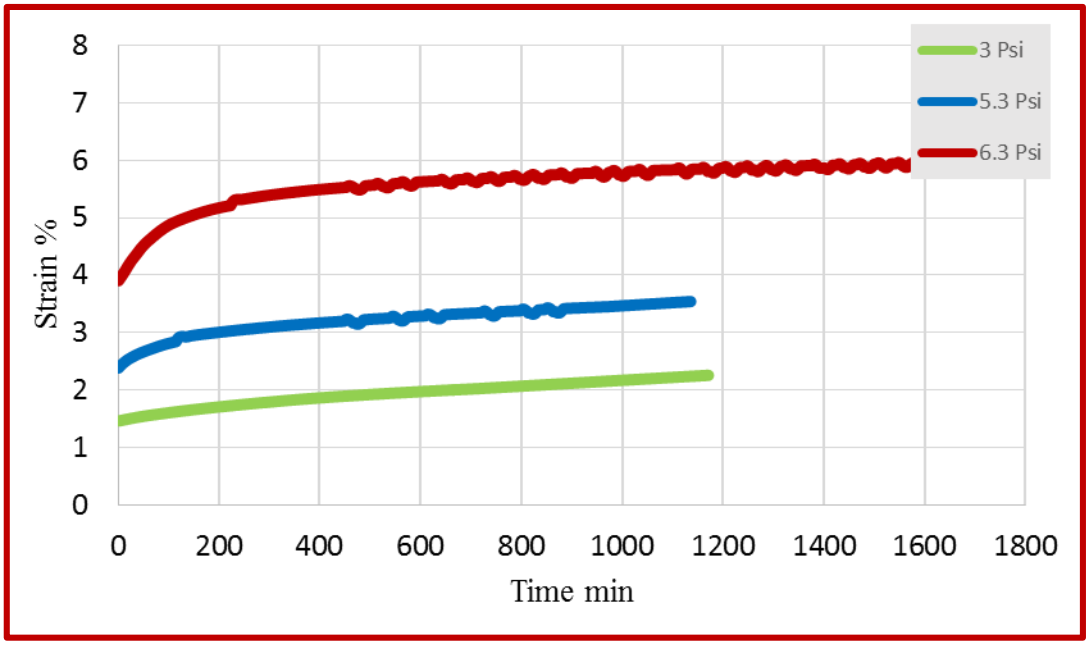

Figure 65 Strain-time curves from a triaxial uu creep test performed on the sample from Beaumont project at a depth between 12 ft.

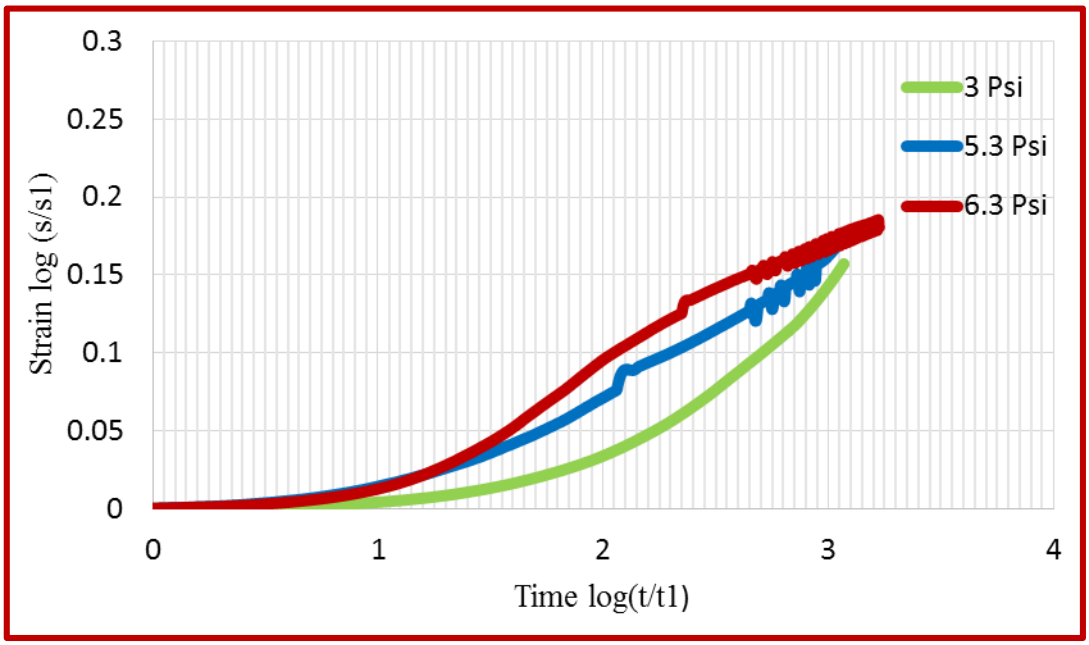

Figure 66 Strain–time curves for all the holding stress plotted in log-log scale on the soil samples from the Beaumont project from depth between 12 ft.

Stress strain curve, increase of strain with time, log time vs log deformation plots of sample at depth 22ft with full saturation is shown in Figure 67, Figure 68 and Figure 69 respectively.

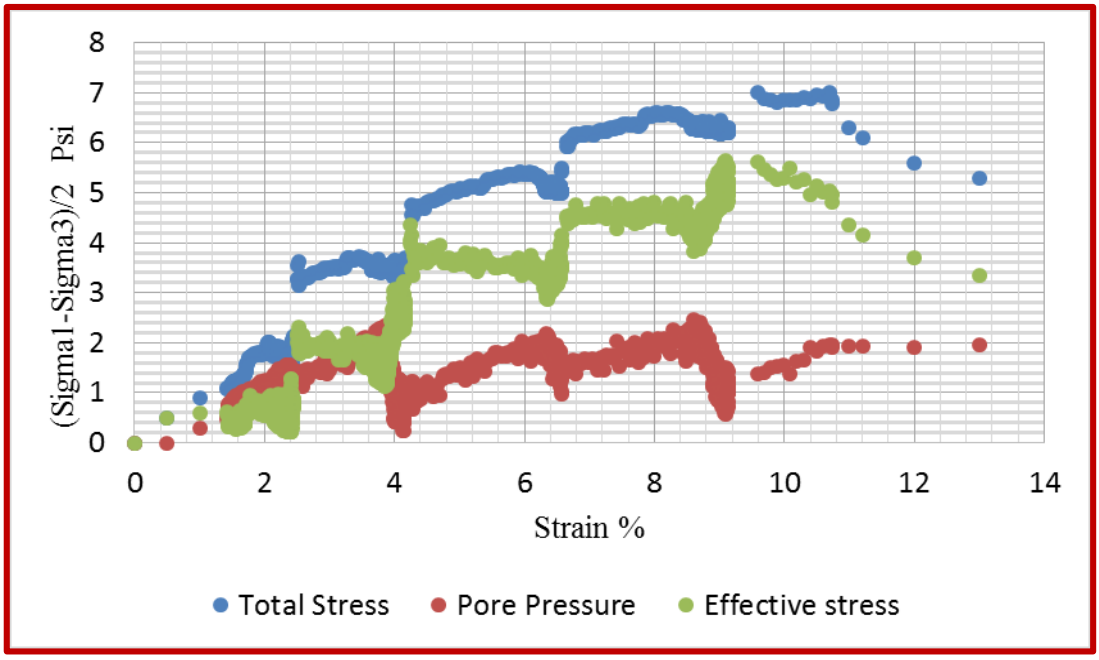

Figure 67 Total stress, effective stress, and pore-water pressure from triaxial uu creep test on the soil sample from the Beaumont project from a depth between 22ft.

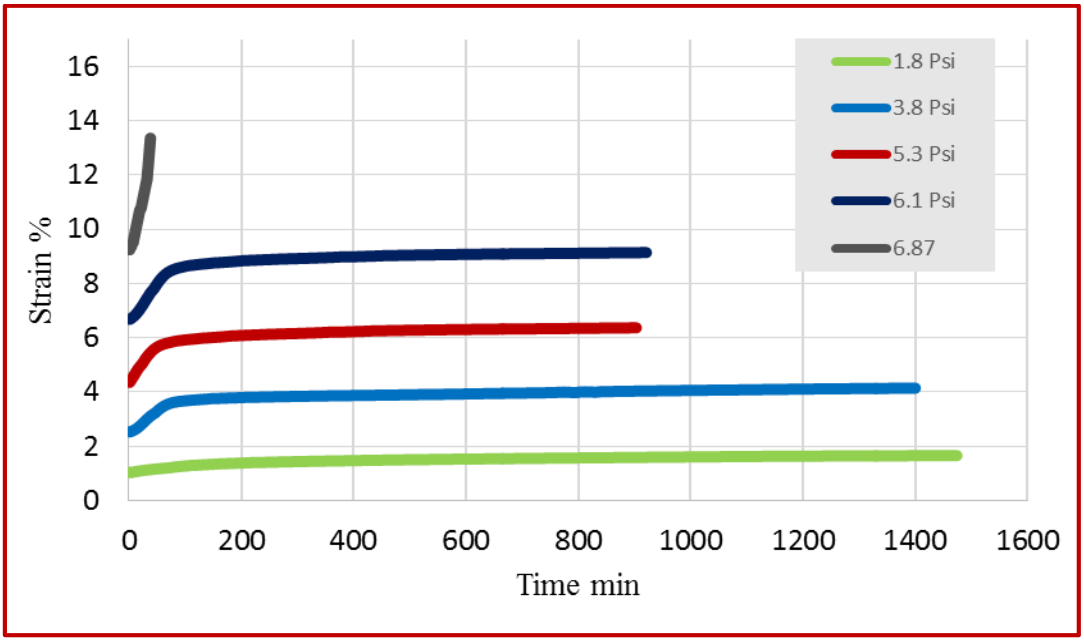

Figure 68 Strain-time curves from a triaxial uu creep test performed on the sample from Beaumont project at a depth between 22ft.

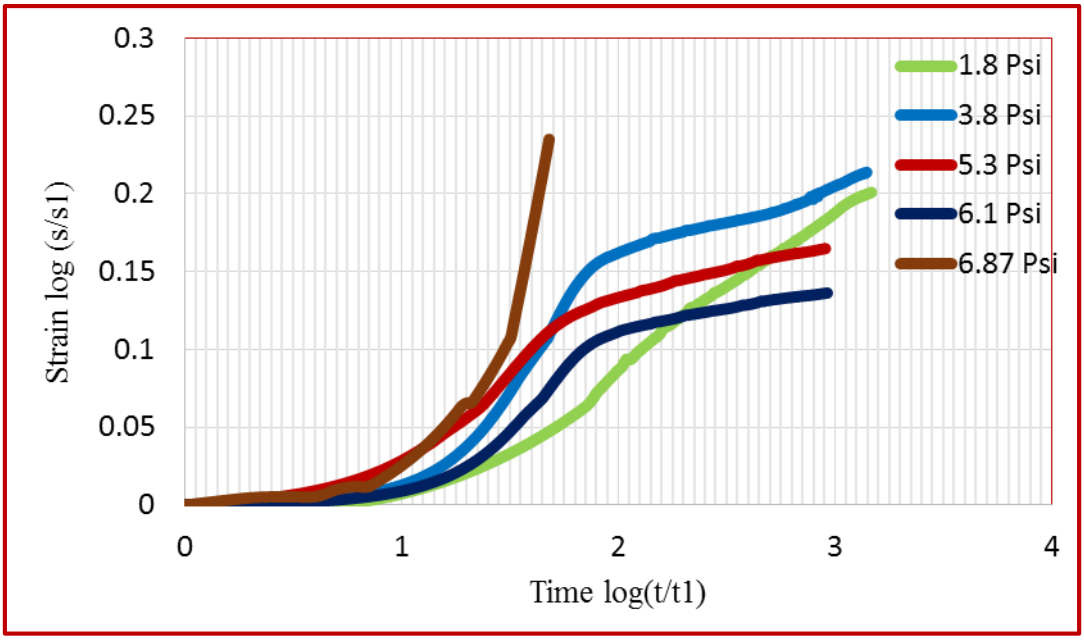

Figure 69 Strain–time curves for all the holding stress plotted in log-log scale on the soil samples from the Beaumont project from depth between 22 ft.

The range of n values calculated based on the equation given by Briaud and Garland (1985) was found to be between .05-0.1. The n value calculated on basis of equation n=.035 +.00066PI was around .079. All the 'n' values obtained from experiments are in this range. The soil from depth 23ft had the lowest 'n' values and high viscosity while the soil from 4ft depth had highest 'n' value and lowest viscosity. The n value for saturated test are shown in Figure 70 and that for unsaturated are shown in Figure 71.

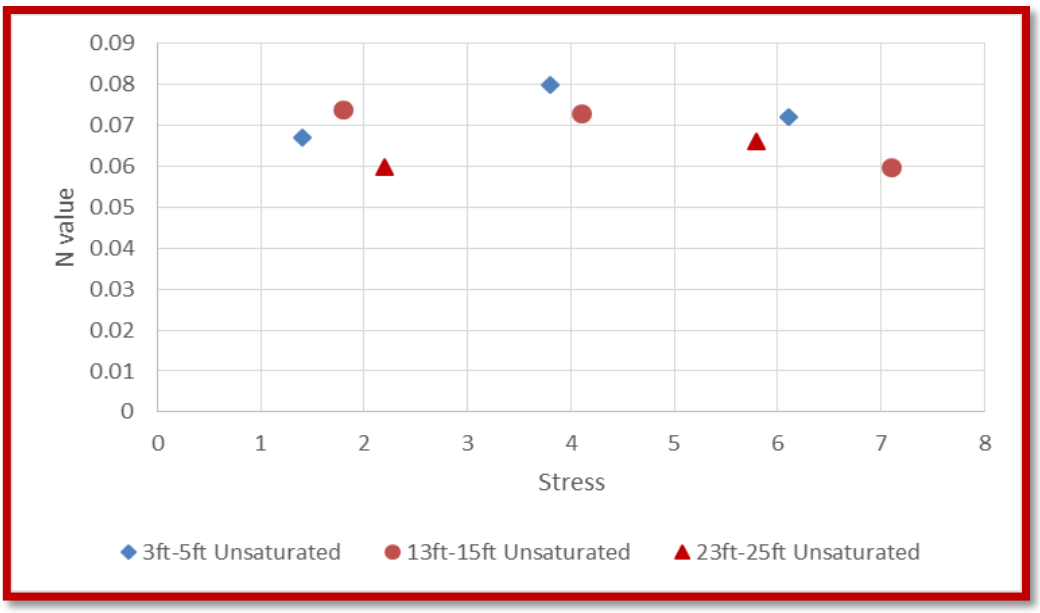

Figure 70 n values obtained from unsaturated tests.

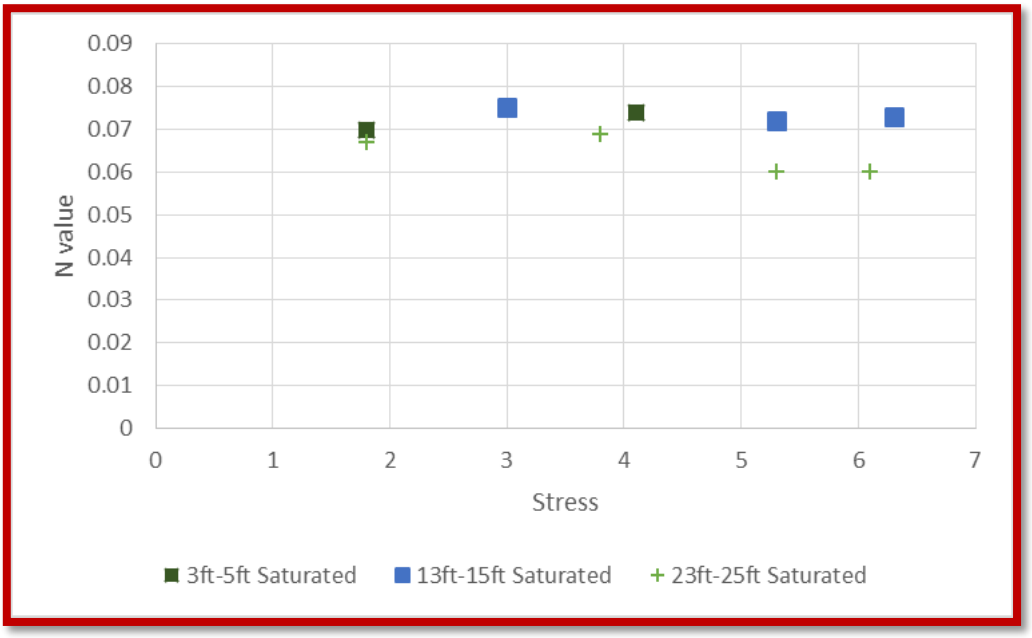

Figure 71 n values obtained from various saturated tests.

CHAPTER IV

NUMERICAL MODELLING

4.1 Introduction

Numerical modeling was an integral part of this thesis. Modelling of soil nail wall constructed at an emergency slope repair in Beaumont is discussed in this section. The wall was monitored during construction. The monitoring of the wall was continued for a year after construction. The wall horizontal deflection, and the strains in the nail was subject to monitoring. Inclinometers were installed at two sections from which the horizontal displacements could be calculated and strains in each row of nails were monitored using strain gauges which could be used to obtain the stress in the nails.

4.2 Finite element software

From literature review it was found that Snailz and Goldnail were some of the limit equilibrium software's used for limit equilibrium analysis. Other methods on same concept like Anthoine (1990) Bridle (1990) differed in the way the failure surface was calculated and its shape.

Akhavan et al (2011) found that the numerical modelling using Hardening soil model in Plaxis gave a very good accordance between the horizontal displacement and the deformation obtained from modelling. Here modelling was done for a depth of 28 meters. Studies by Liew and Khoo (2006) using Plaxis also revealed some information about the dependency of the behavior of the soil mass behind the wall on slope mass movements. Other noticeable studies using Plaxis were by Singh and Babu (2010) and Fan and Luo

(2008), from which it can be inferred that Plaxis can be used for the modelling construction phase of the soil nail wall.

Flac 3D is another prominent software based on finite difference. Lima et al (2003) studied the influence of slope and construction procedure on the stress-strain behavior of the wall. He considered Elastic –perfectly plastic model and also inferred that the slope geometry has an influence on the soil nail length. Briaud and Lim (1997) modelled the complete sequence of excavation and placement of nails. It was validated against an instrumented case history. The results from this study were used to suggest design guidelines.

Zhou et al (2013) used ABAQUS to model 3D soil nail wall and observed that the stability increases if soil nails are present in case of surcharge loading. They also concluded from modelling and field observation that the maximum nail force is mobilized at the middle of the height which will correspond to depth of potential sliding plane. Y.D. Zhou et al (2009) also used ABAQUS to back analyses and study the effect of soil nails in loose fills, like internal deformation, water content redistribution etc, with surcharge loading.

In this study undrained modelling of soil nail wall was modelled. The results from drained modelling done by Kharanaghi (2015) were compared. Failure at section 2+00 was to be modelled, so Flac 3D being finite difference software will serve this purpose and was adopted for this study.

4.2.1 Soil model

The common soil models used were Mohr-Coulomb and hardening soil model, Akhavan et al (2011), Singh and Babu (2010) etc. In the present study one of the important aspect is to characterize of the creep in soils. So it is important to select a model which will give a very good prediction of creep in soils. The common soil models mentioned above are not used for modelling creep. Plaxis provides soft soil creep model. The drawback with this model is that it has not yet been completely verified to use in excavation problems, Sivasithamparam et al (2013). Other soft soil models commonly used are anisotropic creep model and non-associated creep model for structured anisotropic clay Gustafsson and Tian (2011). FLAC-3D provides 8 models for study of creep. These models include the Maxwell model (as explained in background), power law models and the Burgers model in addition to others. From the information studied above it was decided to use FLAC-3D to model construction and creep stages of the soil nail wall.

Mohr-Coulomb was adopted for modelling construction stage of the retaining wall. The parameters required for modelling were obtained from laboratory experiments. Undrained modelling was simulated for the construction stage. This was adopted because during construction sufficient time is not available for the pore pressure to dissipate. In excavation situations long term stability should be considered as drained conditions.

To model creep Burger model in FLAC 3D was adopted. Burger model is a combination of Kelvin and Maxwell's model. It is thus a viscoelastic model proposed by

Singh and Mitchell (1968). These models are placed in series in a Burger Model. The dashpot represents deformation in the Burger model. Unlike in Maxwell's model the strain rate is not constant for constant shearing. Elastic deformations occur initially after the shearing load is applied after which the strain rate decreases and becomes constant. Unconsolidated creep tests were simulated by Segalini et al (2009) and results showed good conformation with the laboratory test for the soil obtained to study the creep induced landslides in Italy. Figure 72 shows stages of creep simulated by Segalini et al (2009).

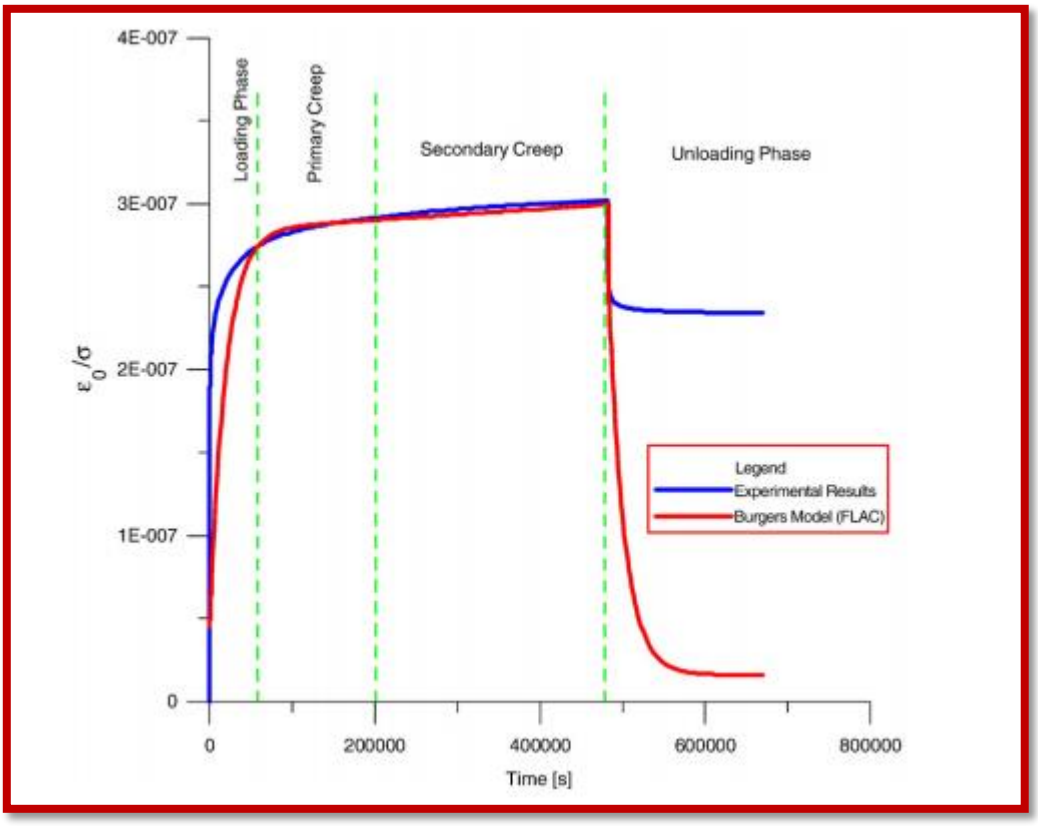

Figure 72 Comparison of creep test modelled using Burger model and experimental results, Segalini et al (2009).

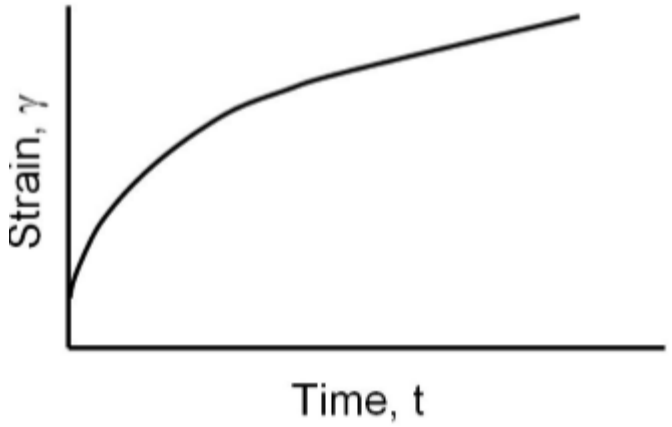

Figure 73 Creep deformation in Burger model.

From creep tests it is clear that the strain vs time behavior of soil is not linear. Maxwell's model, Kelvins model etc are simplistic representation of the creep behavior. As can be seen from Figure 72, Segalini was able to model creep tests using Burger model. Burger model as can be seen from Figure 73 gives strain vs time plots similar to observed from experimental strain vs time curves obtained dint his study. Hence it is proposed in this study to model creep behavior using Burger model.

4.3 Beaumont wall

Kharanaghi (2015) calibrated the creep parameter models using the unconsolidated undrained creep tests conducted in the laboratory for the soil from Beaumont field site. He was able to reproduce the tests efficiently. The variation of Burger creep parameters with respect to 'n' value was given by Kharanaghi (2015). These parameters were used for the modelling creep behavior of the retaining wall. Since the soil is classified as showing high plasticity, to determine long term movement of the wall a null cohesion and residual friction angle is used Tavenas and Leroueil (1981). Cable elements can be used to simulate

the support provided by materials like soil nails in embankments Itasca (2009). CableSEL cable elements are elastic, perfectly plastic material. Since bending is relatively small in soil nails are neglected in this study. In this study cables are considered as grouted so that tension force develops along the length in response to small displacement e between cable and grid. It has two nodes and one translational degree of freedoms per node. The cable soil interface is idealized as spring-slider system and it is cohesive and frictional, Itasca (2009). Cables are pretension using SEL cable pretension command. Figure 74 shows the idealization of grouter cable system. As mentioned before Mohr-Columb was used to model the construction stages of the wall. The cohesion and internal friction obtained from laboratory test was used as strength parameters in the model. Young's modulus and poisons ratio corresponding to undrained shear strength were chosen from Briaud (2013). Grout properties were found by Kharanaghi (2015) by simulating the pullout test in the filed using FLAC 3D. Summary of parameters used in this study are given in the Table 8.

Material	Constitutive model	Properties
Embankment soil	Mohr-Coulomb	ϕ'=20, c'=0, γ =125 pcf, E=2.9e5 psf. , υ=0.3
Soil nails (cable element)	Elastic-perfectly plastic	E steel=4.17e9 psf (200 GPa), c_grout=1e3 psf , ϕ_grout=20 degree
Shotcrete (shell element)	Elastic (isotropic)	E shot = 2.2e8 psf, υ=0.25, thickness=4 in.

Table 8 Parameters used in Flac-3D modelling construction of the Beaumont wall

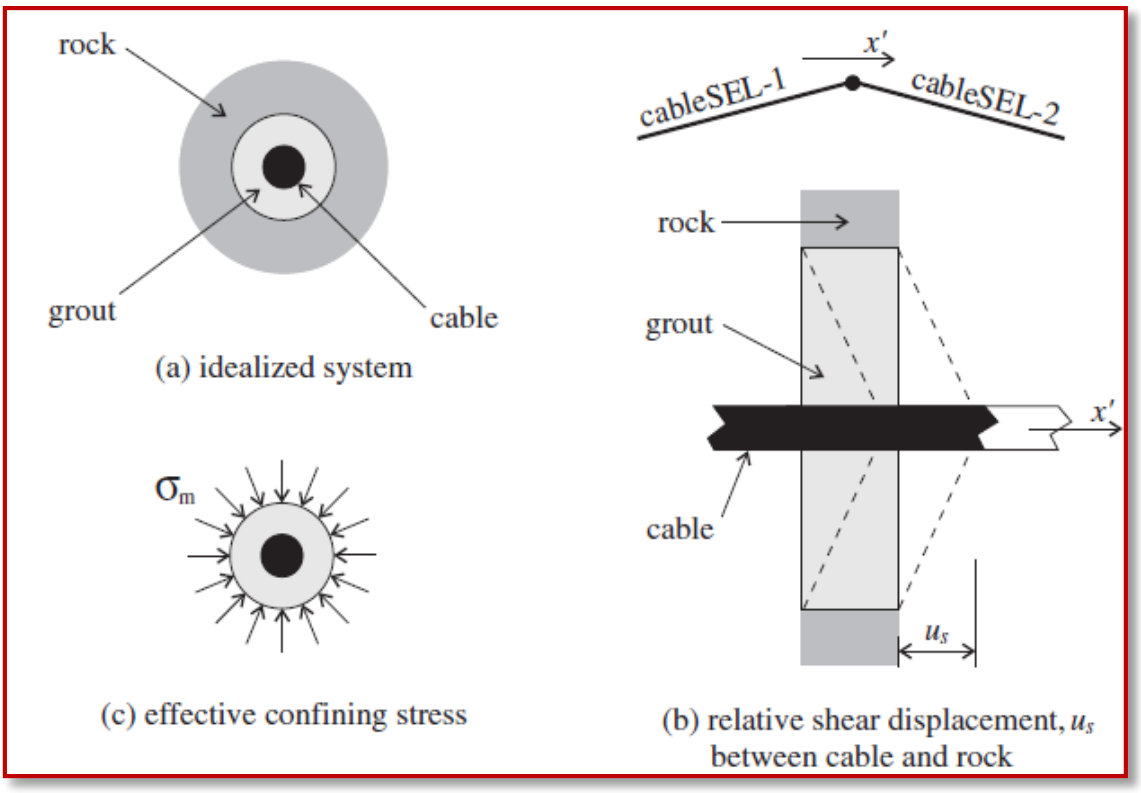

Figure 74 Grouted cable system, Itasca (2009).

4.4 Section 2+00

During construction the retaining wall failed due to over excavation. This happened at the second stage of excavation. Local failure at depth of 12 ft was observed. The construction was continued after inserting pretension bars. At the first stage an excavation of 3.6 ft was done. Soil nails were installed after grouting. Limit equilibrium analysis using UTEXAS software is done to check the factor of safety at this stage of construction. The expected factor of safety was less than one, which will imply that there is more unbalanced force than resisting force. Cohesion of 3kpa and internal frictional

angle of 19.8 degrees were used for this analysis. To represent soil nails reinforcement option in the software was used. The result is shown in Figure 75.

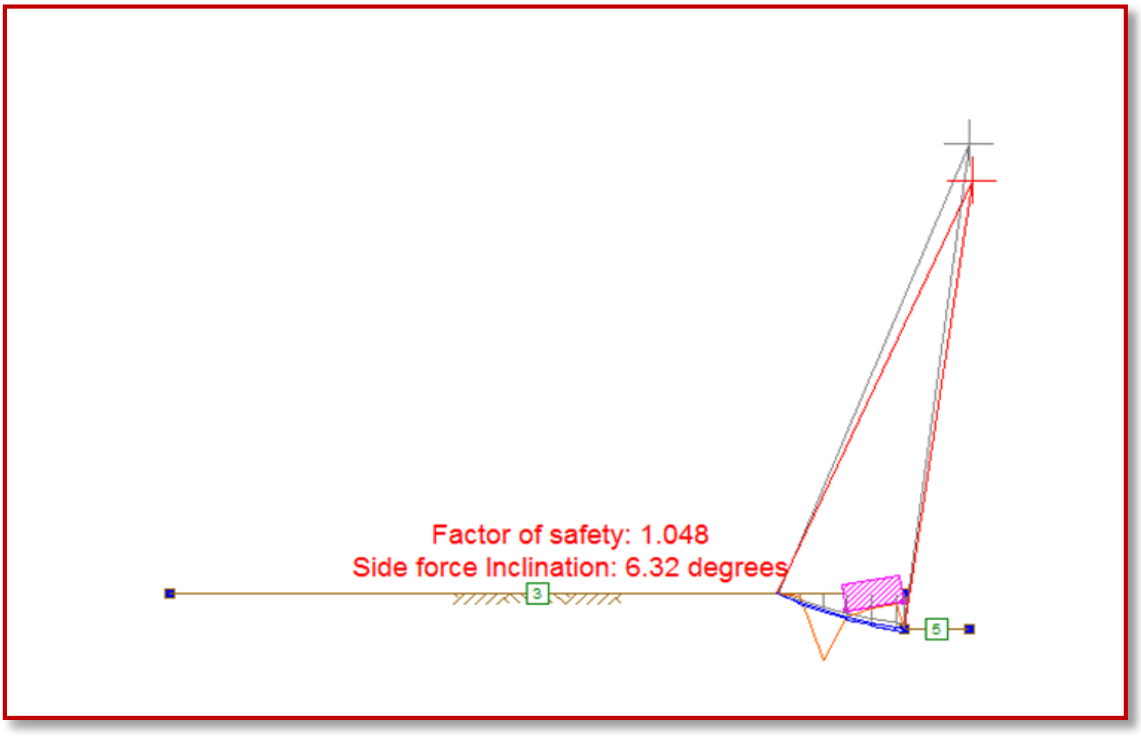

Figure 75 Limit equilibrium analysis using UTEXAS at section 2+00.

As expected the factor of safety is near to zero. So after excavation and leaving the excavation without any support for two nights would have led to failure of the slope. The same was modelled in finite element software FLAC 3D. The Figure 76 shows the construction stages

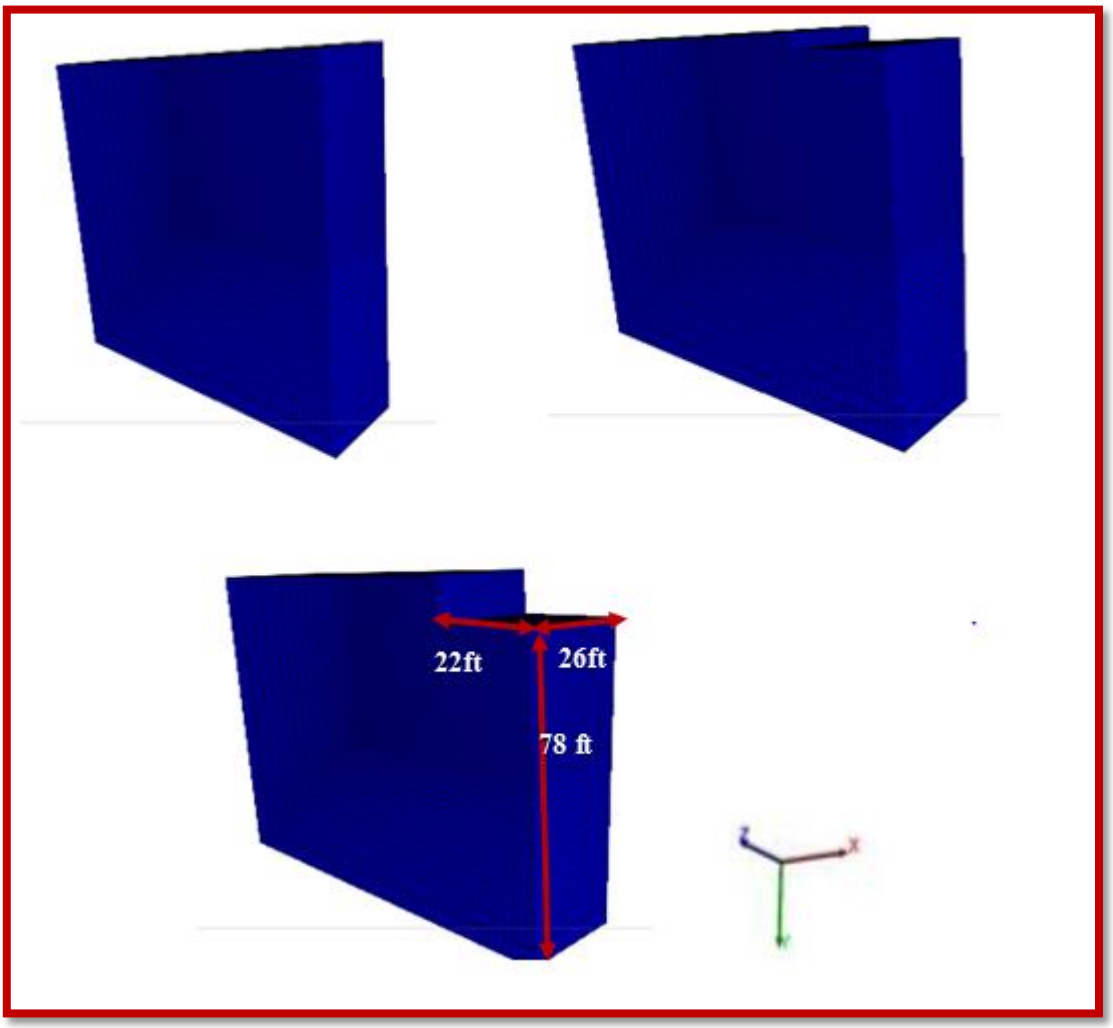

Figure 76 Stages of construction until failure.

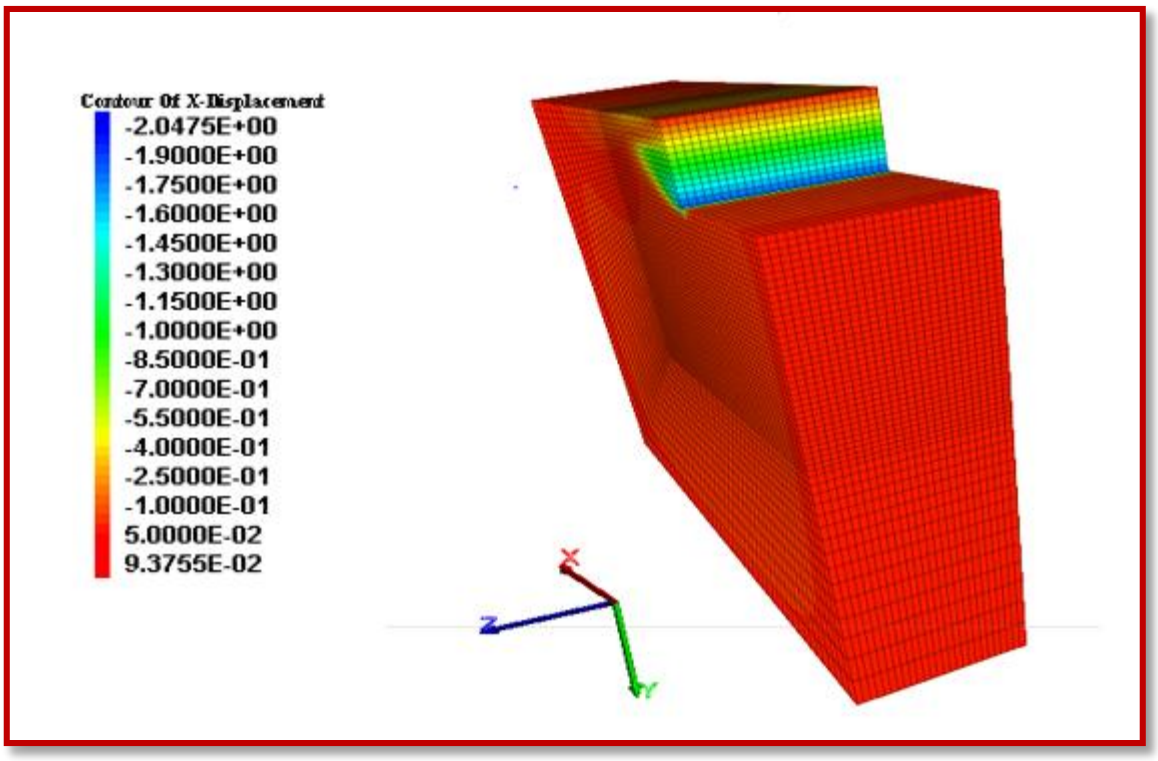

Figure 77 Contour of displacement after second stage of construction before failure.

The contours of displacement is shown in the Figure 77 . It can be seen that the highest displacemnt can be observed at 12 ft depth. The code does not converge which implies and displacement keeps increasing. The displacement with steps at 12 ft depth 4 ft behind the wall is shown in the Figure 78. It is noticed that very less movement is intially observed till the first stage. After the second stage the deformation increases rapidly at at an increases rate.

Figure 78 Horizontal deformation at depth of 12 ft after the second stage of construction.

Modelling the post failure construction had many challenges. Since FLAC is an explicit software the number of steps to be taken during the analysis can be given as input or ratio of unbalanced force at which the next level of analysis can be started can be set. This feature can be used to model the post failure construction stages. Pretension nails were installed after the failure and construction is continued. Since the field instruments were not able to capture the failure correctly, the steps taken should represent the field situation till the failure. This is done so that the horizontal deformation at the time of failure can used to compare and to decide when to input the pretension nails. The displacement at depth of 12 ft. can be used for this comparison, since maximum

deformation is observed at this depth. Another technique is to move to next stage of construction when the displacement is same as the last reading taken at the field before failure. The construction stages is shown in the Figure 79. The contours of displacement are shown in the Figure 80.

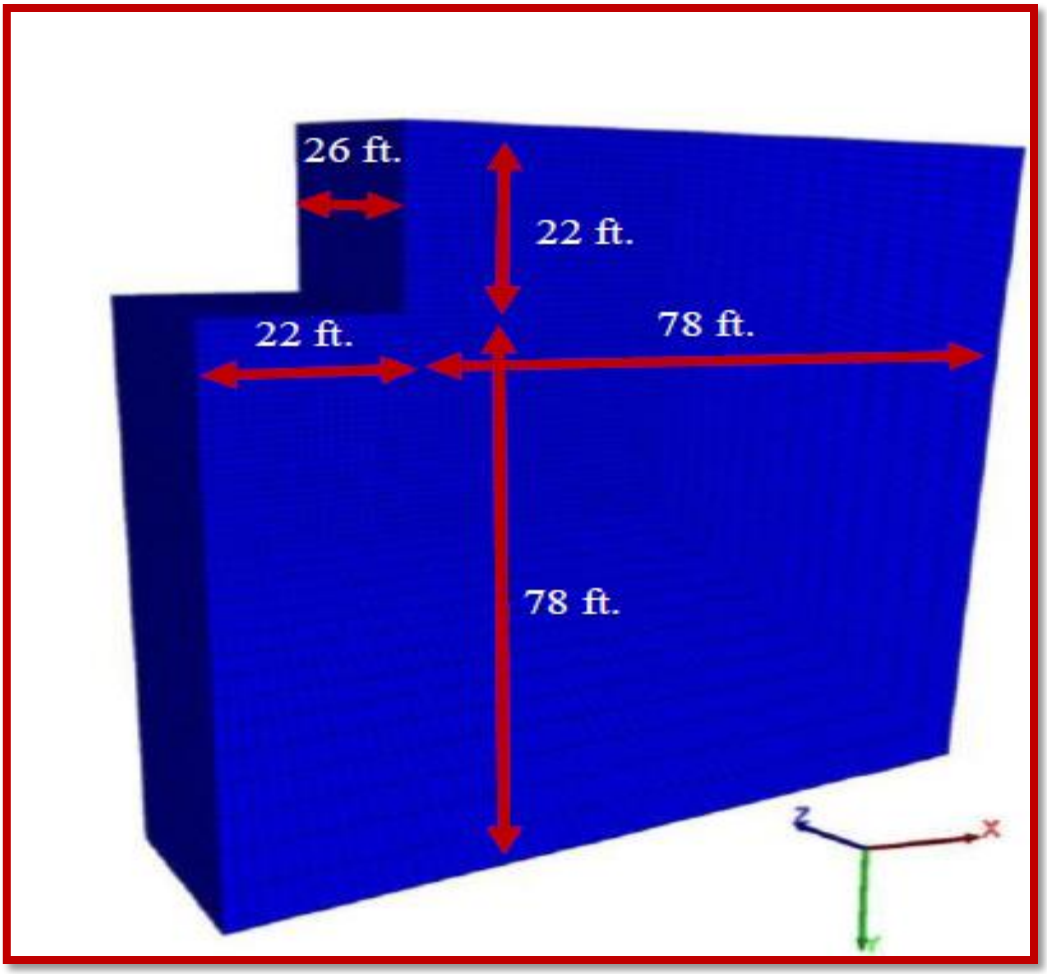

Figure 79 End of construction section 2+00.

The horizontal deformation of the wall obtained from modelling is compared at with the observed reading at the field (Figure 81). Excellent similarity is observed between the two. This is partly because at second stage of construction the horizontal deformation obtained from modelling was matched with the field observations. The next was to see how the forces in the nails compare with the field observations. From the horizontal deformation readings it is expected that the forces in the nails will be higher than the file observations.

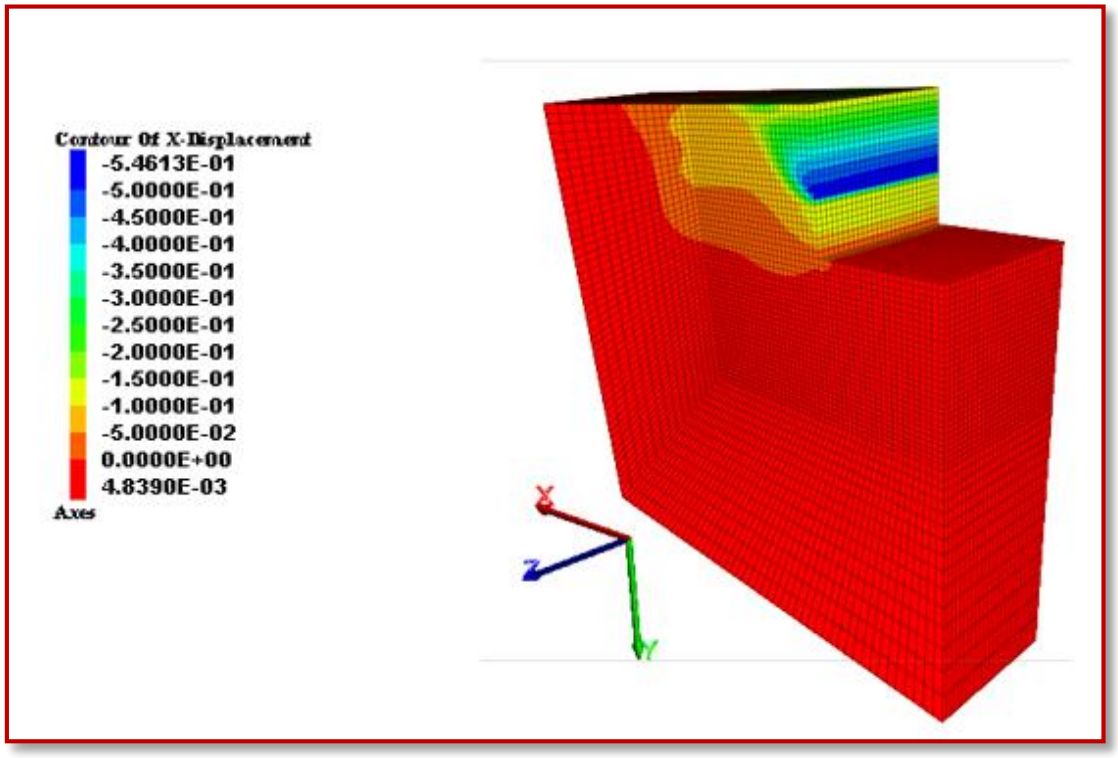

Figure 80 Contour of horizontal deformation after construction at section 2+00.

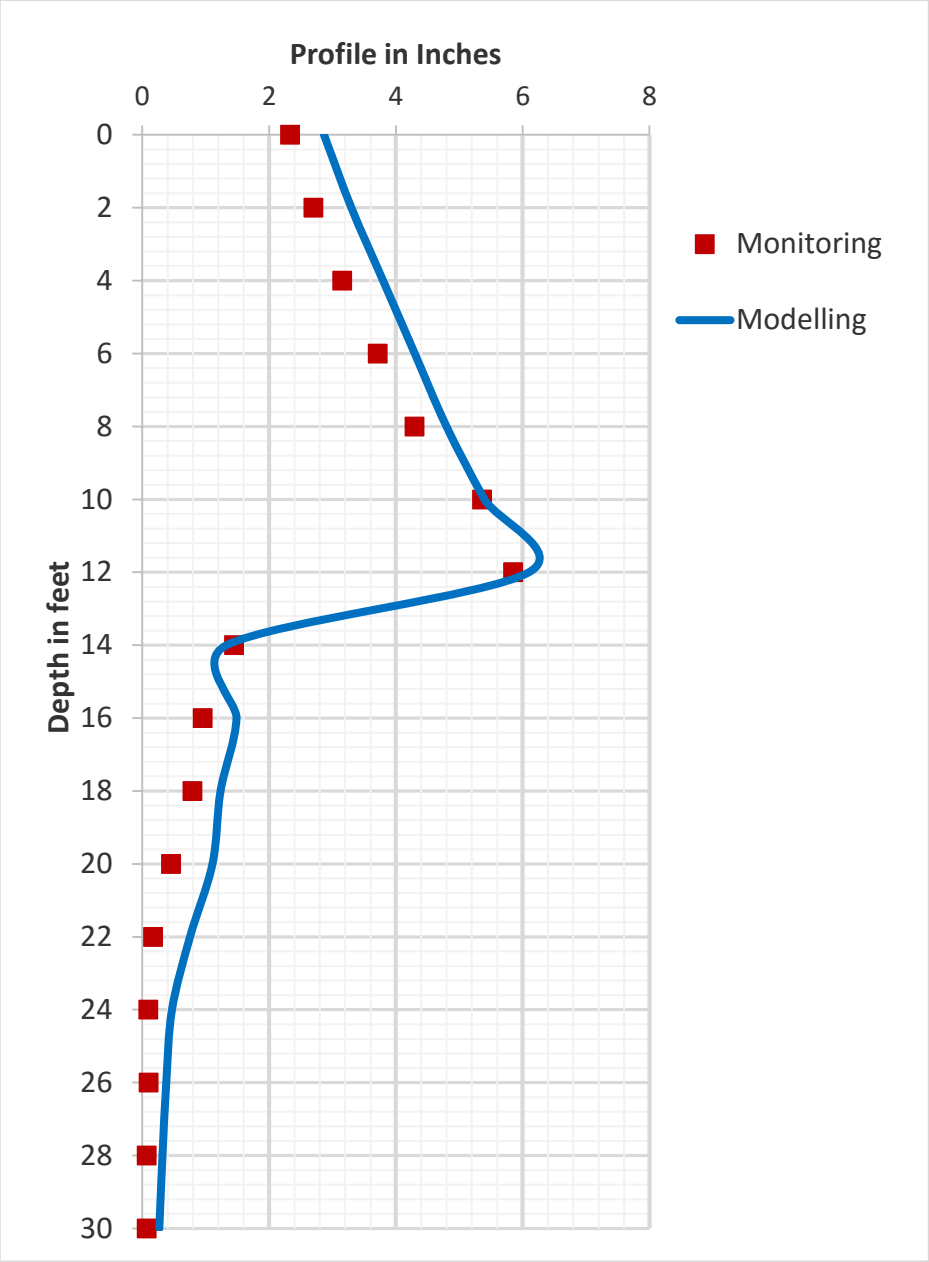

Figure 81 Comparison of monitored and modelled horizontal deformation.

The forces in the nails at end of construction is shown in the Figures 82 to Figure 87.

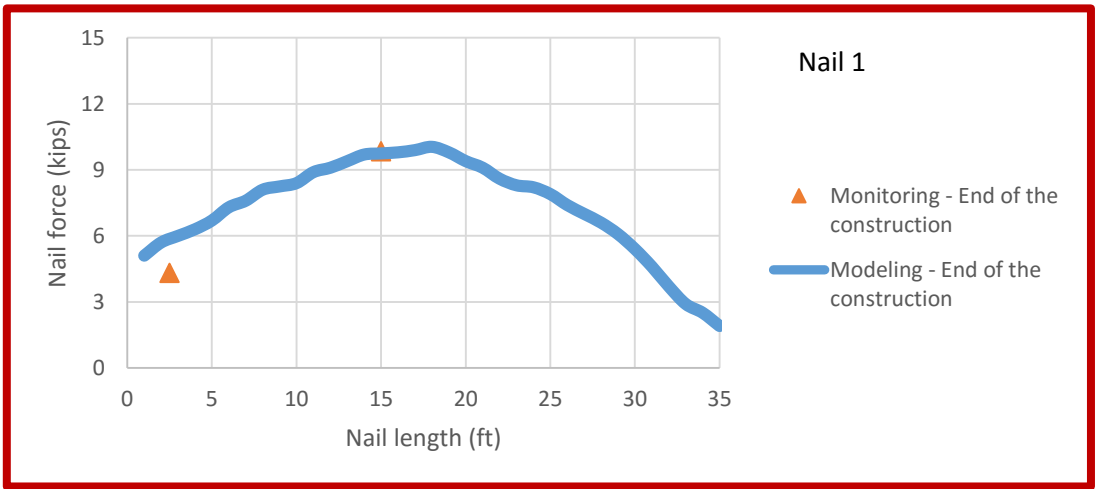

Figure 82 Comparison of service load in nail 1 after construction from numerical modelling and monitoring at section 2+00.

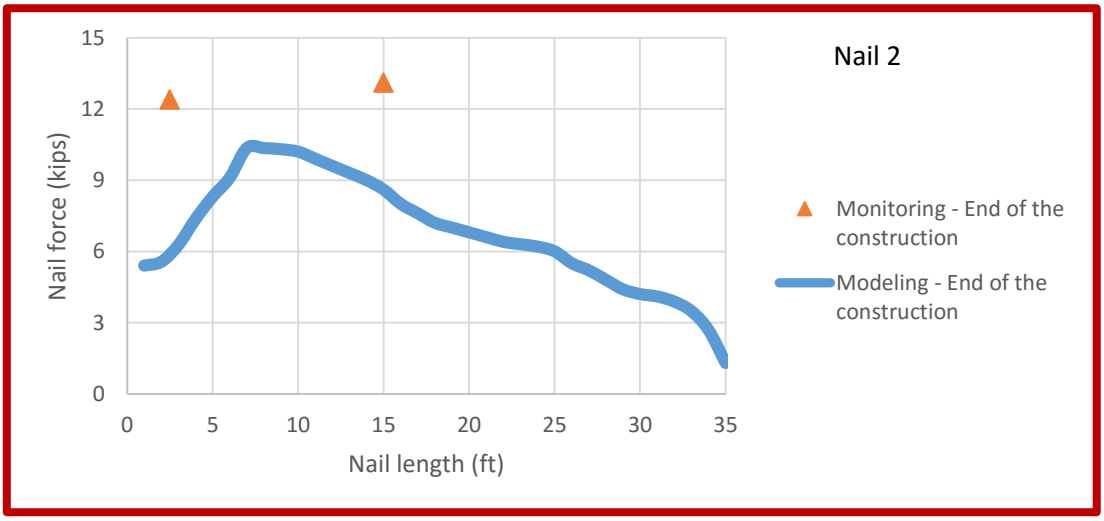

Figure 83 Comparison of service load in nail 2 after construction from numerical modelling and monitoring at section 2+00.

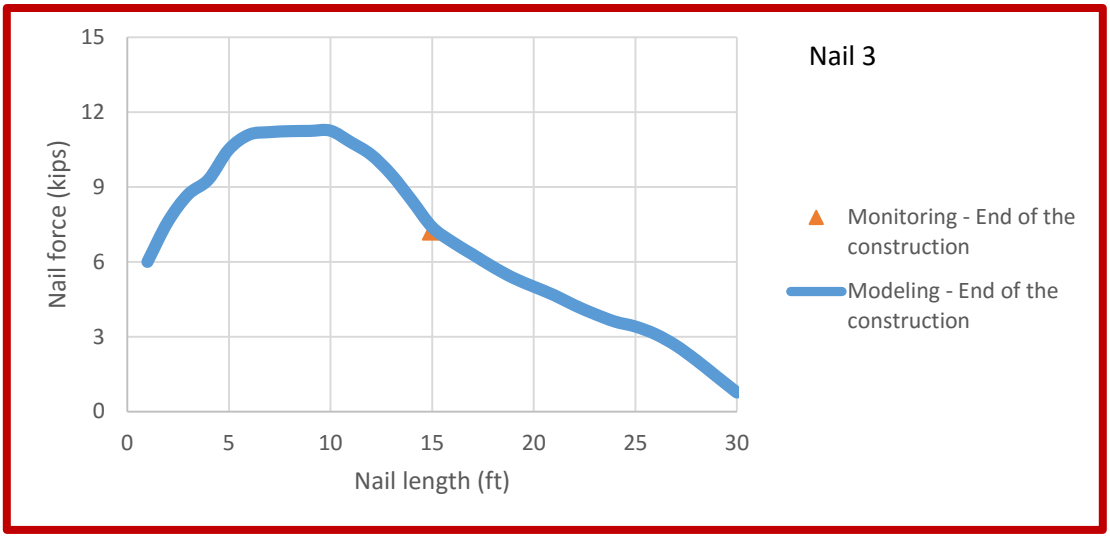

Figure 84 Comparison of service load in nail 3 after construction from numerical modelling and monitoring at section 2+00.

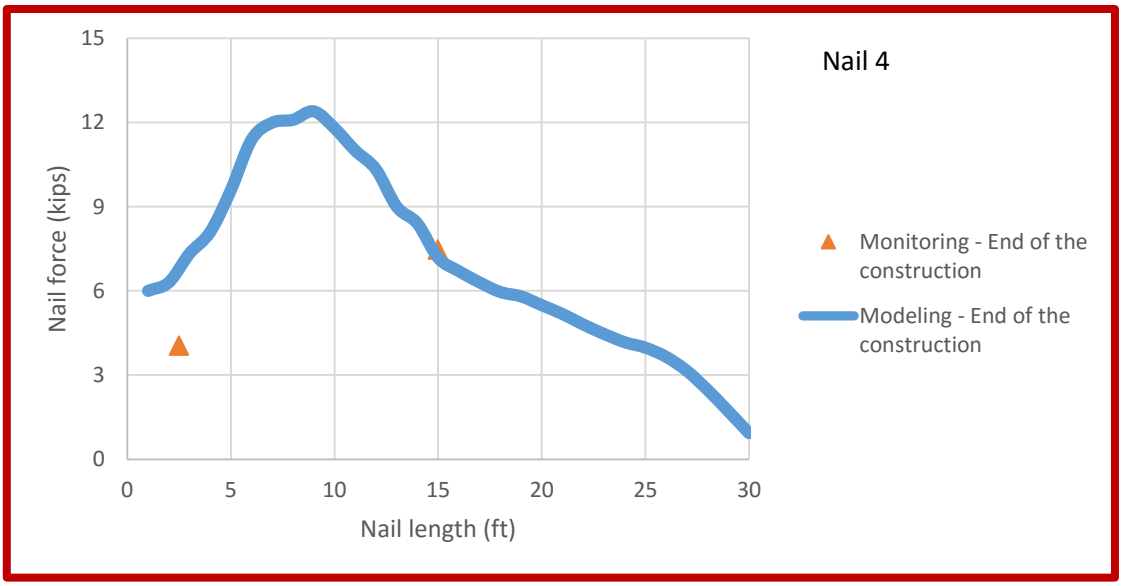

Figure 85 Comparison of service load in nail 4 after construction from numerical modelling and monitoring at section 2+00.

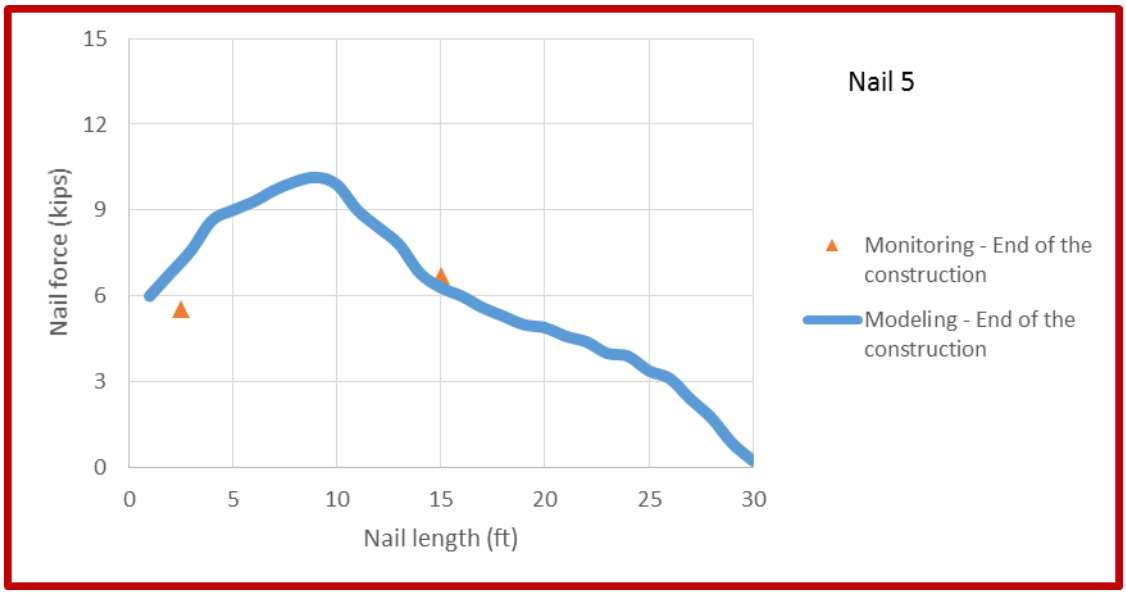

Figure 86 Comparison of service load in nail 5 after construction from numerical modelling and monitoring at section 2+00.

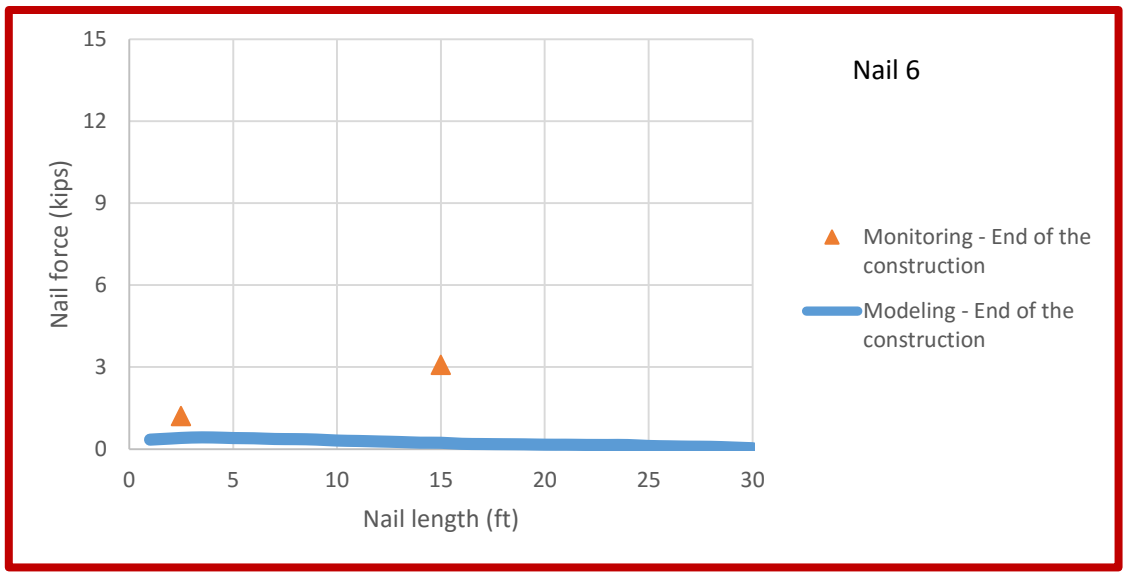

Figure 87 Comparison of service load in nail 6 after construction from numerical modelling and monitoring at section 2+00.

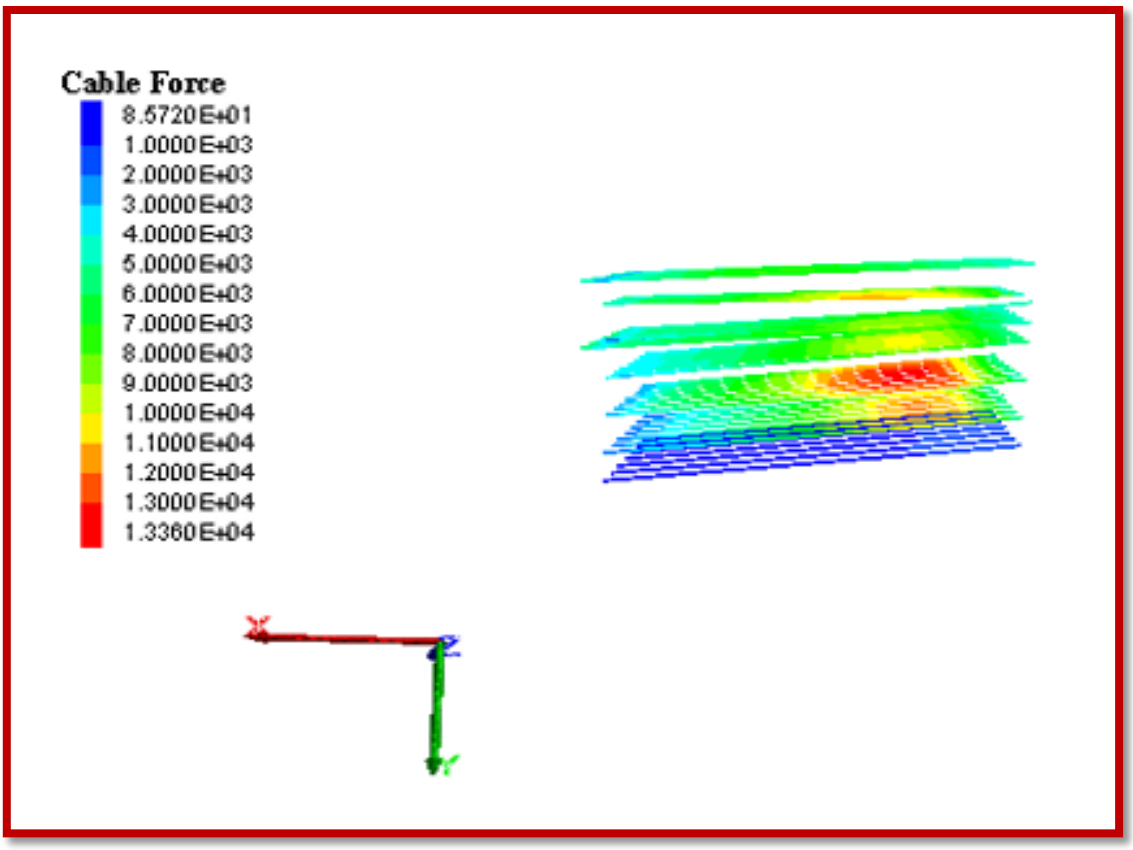

Figure 88 Load distribution in nail after construction at section 2+00.

The contour of load in nails is shown in Figure 88. It can be seen that max load is seen in fourth row of nails.

4.5 Creep modelling

The wall in Beaumont was monitored for one year by Kharanaghi (2015). The horizontal deformation and the load in the nails were monitored every month. The creep of soil nail wall at section 2+00 was modelled. The ‘n’ value obtained from laboratory was the key parameter to obtain other parameters to be used in the creep model. Burger viscoelastic model was used for modelling the creep behavior of the soil. The following

parameters shown in Table 9 were input into the model for obtaining the creep behavior based on the obtained n value from field observations

***n* value**	**Viscous parameters for the Burger model**
$0.02 < n < 0.04$	m shear =1.04e9 lb /ft^2, m vis= 5.91e14 lb*s/ft^2., k shear = 3 e6 lb /ft^2, k vis = 2.5e13 lb*s/ft^2.
$0.05 < n < 0.07$	m shear =1.04e9 lb /ft^2, m vis= 2e14 lb*s/ft^2., k shear = 5e5 lb /ft^2, k vis = 3.5e12 lb*s/ft^2.
$0.07 < n < 0.09$	m shear =1.04e9 lb /ft^2, m vis= 1.28e14 lb*s/ft^2., k shear = 2.37e5 lb /ft^2, k vis = 1.55e12 lb*s/ft^2.

Table 9 Viscous parameters for various n values given by Kharanaghi (2015).

The obtained n value in the laboratory was around .05-.08. Thus the mshear, mvis, k shear and k vis was taken from the Table 9. The contour of displacement is shown the Figure 89. The maximum displacement was observed at a depth of 12 ft after one year. The movement of the wall for one year after construction for both the section is shown in the Figure 90

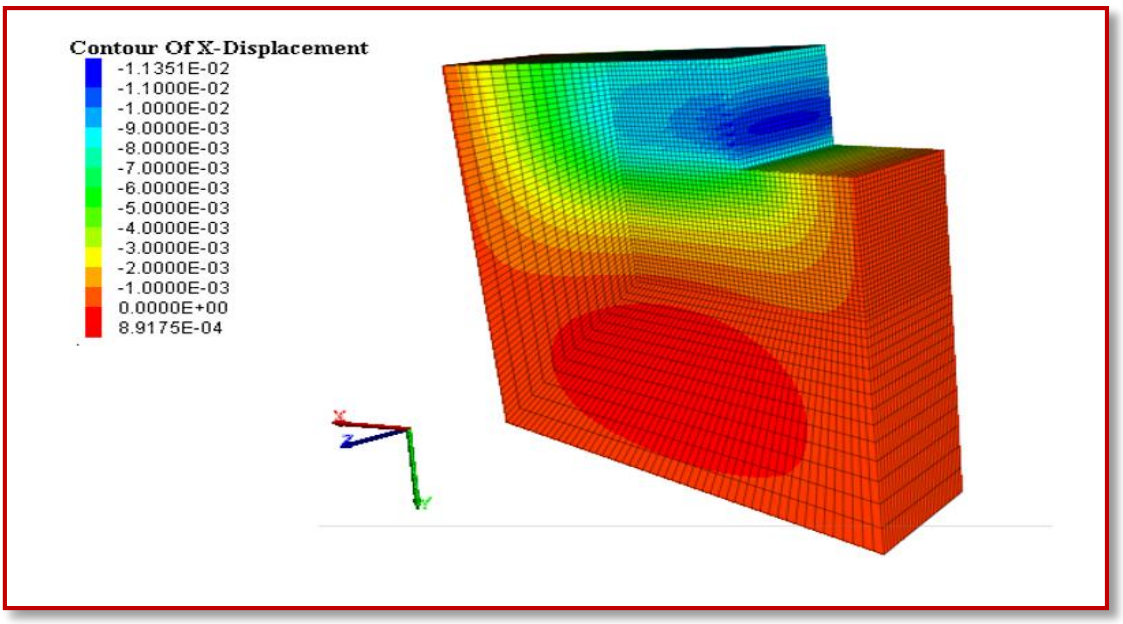

Figure 89 Contour of creep deformation at section 2+00 one year after construction.

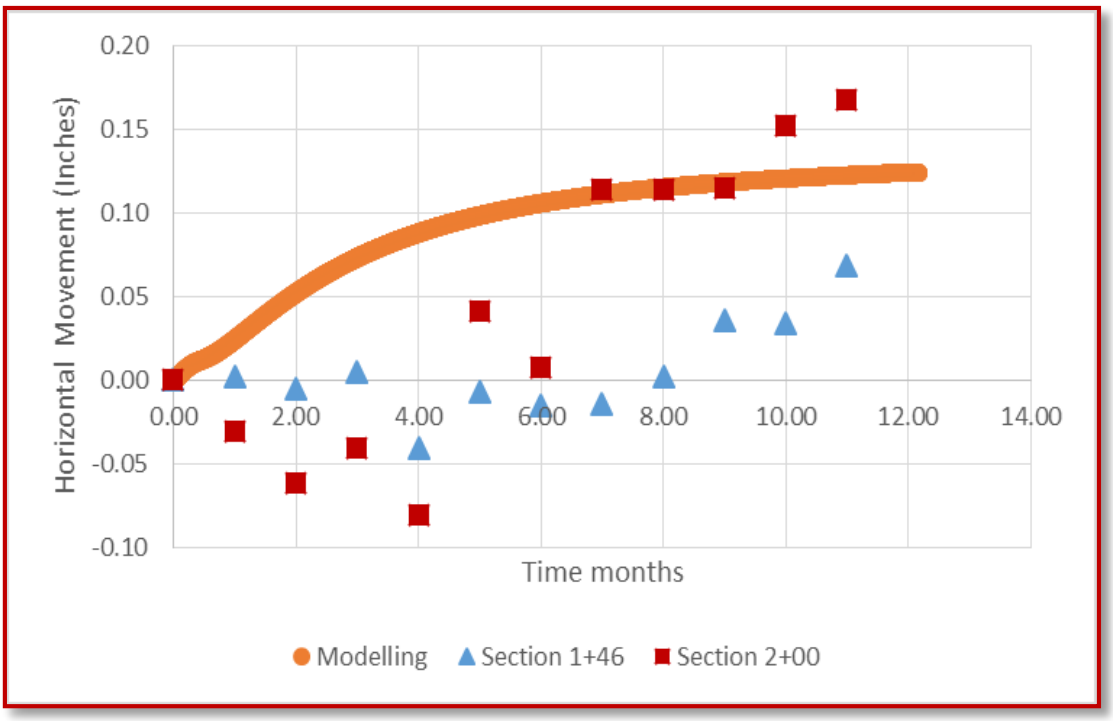

Figure 90 Wall movement for one year after construction at depth of 12ft.

Maximum movement occurred at a depth of 12ft. The model fits well with the observed readings for the section 1+46 after a period of 6 months. The wall shows the creep behavior, that is an increase in displacement after an initial settling period of 4 months. This is clear from observations at both the sections. This can also be due to weather conditions including changes in water content. Having said that the model over predicts the creep for most of the period and can hence be used to study if creep is to be considered in the design of walls. The comparison of load distribution along nails with observed and monitored readings is shown in Figure 91 to Figure 96. It was be key to observe the increase in load with time. The predicted load by the model is expected to exceed the monitored load because the worst case scenario parameters are adopted in the modelling.

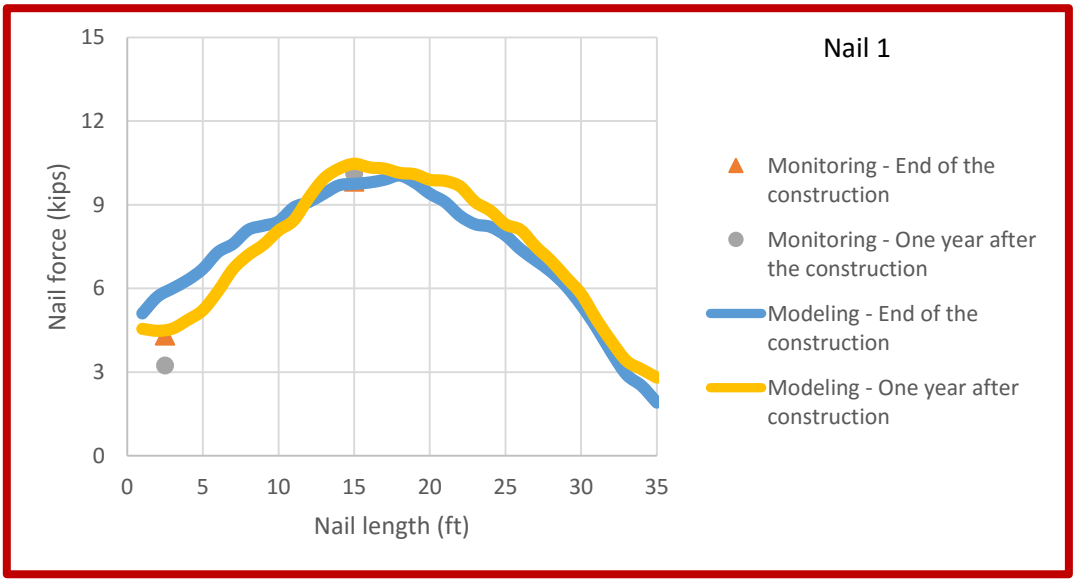

Figure 91 Load distribution in nail 1 at the end of construction and after one year of operation. Comparison between monitored and numerical results.

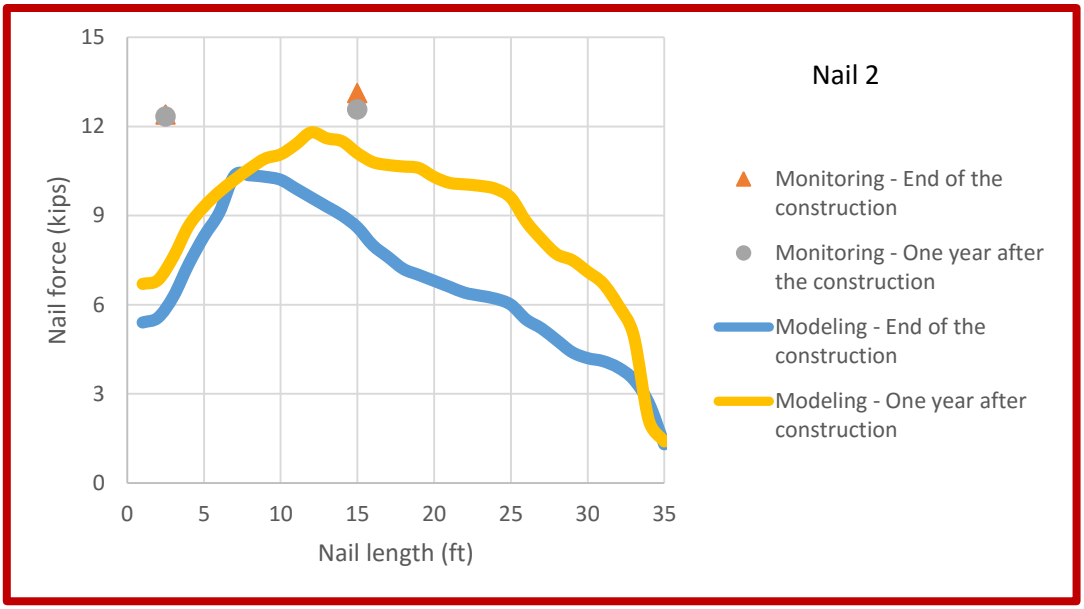

Figure 92 Load distribution in nail 2 at the end of construction and after one year of operation. Comparison between monitored and numerical results.

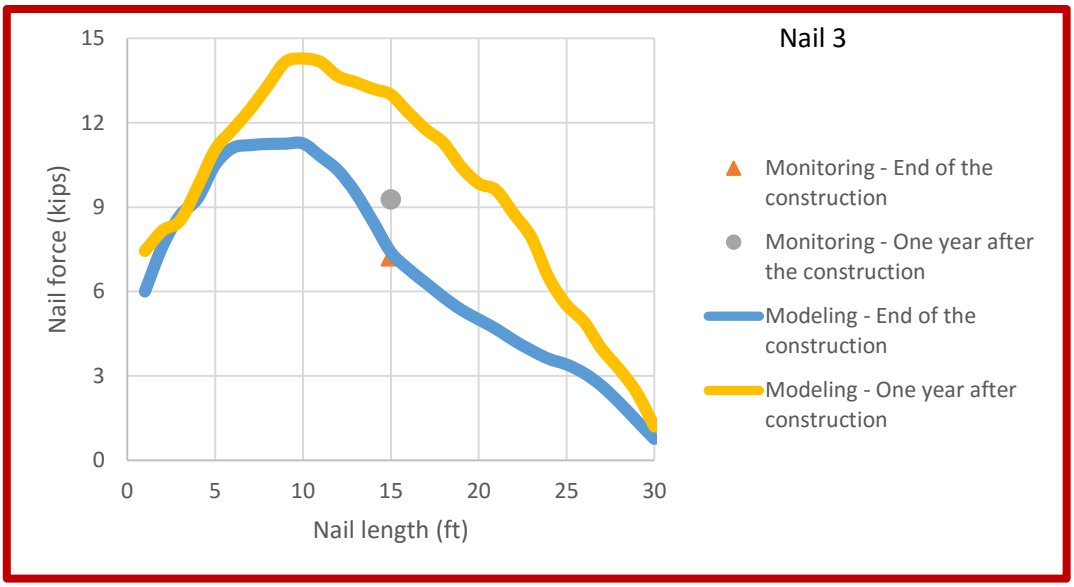

Figure 93 Load distribution in nail 3 at the end of construction and after one year of operation. Comparison between monitored and numerical results.

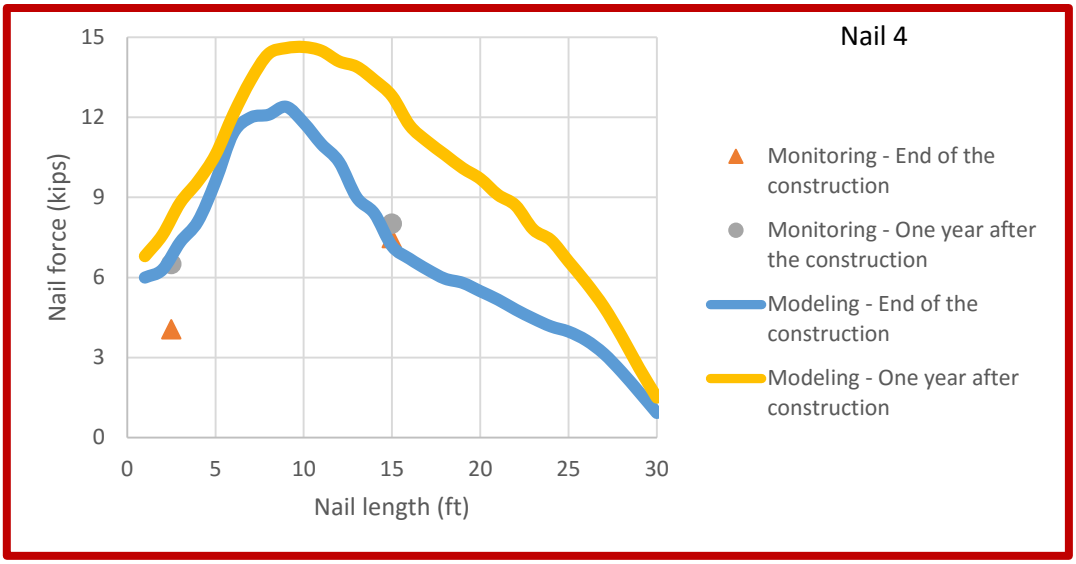

Figure 94 Load distribution in nail 4 at the end of construction and after one year of operation. Comparison between monitored and numerical results.

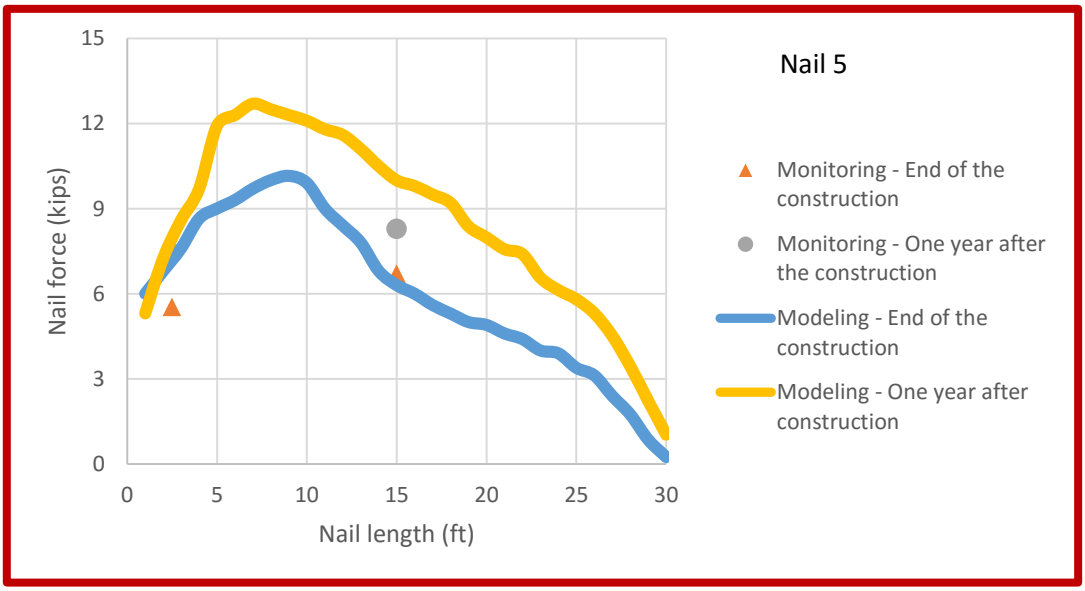

Figure 95 Load distribution in nail 5 at the end of construction and after one year of operation. Comparison between monitored and numerical results.

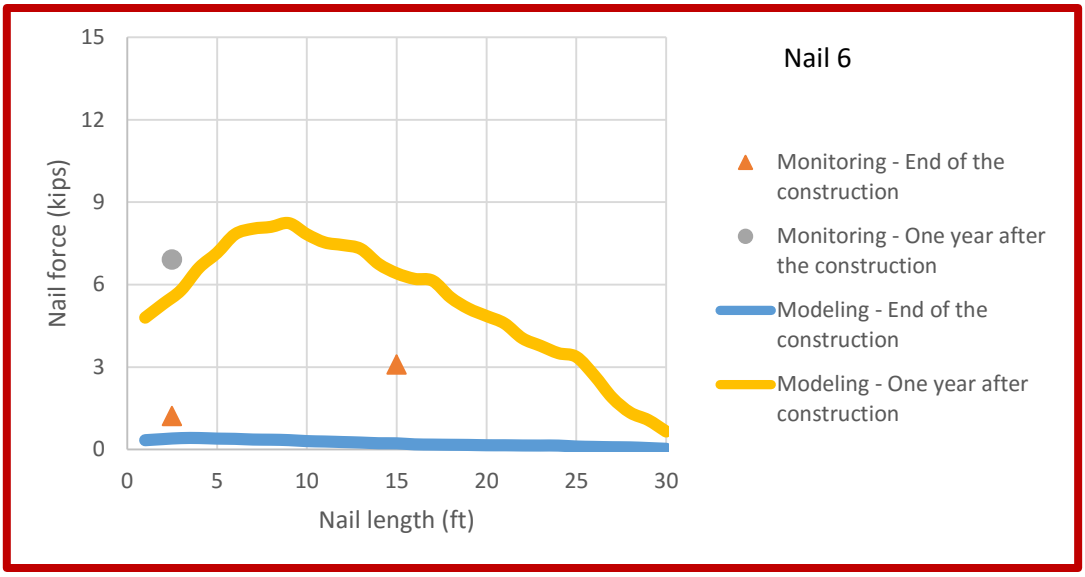

Figure 96 Load distribution in nail 6 at the end of construction and after one year of operation. Comparison between monitored and numerical results.

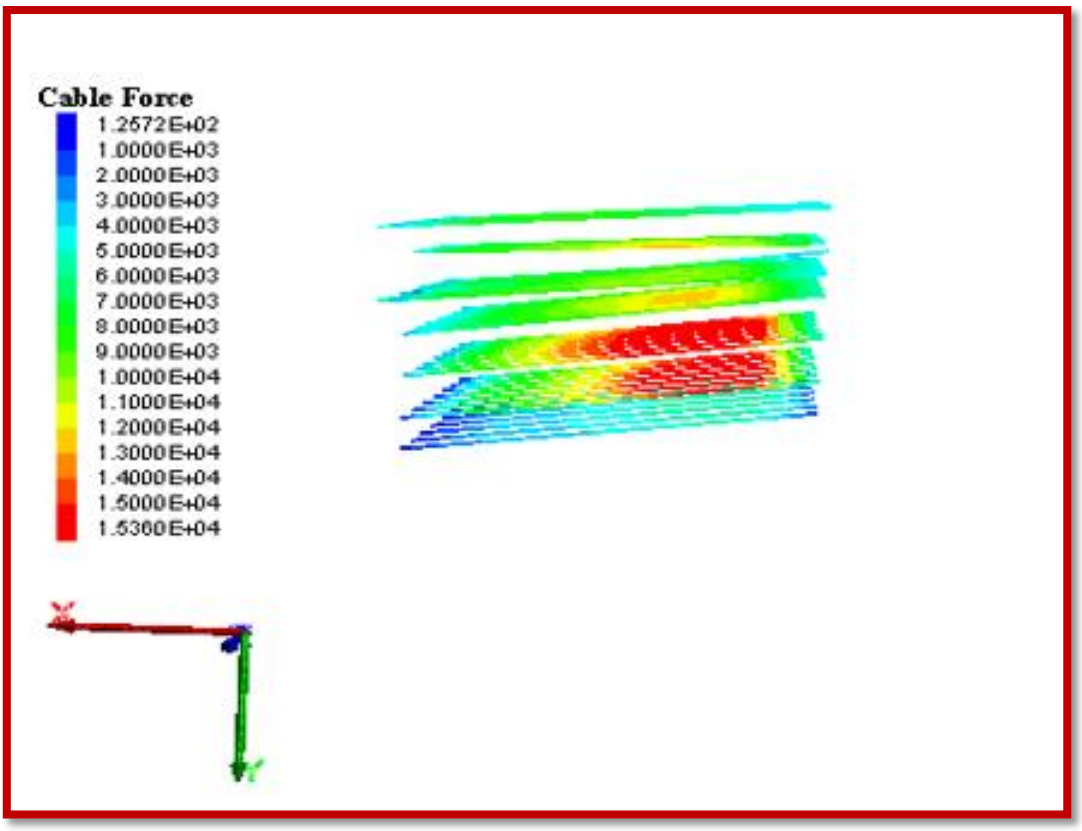

Figure 97 Load distribution on nails at section 2+00 one year after construction.

The load in the nails after one year of creep is shown in Figure 97. It can be concluded that modelling using FLAC 3D gives a very good correlation with observed reading. The increase of load in nails were also predicted using the model. A comparison of increase in load is shown in Table 10.

Nail#	Max load in the nails at end of the construction (kips)	Max load in the nails one year after the construction (kips)	Increase in the axial load due to the creep (kips)	Increase in the axial load due to creep (%)	Increase in axial load due to creep observed in field (%)
1	10.35	10.62	0.27	2.6	3
2	10.35	11.5	1.15	11	-
3	11.25	14.35	1.1	27.5	28
4	12.40	14.60	2.2	17	7
5	10.00	14.32	4.32	43	24
6	0.5	5.3	4.8	960	573

Table 10 Comparison of increase in load in nails before and after creep**.**

The maximum load was observed in the row 4 after construction. There was an increase of 2.2 kips. The corresponding increase of 17% was predicted by the model. The actual increase was 7%. Thus the model is over predicting the creep but still the max load is within the design load of 21 kips. Similarly at row 3 very the model predicts the increase in load which was observed in the field.

Using the same model the creep for 75 years was predicted. The failure of the soil nail wall will occur when the load in the nails will be more than pull out capacity of the nail. In this project the design load on nails is 21 Kips. Here after 75 years it is expected that the load in the nails is below the design load. The load distribution in the nails is given by the Figure 98. The creep deformation is shown in the Figure 99. Thus using this

procedure creep deformation and the load in the nails can be simulated for the lifetime of the structure.

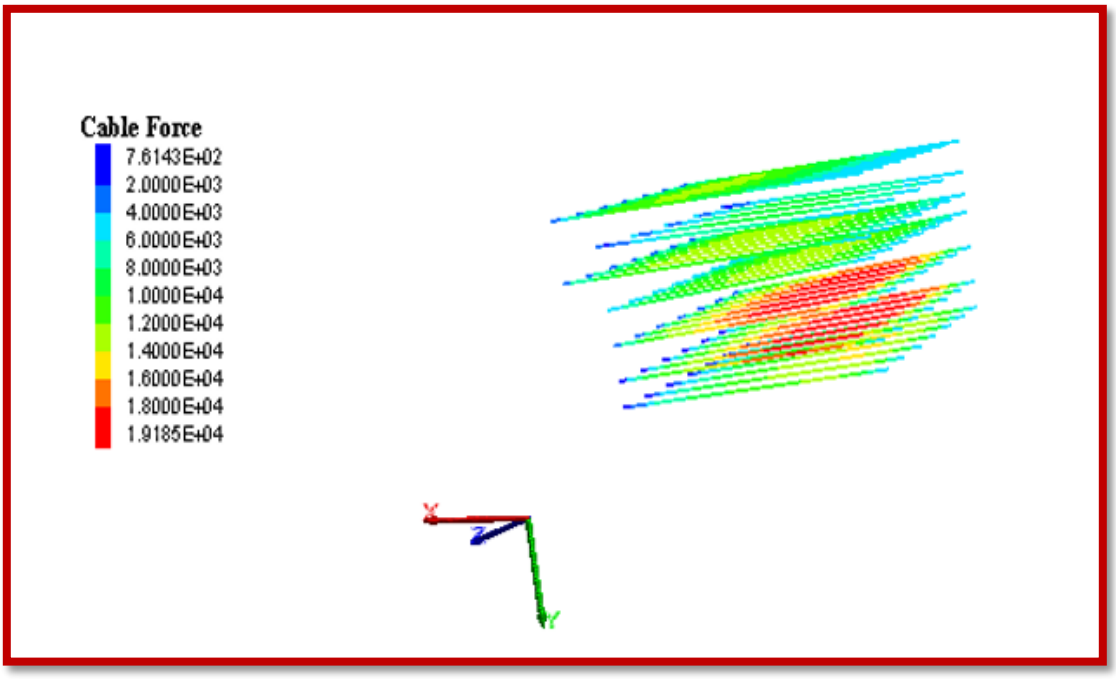

Figure 98 Load distribution in nail 75 years after construction.

Comparison of load distribution in nails one year after construction and 75 years of operation is shown in Figure 100.

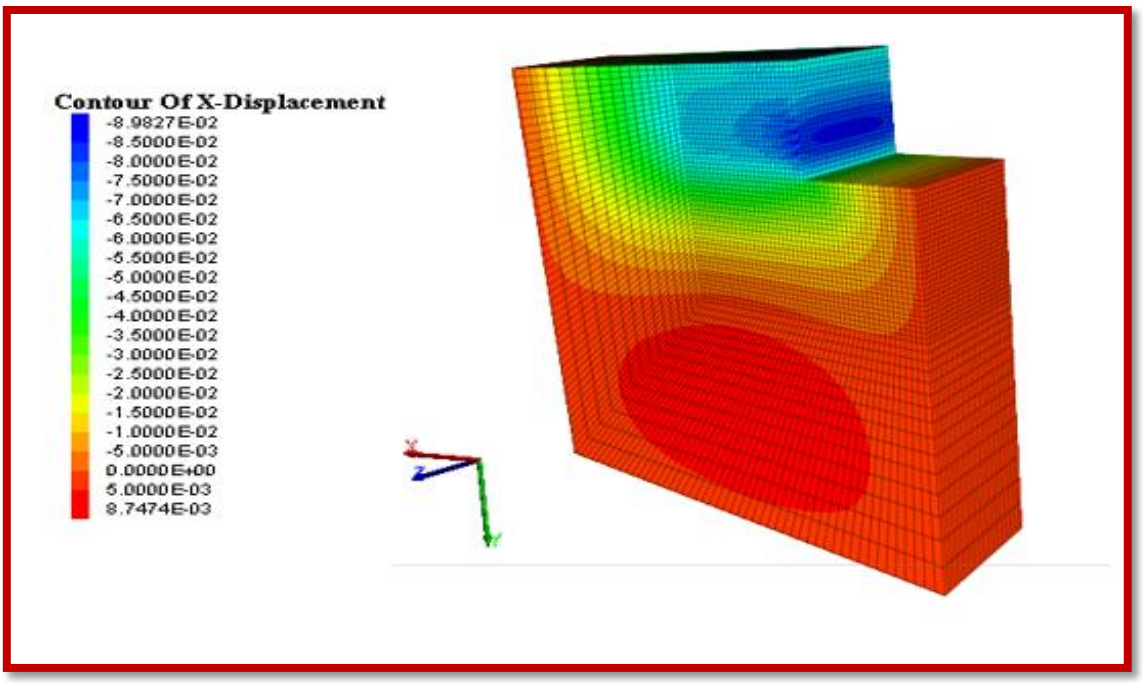

Figure 99 Creep contours after 75 years of construction.

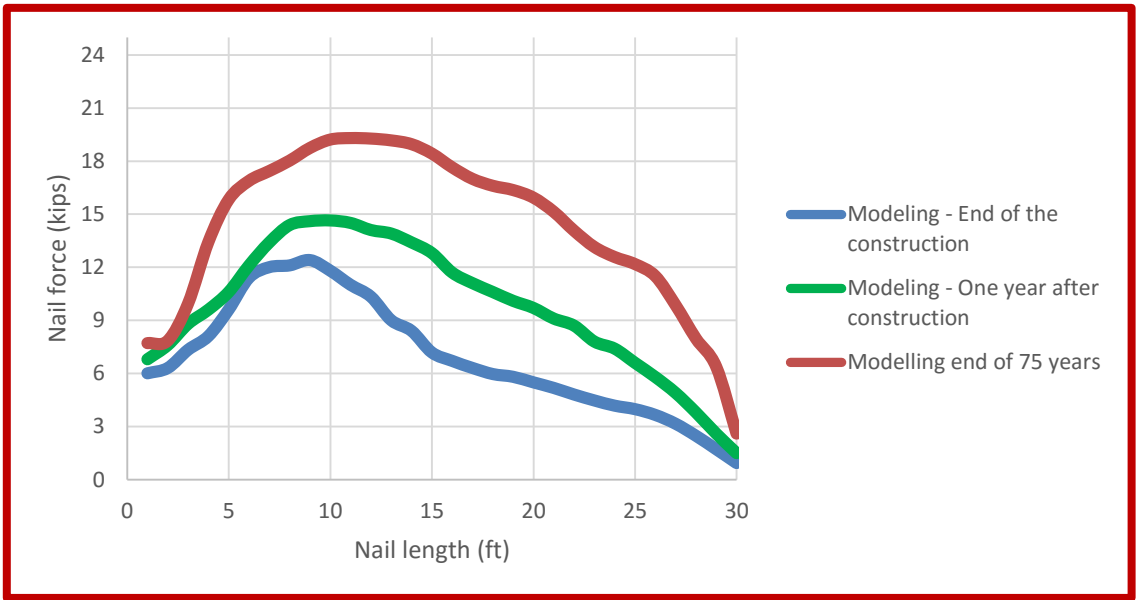

Figure 100 Comparison of increase in load in nails from end of construction to one year after construction to 75 years after construction.

4.6 Section 1+46

Construction at this stage went according to the design. The contour of displacement at end of construction stage is shown in Figure 101. This gives a very good conformation with the observed field reading. The comparison of monitored and modelled deformation is shown in Figure 102.

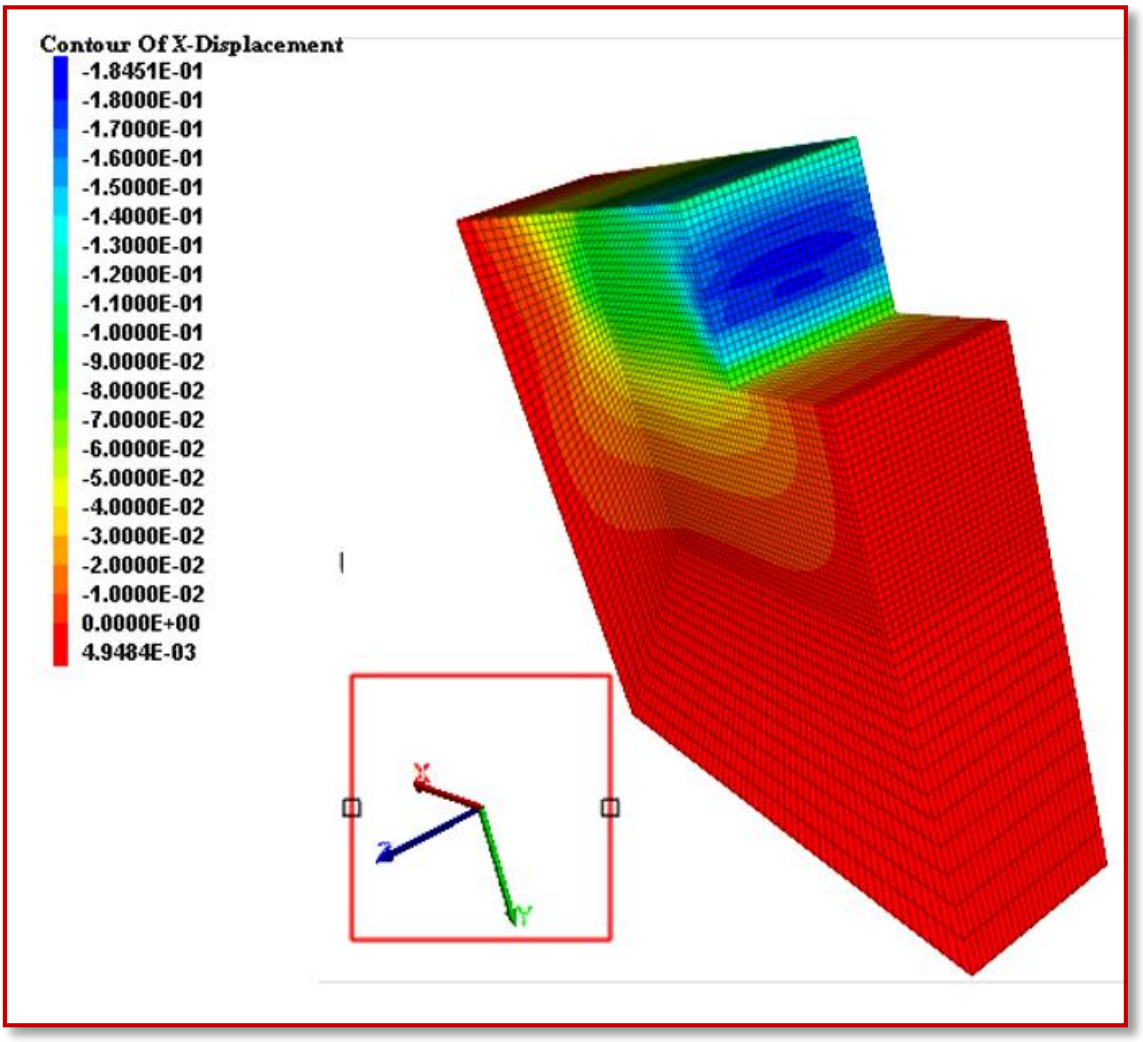

Figure 101 Contour of displacement after construction for section 1+46.

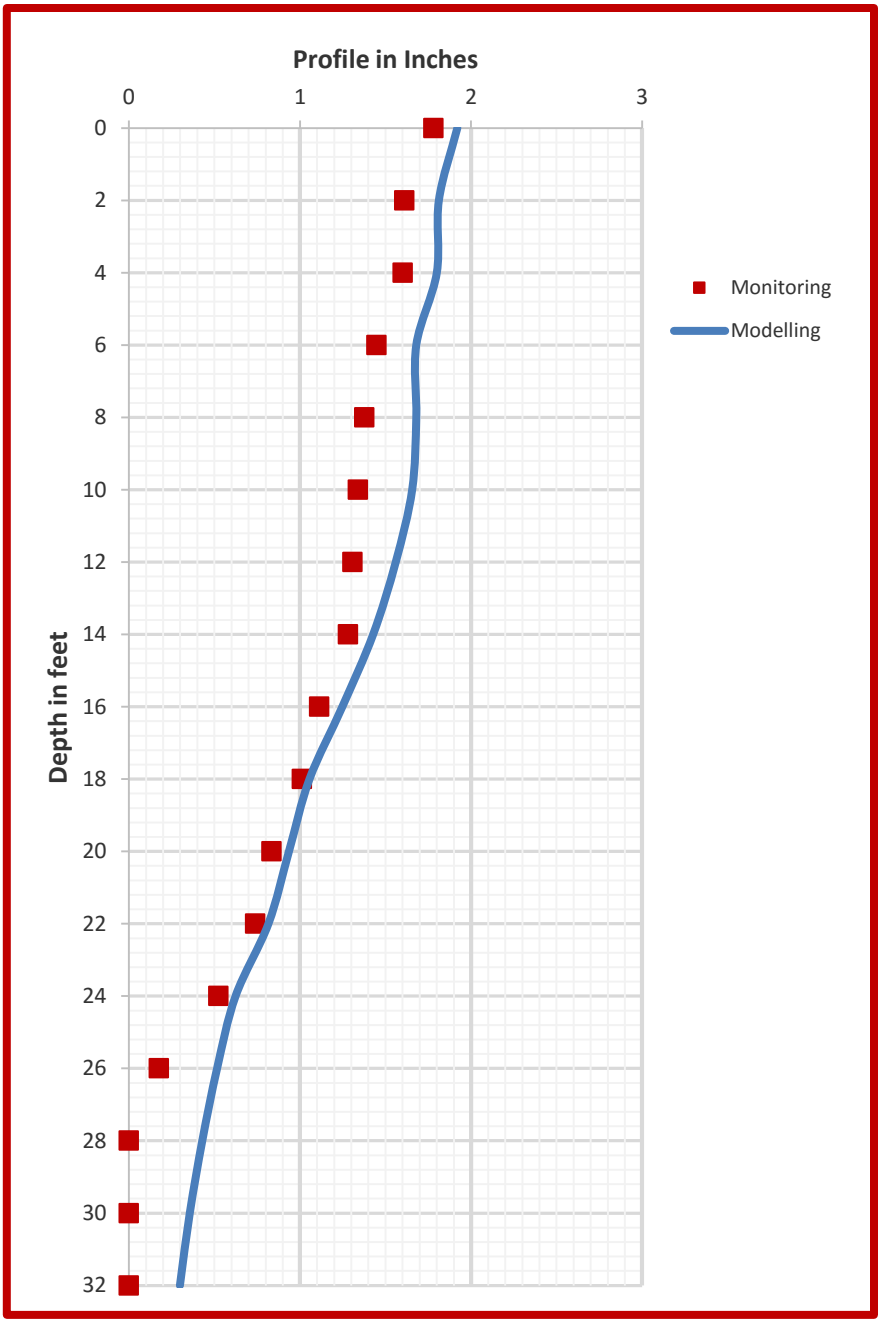

Figure 102 Comparison of monitored and modelled horizontal deformation.

The load in the nails at section 1+46 after construction are shown in Figures 103 to Figure 108.

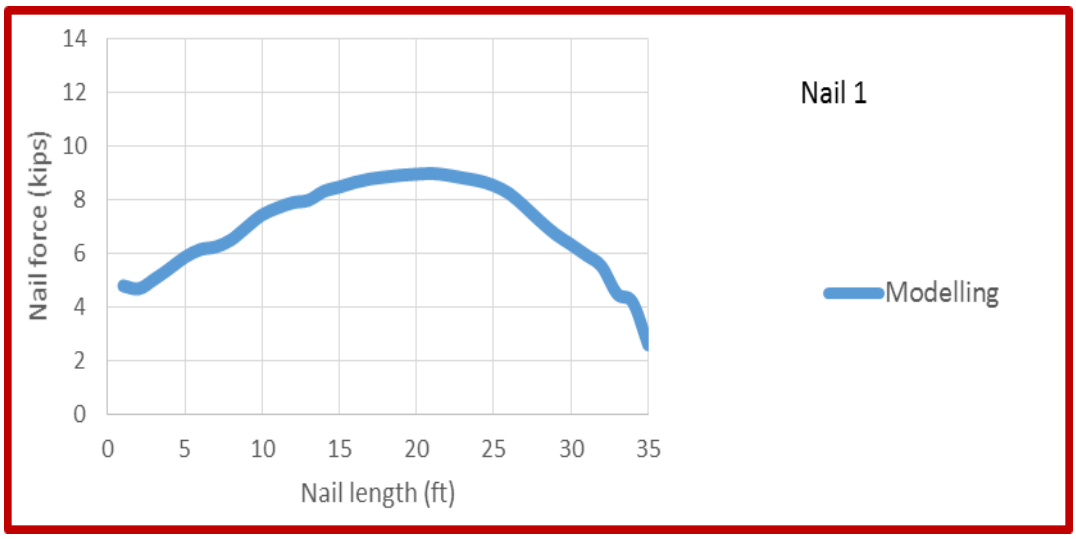

Figure 103 Service load in nail 1 after construction from numerical modelling at section 1+46.

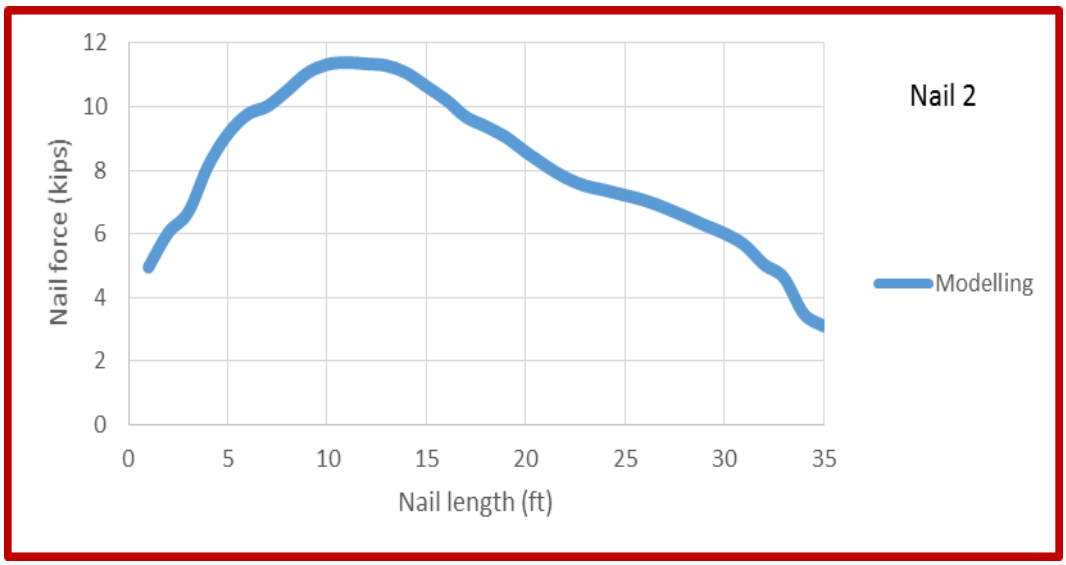

Figure 104 Service load in nail 2 after construction from numerical modelling at section 1+46.

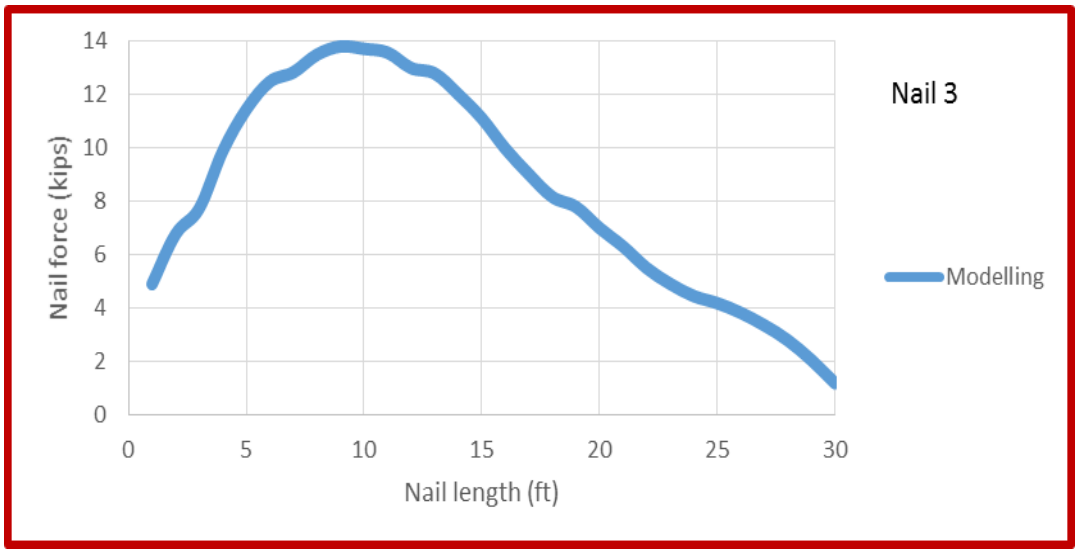

Figure 105 Service load in nail 3 after construction from numerical modelling at section 1+46.

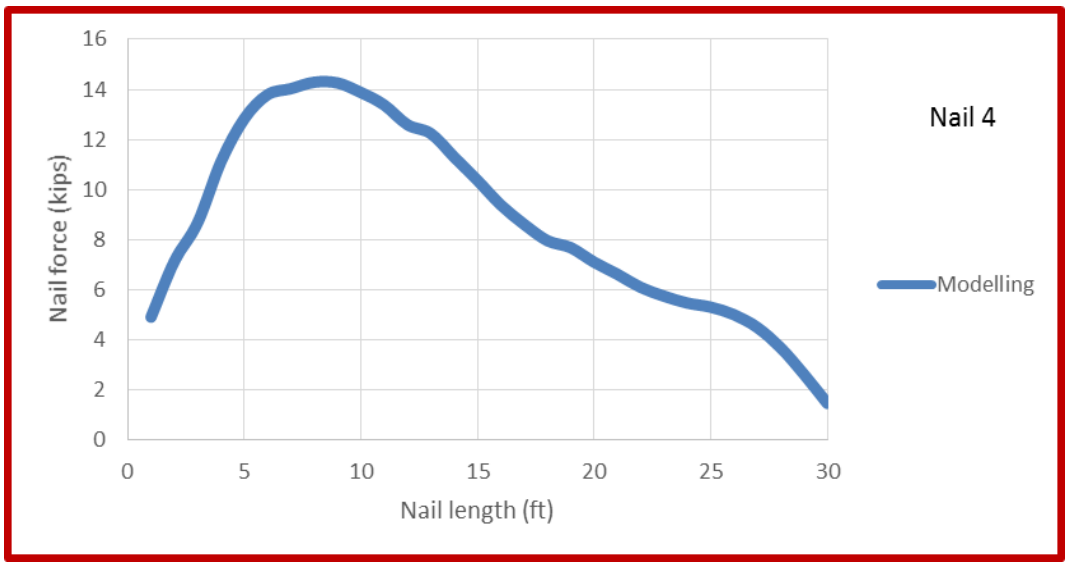

Figure 106 Service load in nail 4 after construction from numerical modelling at section 1+46.

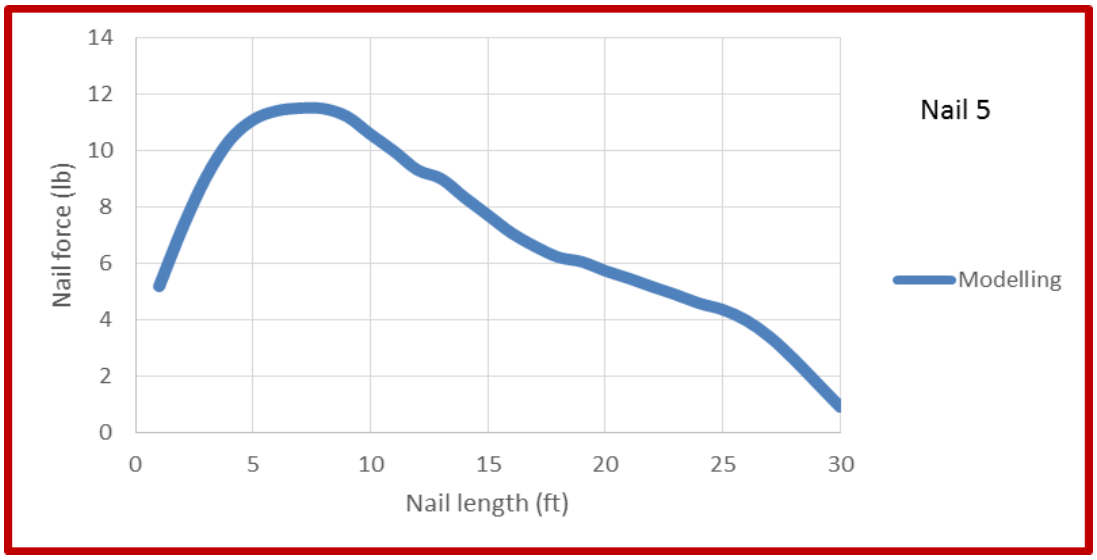

Figure 107 Service load in nail 5 after construction from numerical modelling at section 1+46.

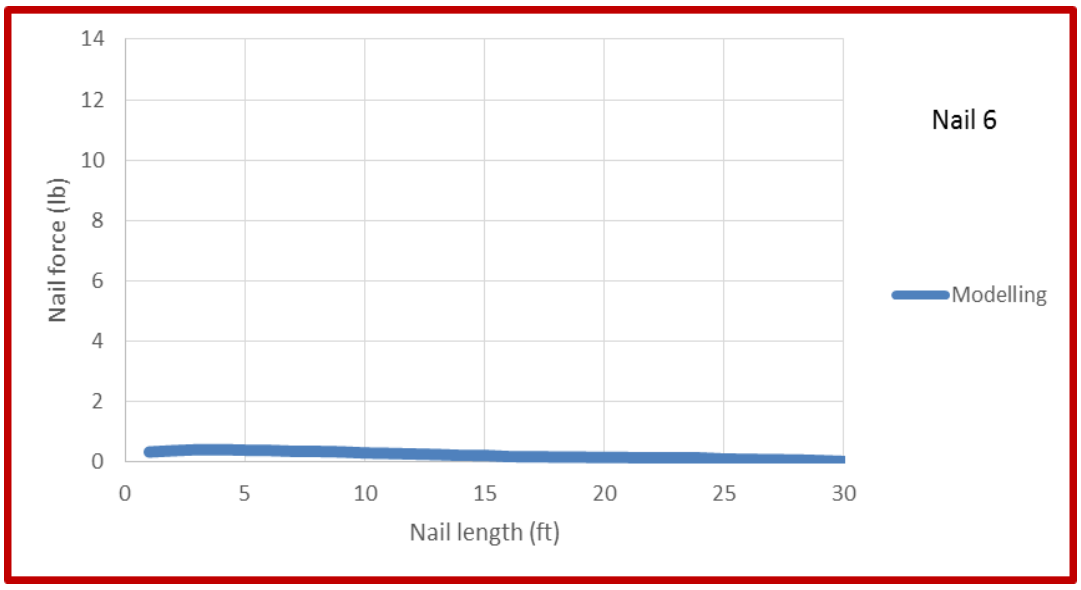

Figure 108 Service load in nail 6 after construction from numerical modelling at section 1+46.

The same procedure for creep was adopted to model this section as in section 2+00. After resting the retaining wall after construction, Burger model was imposed to model creep. The increase in load in nails after one year is shown in Figure 109 to 114.

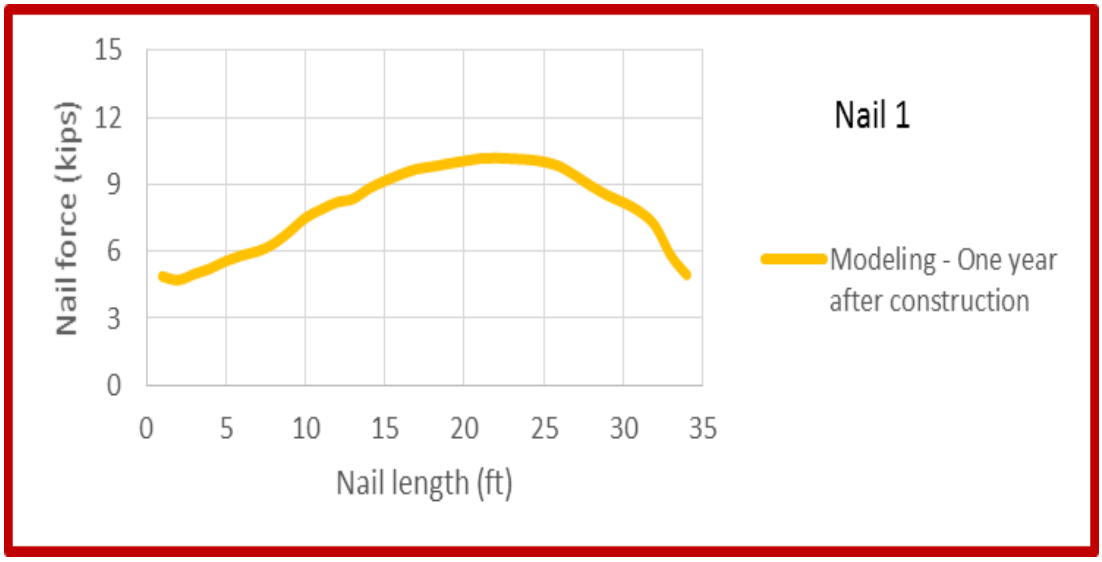

Figure 109 Service load in nail 1 one year after construction from numerical modelling at section 1+46.

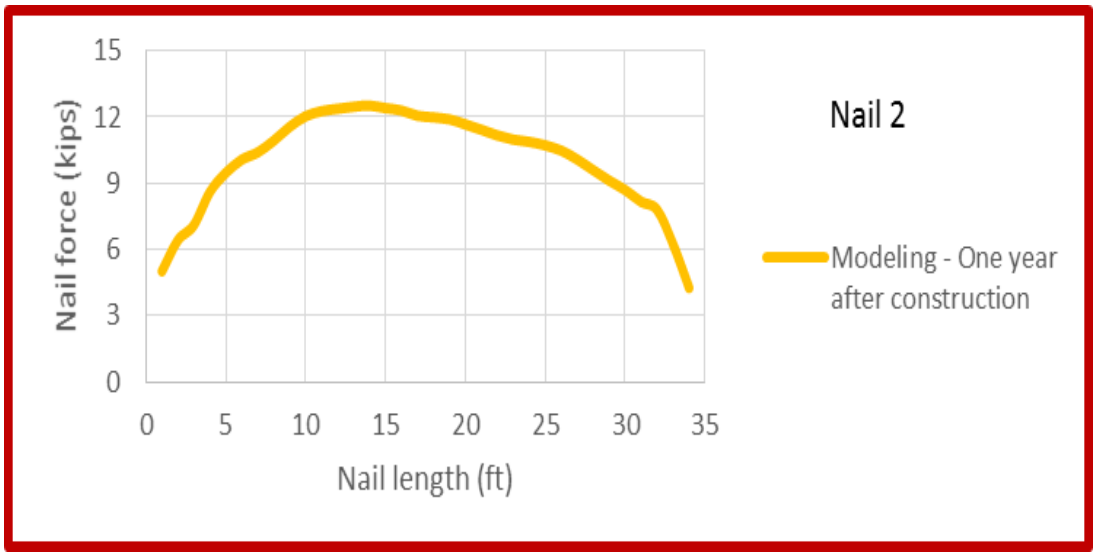

Figure 110 Service load in nail 2 one year after construction from numerical modelling at section 1+46.

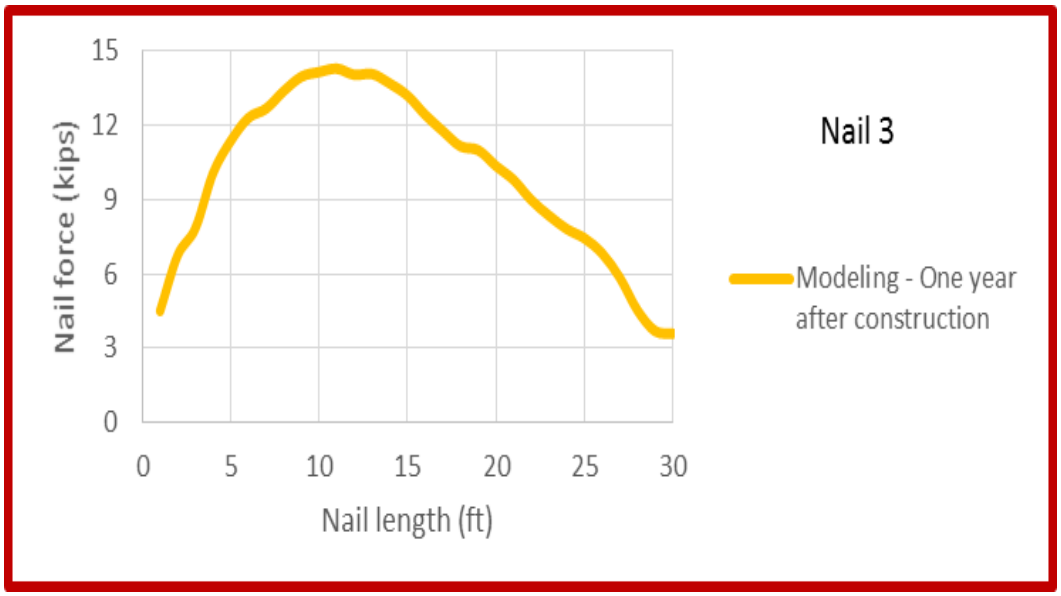

Figure 111 Service load in nail 3 one year after construction from numerical modelling at section 1+46.

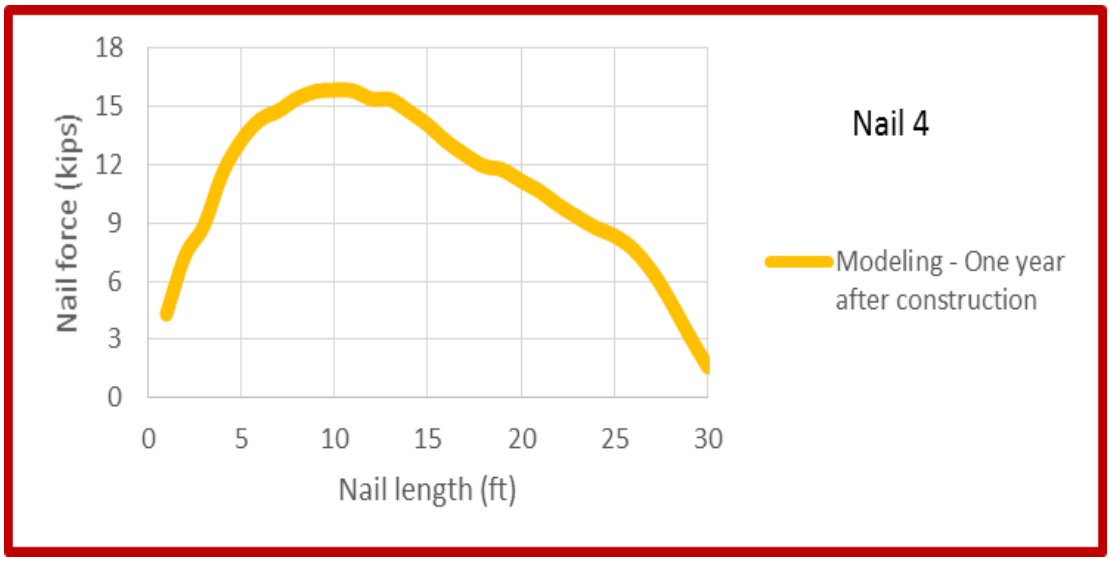

Figure 112 Service load in nail 4 one year after construction from numerical modelling at section 1+46.

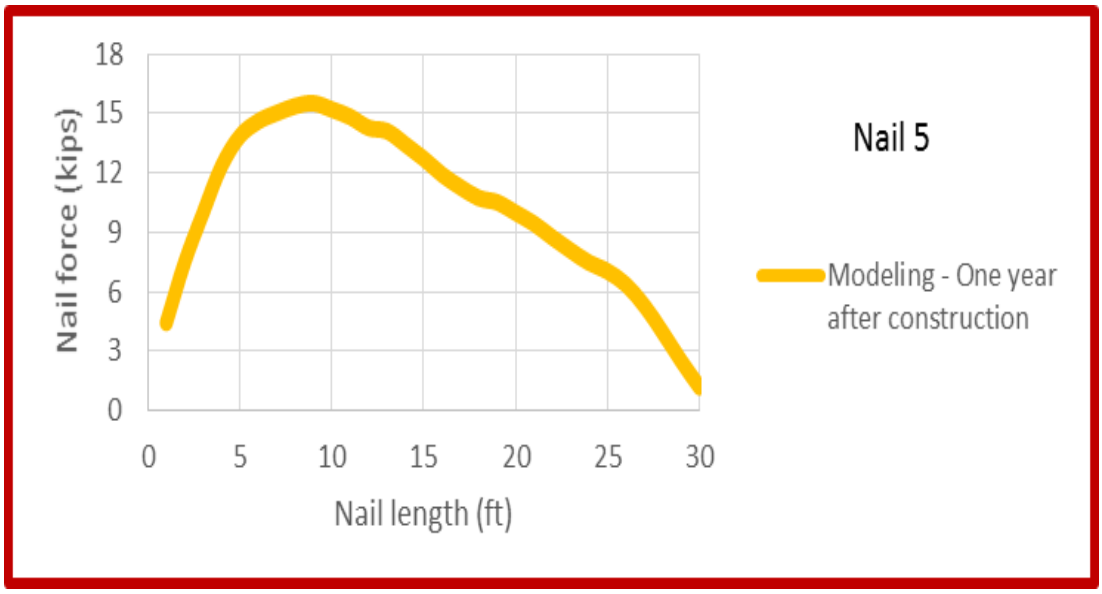

Figure 113 Service load in nail 5 one year after construction from numerical modelling at section 1+46.

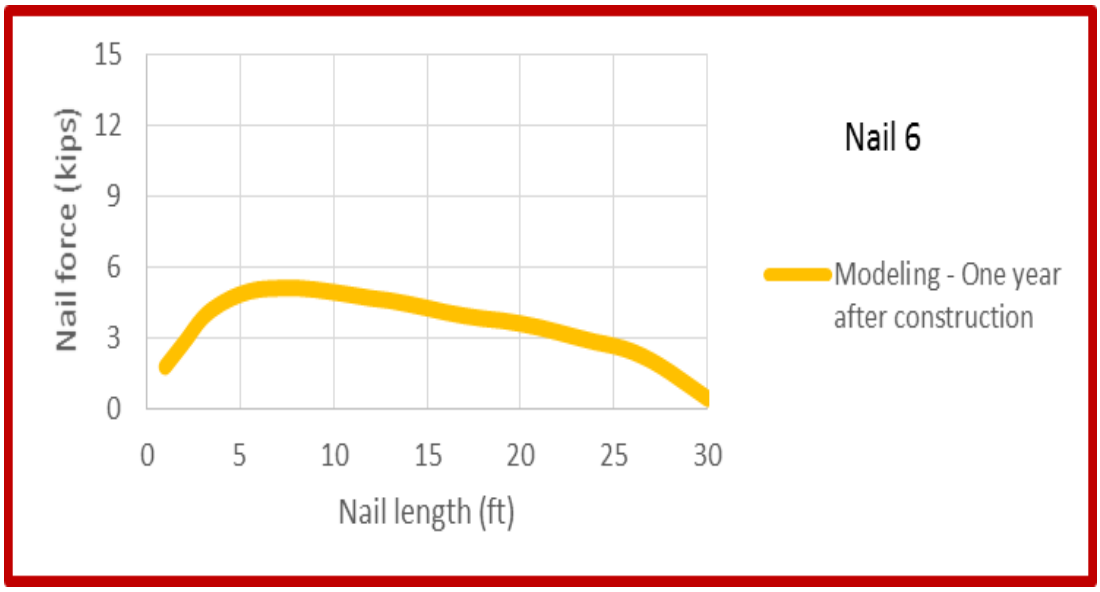

Figure 114 Service load in nail 6 one year after construction from numerical modelling at section 1+46.

In this chapter the wall that was constructed in Beaumont was modelled. Undrained modelling was adopted to model the construction phase of the wall. The deformation and the load in the nails were compared with the monitored readings. The creep behavior of the wall was modelled using Burger model. The load in the nails was compared with observed load in nails. Good confirmation with monitored readings were observed. The percentage of increase in loads in monitored and from model were compared and the increase was found to be matching. Creep for 75 years was modelled, the load increase in nails was below the pullout capacity of the nails which show that the wall will not fail due to creep.

CHAPTER V

CONCLUSIONS

From the literature it was understood that clayey soils show creep behavior under sustained loading. It was also inferred that there was a reduction in strength and an increase in creep with increasing water content. Direct shear tests done as a part of this thesis showed an increase in shear stress with decreasing water content. When the sample was inundated with water and tested under drained conditions lower shear strength was obtained when compared to sample which was 90% saturated. Thus it was inferred to model the soil with fully saturated conditions during modelling stage. It is also to be mentioned that the soil in the field was fully saturated.

Unconsolidated undrained tests on fully saturated and 85% saturated samples were conducted on remolded samples from three depths. The strength was seen to increase with increasing confining pressure and depth. The strength variation with depth was obtained from this test. The strength increased with decrease of saturation. When modelling, fully saturated conditions was assumed so that we could predict the creep behavior at worst case scenario and as can be seen from this test strength is increasing with decrease in water content due to suction affects. These tests gave a clear idea about holding loads for creep tests. It was decided to have at least three holding stress levels for each sample. The maximum stress level was known from uu test and based on this three stress levels were decided. Based on unconsolidated undrained creep tests the ‘n’ value for the soil was obtained. It can be seen that generally an increase in ‘n’ value and hence creep for soils increase with saturation. From these observations it was concluded that for this soil, creep

increases with saturation, however to extend this conclusion to extend this to all soils, an extensive lab test program will be necessary. From the literature it is concluded that creep increases with saturation. It is also concluded that in the working load range stress have very little effect on n value and hence on creep. The 'n' value obtained from these tests was later used in the modelling stage to find the creep parameters in the Burger model. Consolidated undrained tests provided the effective stress parameters to be used for the Mohr-Columb model used in the modelling stage.

Numerical modelling:

The soil nail wall was modelled using finite difference software FLAC 3D. Undrained parameters obtained from lab tests were used during the construction stage.

The failure that occurred in the section 2+00 during construction was also modelled in this thesis. Post failure construction stage was modelled by stepping the model to the last monitored deformation reading. A very good correlation was obtained between the observed field deformation and the predicted deformation from the model. The load in the nails predicted by the nail was compared with post construction monitored load in the field. Though the model over predicted the force in two rows of nails, overall it shown good conformation with monitored reading. The same procedure was adopted for section 1+46 and here also very good relation between the observed reading and predicted by modelling was obtained.

Creep was modelled using Burger visco elastic model. The model after construction was rested and shifted from Mohr Columb to Burger model. The model parameters were found by modelling the lab creep tests. The model was able to predict the

creep movement at the top of the wall for the section 1+46. The model was over predicting the creep for the section at 2+00. But it can be seen from the movements of the wall at section 2+00 at depth 12ft the creep is in an increasing rate. The reason is probably because the failure and the inclusion of pretension nails must have stabilized the wall for the initial few months and with time it has started to creep. This can be confirmed by further monitoring the wall.

Failure of soil nail wall will occur when the load in the nails is more than the pullout capacity of the nail. In this project the design load was 21kips. In 75 years the load is increased to 20kips. So with the model considering the worst case scenario, the wall is stable for a minimum of 75 years with the load below design load. The pullout capacity of the nails are 65 kips. So it is proposed that with the 'n' value hitting the maximum, the creep of the nails in high plasticity soil is safe for the common design period of 75 years.

5.1 Future research

1. In this study samples with two water contents were tested. It should be extended to different saturations to better understand the variation of creep and the creep parameter 'n' with water content.
2. Different types of soil with different plasticity need to be tested to understand the creep behavior of soils and their effect on soil nail walls. Here only one type of high plasticity clay has been considered. Another interesting study will be to study creep behavior of composite soils.
3. The wall needs to be monitored for longer time. As it can be observed the movement of the wall for the failure section is increasing, so it is required to

monitor the wall for more duration of time and to confirm the results from modelling.

REFERENCE

1. Akhavan, M., Ghareh, S. and Naeini, M.B., 2011. Comparing the results of numerical analysis and monitoring about the behavior of cracks occurred nearby soil-nailing walls. *Electronic Journal of Geotechnical Engineering*, *16*, pp.1239-1252.
2. Anthoine, A., 1990. Une méthode pour le dimensionnement à la rupture des ouvrages en sols renforcés. *Revue Française de Géotechnique*, (50),pp. 5-21
3. Bi, G., 2015. *A Power law model for time dependent behavior of soils* (Unpublished Doctoral dissertation). Texas A&M University, College Station, TX.
4. Briaud, J.L. and Garland, E., 1985. Loading rate method for pile response in clay. *Journal of Geotechnical Engineering*, *111*(3), pp.319-335.
5. Briaud, J.L. and Gibbens, R., 1999. Behavior of five large spread footings in sand. *Journal of Geotechnical and Geoenvironmental Engineering*, *125*(9), pp.787-796.
6. Briaud, J.L. and Lim, Y., 1997. Soil-nailed wall under piled bridge abutment: simulation and guidelines. *Journal of Geotechnical and Geoenvironmental Engineering*, *123*(11), pp.1043-1050.
7. Briaud, J.L., 2013. *Geotechnical engineering: unsaturated and saturated soils*. John Wiley & Sons.
8. Bridle, R.J. and Barr, B.I.G., 1990, September. The analysis and design of soil nails. *In Proceedings of the International Reinforced Soil Conference*, Glasgow, pp. 10-12.
9. Sivasithamparam, N., Karstunen, M., Brinkgreve, R.B.J. and Bonnier, P.G., 2013. Comparison of two anisotropic creep models at element level. *In Proc. International Conference on Installation Effects in Geotechnical Engineering*, Rotterdam, pp. 72-78.

10. Carlos, A.L., Elias, V. and Espinoza, D., 2003. *Geotechnical engineering circular N\no. 7 soil nail walls*. FHWA0-IF-03-017 Washington DC: Federal highway administration, US department of transportation.
11. Fan, C.C. and Luo, J.H., 2008. Numerical study on the optimum layout of soil–nailed slopes. *Computers and Geotechnics*, *35*(4), pp.585-599.
12. Feda, J. 1992. *Creep of soils and related phenomena, Development in geotechnical engineering 68*, Amsterdam, Elsevier, Printed in Czechoslovakia, p. 422
13. Galvan, M., 2012. TxDOT Bridge Division, Proposal Meeting RMC5 - 0-6784.
14. Gasparre, A., Coop, M.R. and Cotecchia, F., 2003. An experimental investigation of creep processes in a crushable sand. *In Proceedings of the Third International Symposium on Deformation Characteristics of Geomaterials*, pp. 773-778.
15. Gassler, G. and Gudehus, G., 1981. Soil nailing-some aspects of new technique. *Proceedings of Tenth ICSMFE*, pp: 665-670.
16. Gassler, G., 1990. In-situ techniques of reinforced soil. *Performance of Reinforced Soil Structures, British Geotechnical Society*, pp.185-196.
17. Germaine, J.T. and Ladd, C.C., 1988. State-of-the-art paper: Triaxial testing of saturated cohesive soils. *In Advanced Triaxial Testing of Soil and Rock*, pp. 421-459.
18. Gustafsson, P. and Tian, T., 2011. *Numerical study of different creep models used for soft soils*. (Master of science thesis) Chalmers University of Technology Sweden. Retrieved from : http://publications.lib.chalmers.se/records/fulltext/143846.pdf

19. Havel, F., 2004. *Creep in soft soils*. (Doctoral dissertation). Norwegian University of Science and Technology, Norway. Retrieved from: http://www.diva-portal.org/smash/get/diva2:124915/FULLTEXT01.pdf
20. Hunter, G.J. and Khalili, N., 2000, November. A simple criterion for creep induced failure of over-consolidated clays. *In Proceedings of Geo Engineering Conference*, Melbourne, Australia (CD format, Paper ID: IS-2000-474).
21. Itasca, F.L.A.C., 2009. 3D version 4.0 user's manual. *Minneapolis: Itasca*.
22. Janbu, N., 1954. Application of composite slip surfaces for stability analysis. In *Proc. European Conf. on Stability of Earth Slopes*, Stockholm, Vol. 3, pp. 43-49.
23. Jang, J. and Santamarina, C.J., 2015. Fines classification based on sensitivity to pore-fluid chemistry. *Journal of Geotechnical and Geoenvironmental Engineering*, p.06015018.
24. Juran, I. and Elias, V., 1987. Soil nailed retaining structures: Analysis of case histories. In *Soil Improvement@ SA Ten Year Update*, pp. 232-244. ASCE.
25. Lai, X.L., Wang, S.M., Ye, W.M. and Cui, Y.J., 2014. Experimental investigation on the creep behavior of an unsaturated clay. *Canadian Geotechnical Journal*, *51*(6), pp.621-628.
26. Liew, S.S. and Khoo, C.M., 2006, May. Design and construction of soil nail strengthening work over uncontrolled fill for a 14.5 m deep excavation. In*10th International Conference on Piling and Deep Foundations*, Amsterdam, Vol. 31,pp.165-172

27. Lima, A.P., Gerscovich, D.M. and Sayão, A.S.F.J., 2003. Deformability analysis of nailed soil slopes. In *12th Panamerican Conference for Soil Mechanics and Geotechnical Engineering* pp. 2127-2132.

28. Luo, Q. and Chen, X., 2014. Experimental research on creep characteristics of Nansha soft soil. *The Scientific World Journal*, 2014. Article ID 968738.

29. Kharanaghi, M.M., 2015. Creep Behavior of Soil Nail Wall in High Plasticity Index (PI) Soil (Unpublished Doctoral dissertation). Texas A&M University, College Station, TX.

30. Maslov, N.N. 1968, Long-term stability and displacements of retaining structures, *Energiya*, Moscow, p. 160.

31. Pestana, J.M. and Whittle, A.J., 1998. Time effects in the compression of sands. *Geotechnique*, *48*(5), pp. 695-701

32. Schlosser, F., Unterreiner, P. and Plumelle, C., 1992. French research program CLOUTERRE on soil nailing. In *Grouting, Soil Improvement and Geosynthetics* , pp. 739-750. ASCE.

33. Rees, Sean. "GDS instruments - specialists in computer controlled geotechnical soil and rock testing systems." GDS instruments - specialists in computer controlled geotechnical soil and rock testing systems. Retrieved May 18, 2016, from http://www.gdsinstruments.com/__assets__/pagepdf/000037/Part%201%20Introduction%20to%20triaxial%20testing.pdf

34. Segalini, A., Giani, G.P. and Ferrero, A.M., 2009. Geomechanical studies on slow slope movements in Parma Apennine. *Engineering Geology*, *109*(1), pp.31-44.

35. Semi-Automatic Cone Penetrometer. (n.d.). Retrieved June 13, 2016, from http://www.ele.com/Product/semi-automatic-cone-penetrometer-to-bs-1377-part-2/223
36. Singh, A. and Mitchell, J.K., 1968. General stress-strain-time function for soils. *Journal of the Soil Mechanics and Foundations Division*, *94*(1), pp.21-46.
37. Singh, V.P. and Babu, G.S., 2010. 2D numerical simulations of soil nail walls. *Geotechnical and Geological Engineering*, *28*(4), pp.299-309.
38. Skempton, A.W., 1977, July. Slope stability of cuttings in brown London clay. In *Proc. 9th Int. Conference on Soil Mechanics and Foundation Engineering, Tokyo*, Vol. 3, pp. 261-270.
39. RL. Wadsworth construction Co, Soil Nail Walls. (n.d.). Retrieved June 13, 2016, from https://www.wadsco.com/soil-nail-walls/
40. Stocker, M.F. and Korber, G.W., GaÈ ssler G. and Gudehus G., 1979. Soil nailing. In *Proceedings of the International Conference on Soil Reinforcement: Reinforced Earth and Other Techniques*, Paris, Vol. 2, pp. 469-474.
41. Stocker, M.F. and Riedinger, G., 1990, June. The bearing behavior of nailed retaining structures. In *Design and Performance of Earth Retaining Structures*, pp. 612-628. ASCE.
42. Tavenas, F. and Leroueil, S., 1981. Creep and failure of slopes in clays. *Canadian Geotechnical Journal*, *18*(1), pp.106-120.

43. Thompson, S.R. and Miller, I.R., 1990, June. Design, construction and performance of a soil nailed wall in Seattle, Washington. In *Design and Performance of Earth Retaining Structures*, pp. 629-643. ASCE.

44. Vyalov, S. (1986). Rheological Fundaments of Soil Mechanics. *Developments in Geotechnical Engineering*, Vol. 36, pp. 1-564. Elsevier.

45. Zhou, Y.D., Cheuk, C.Y. and Tham, L.G., 2009. Numerical modelling of soil nails in loose fill slope under surcharge loading. *Computers and Geotechnics*, *36*(5), pp.837-850.

46. Zhou, Y.D., Xu, K., Tang, X. and Tham, L.G., 2013. Three-dimensional modeling of spatial reinforcement of soil nails in a field slope under Surcharge loads. *Journal of Applied Mathematics*, 2013. Article ID 926097

APPENDIX A

Time-Deformation Curves

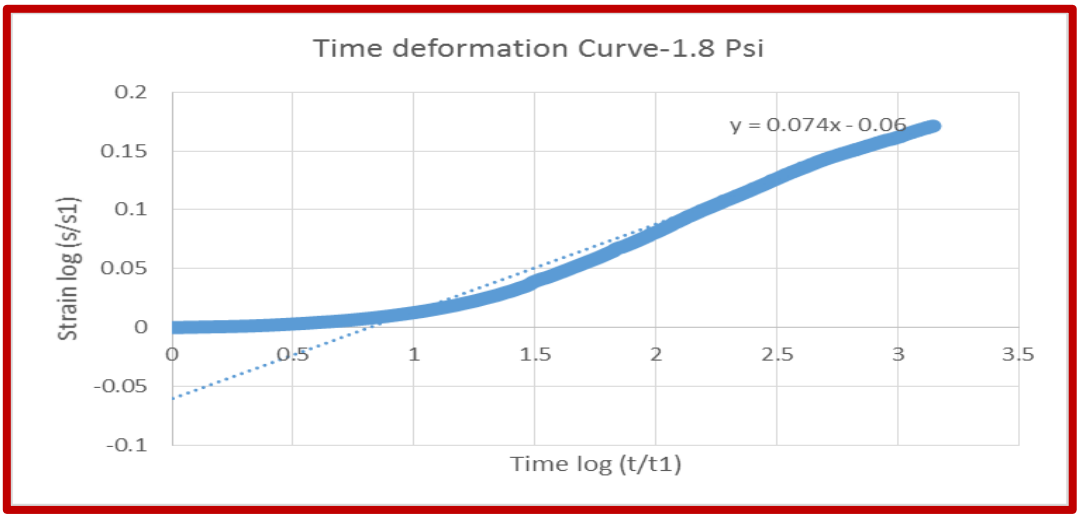

Figure 115 Strain time curve (log-log) at 1.8 psi of triaxial uu creep test at depth 4ft.

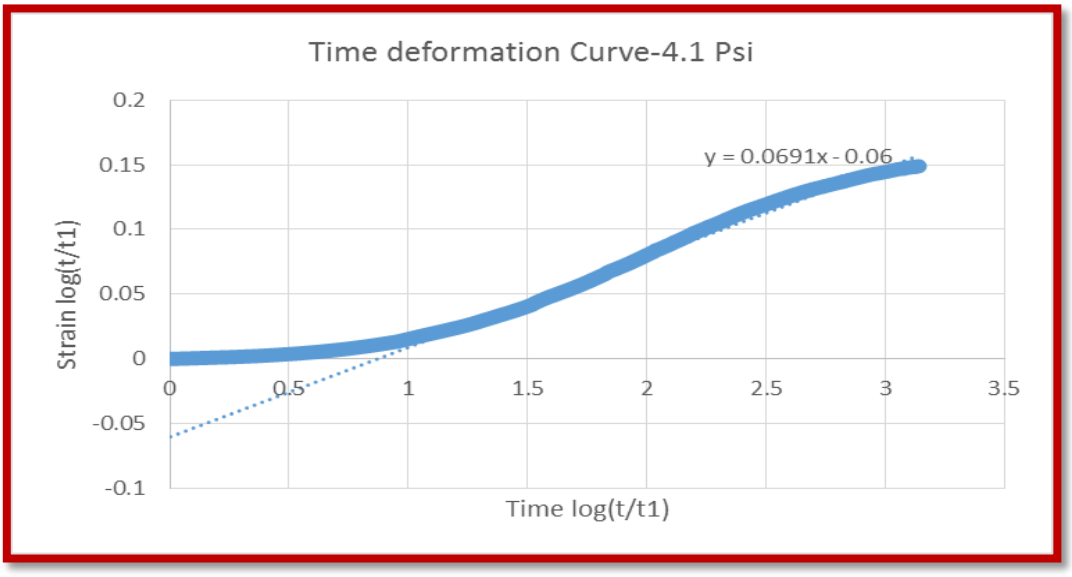

Figure 116 Strain time curve (log-log) at 4.1 psi of triaxial uu creep test at depth 4ft.

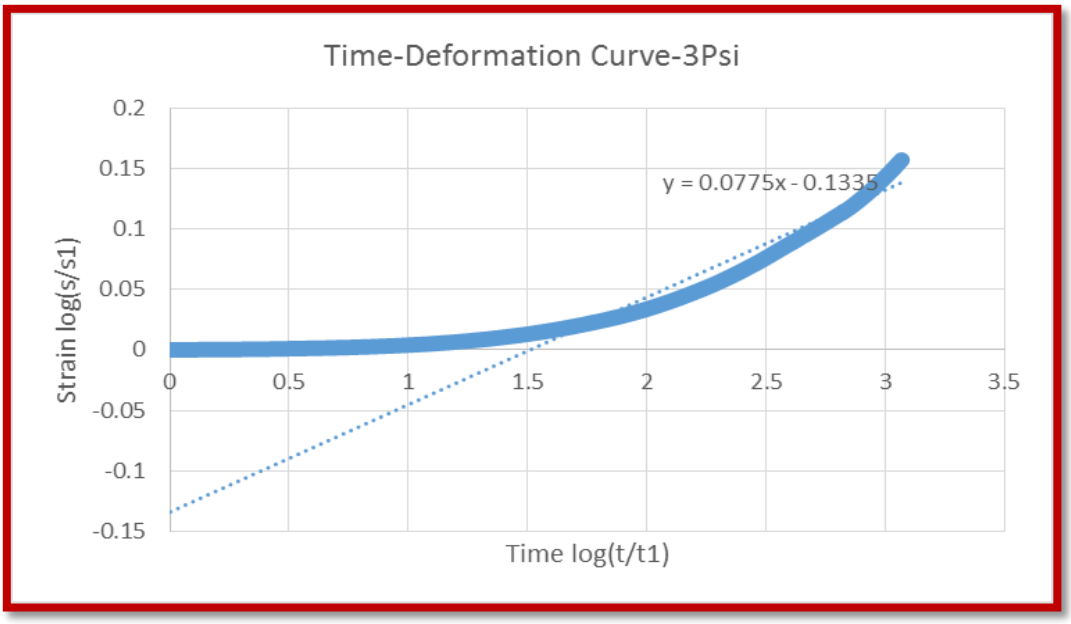

Figure 117 Strain time curve (log-log) at 3 psi of triaxial uu creep test at depth 12ft.

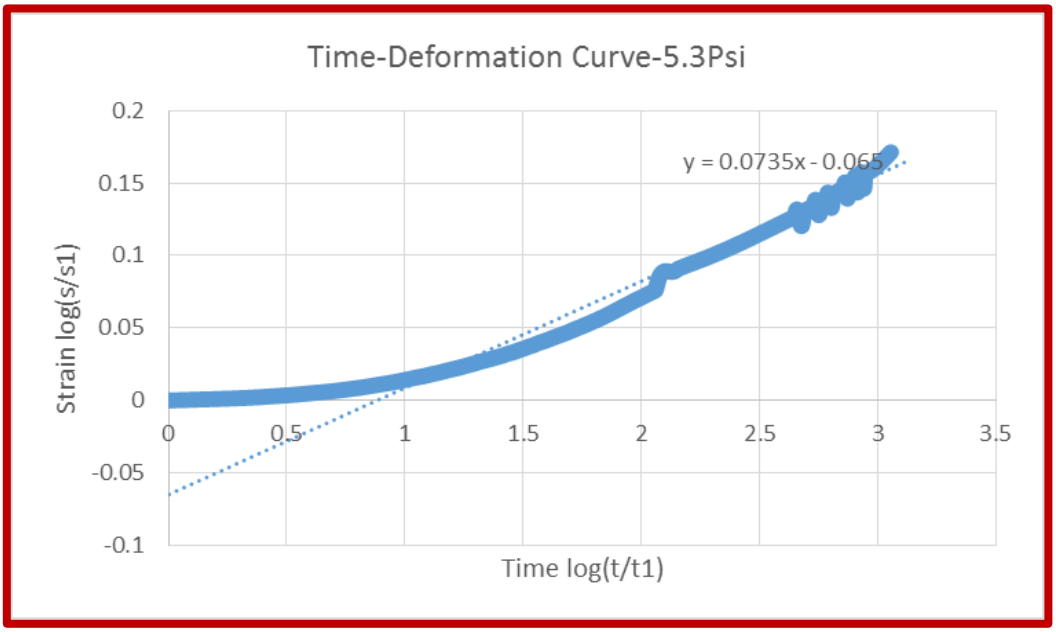

Figure 118 Strain time curve (log-log) at 5.3 psi of triaxial uu creep test at depth 12ft.

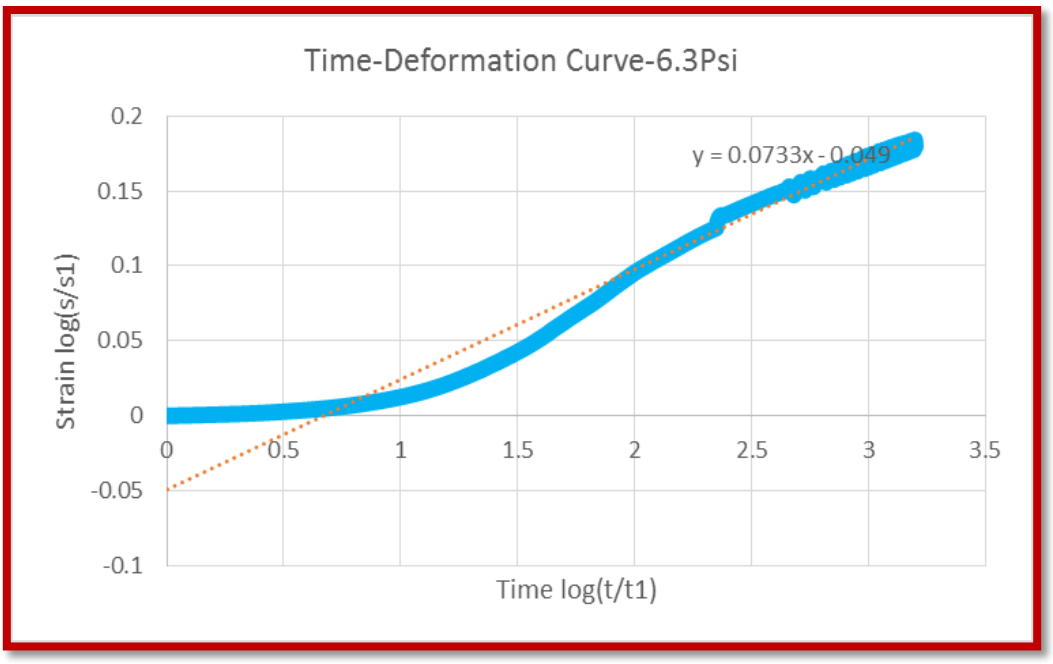

Figure 119 Strain time curve (log-log) at 6.3 psi of triaxial uu creep test at depth 12ft.

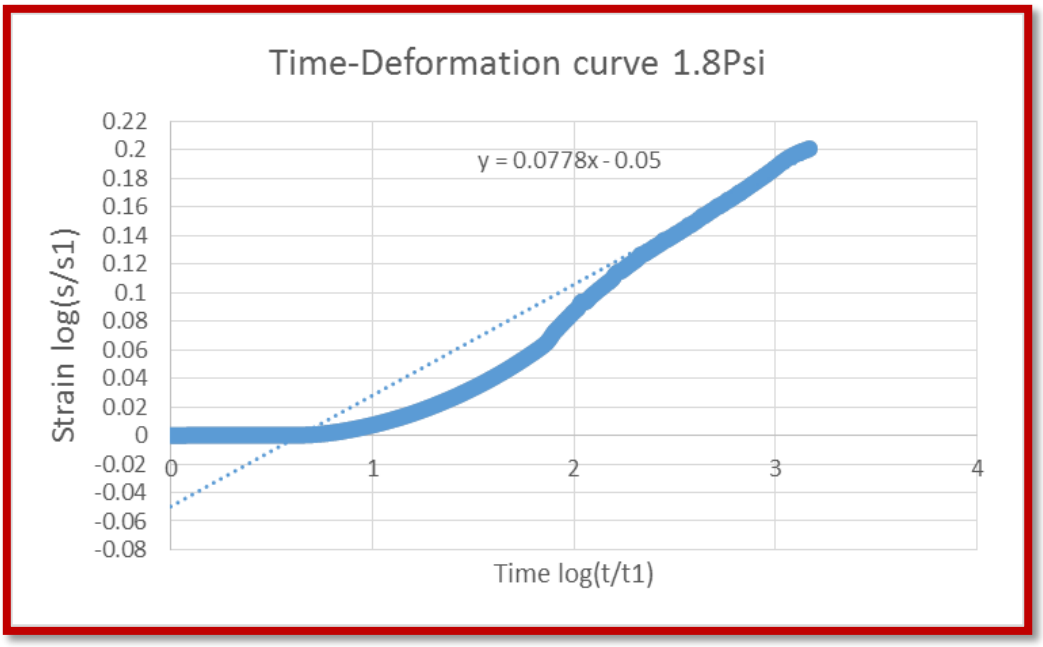

Figure 120 Strain time curve (log-log) at 1.8 psi of triaxial uu creep test at depth 22ft.

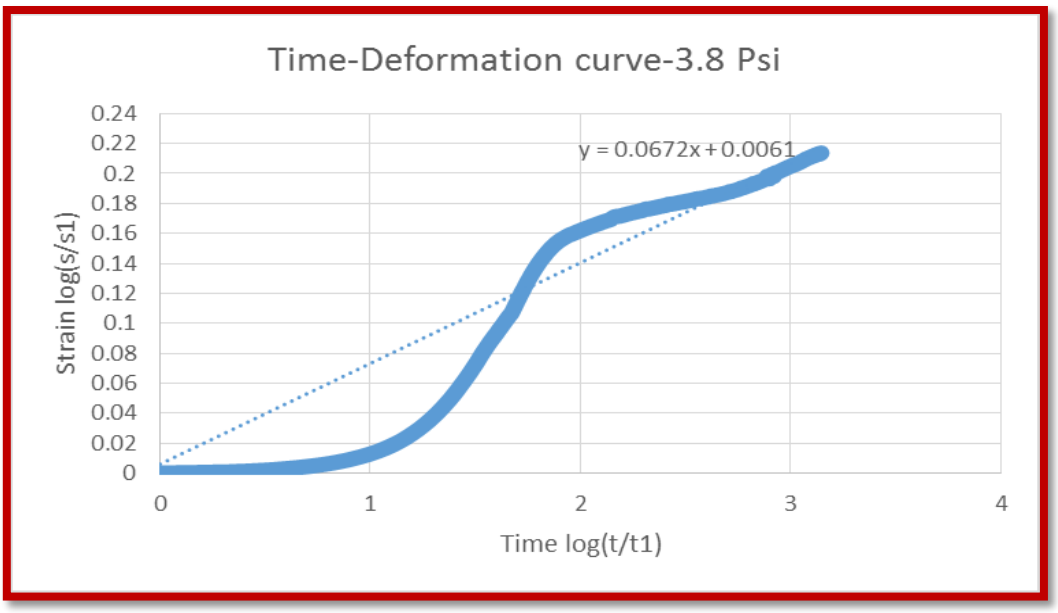

Figure 121 Strain time curve (log-log) at 3.8 psi of triaxial uu creep test at depth 22ft.

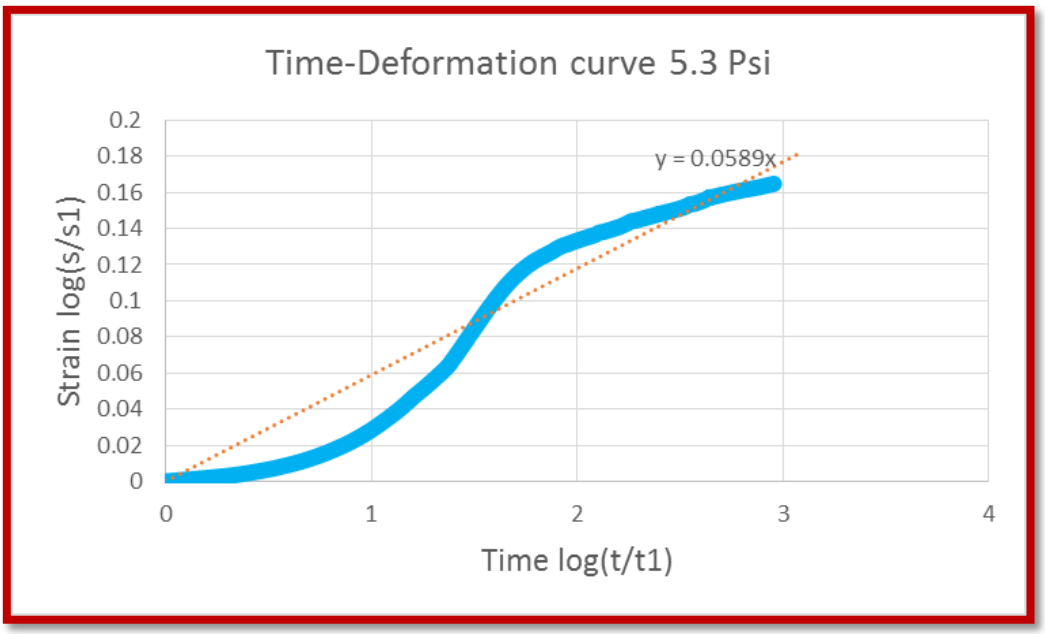

Figure 122 Strain time curve (log-log) at 5.3 psi of triaxial uu creep test at depth 22ft.

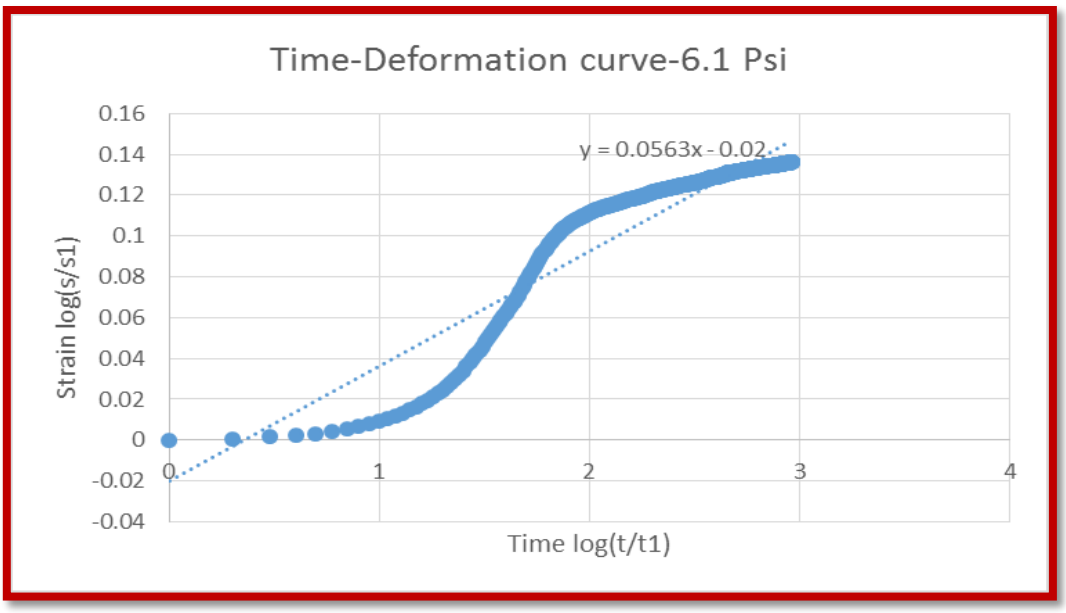

Figure 123 Strain time curve (log-log) at 6.1 psi of triaxial uu creep test at depth 22ft.

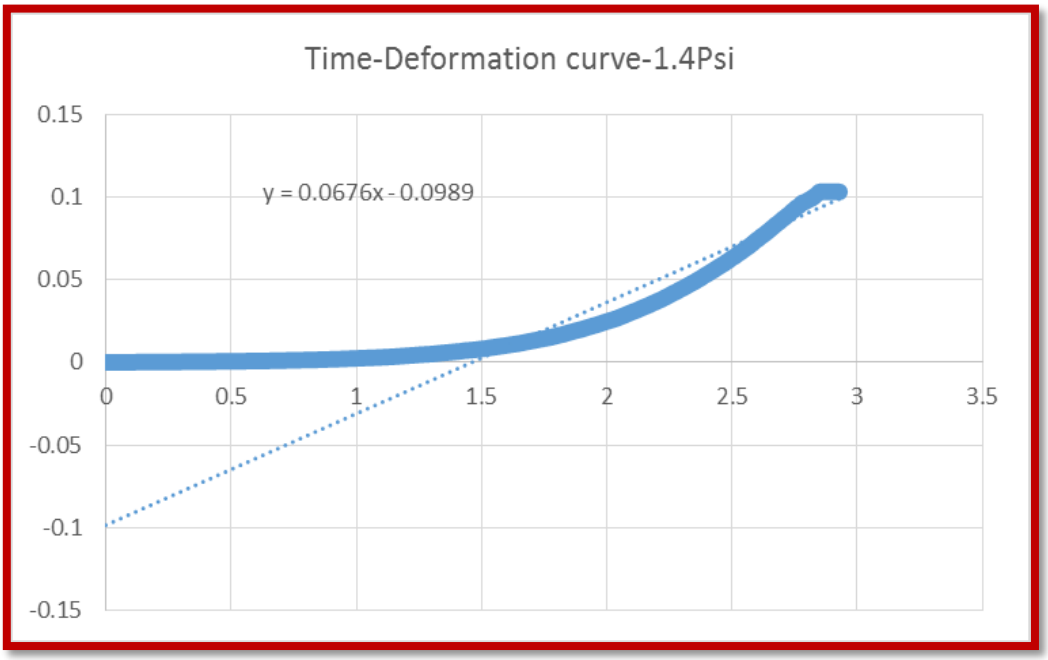

Figure 124 Strain time curve (log-log) at 1.4 psi of triaxial uu creep test at depth 4ft.

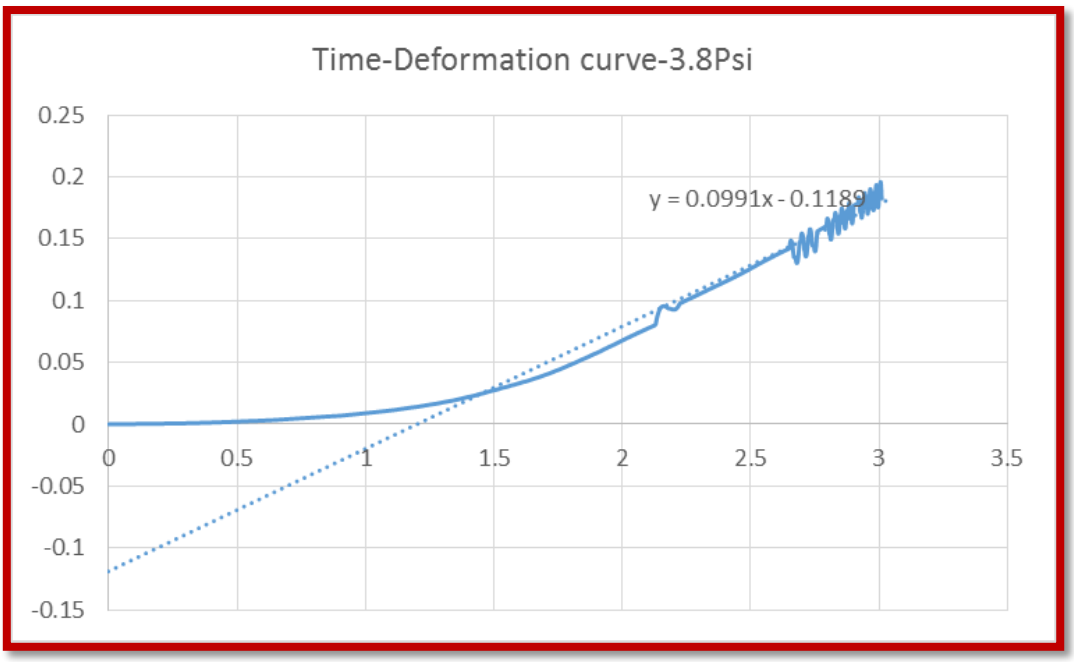

Figure 125 Strain time curve (log-log) at 3.8 psi of triaxial uu creep test at depth 4ft.

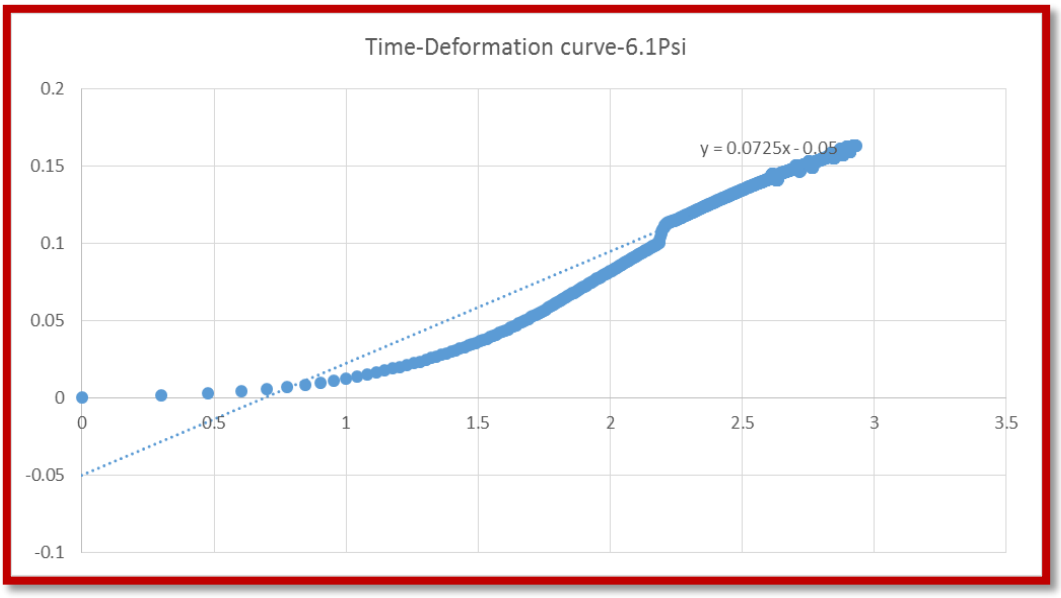

Figure 126 Strain time curve (log-log) at 6.1 psi of triaxial uu creep test at depth 4ft.

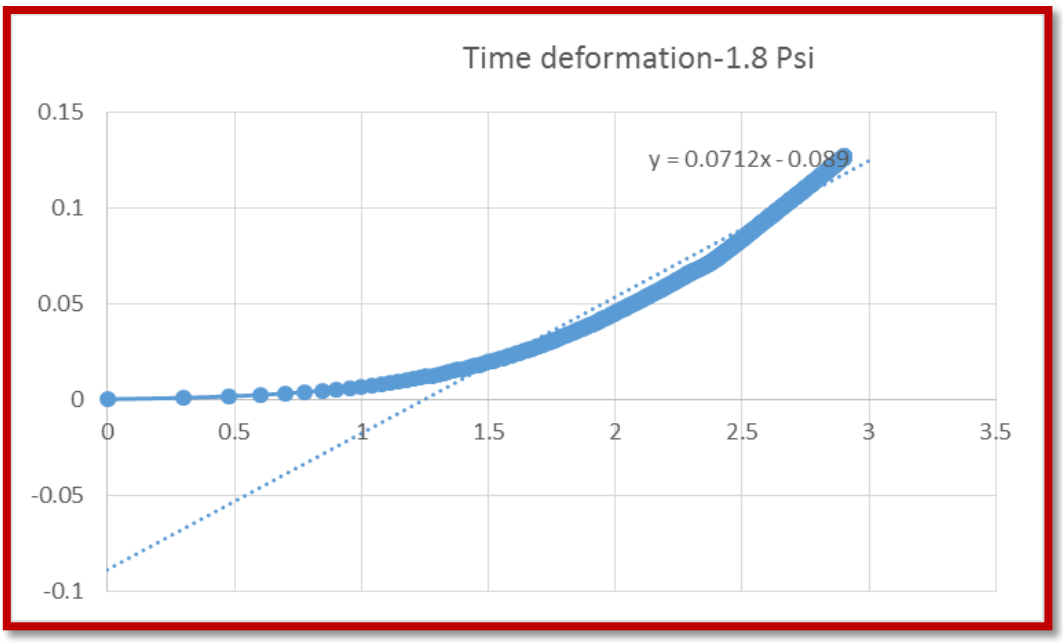

Figure 127 Strain time curve (log-log) at 1.8 psi of triaxial uu creep test at depth 12ft.

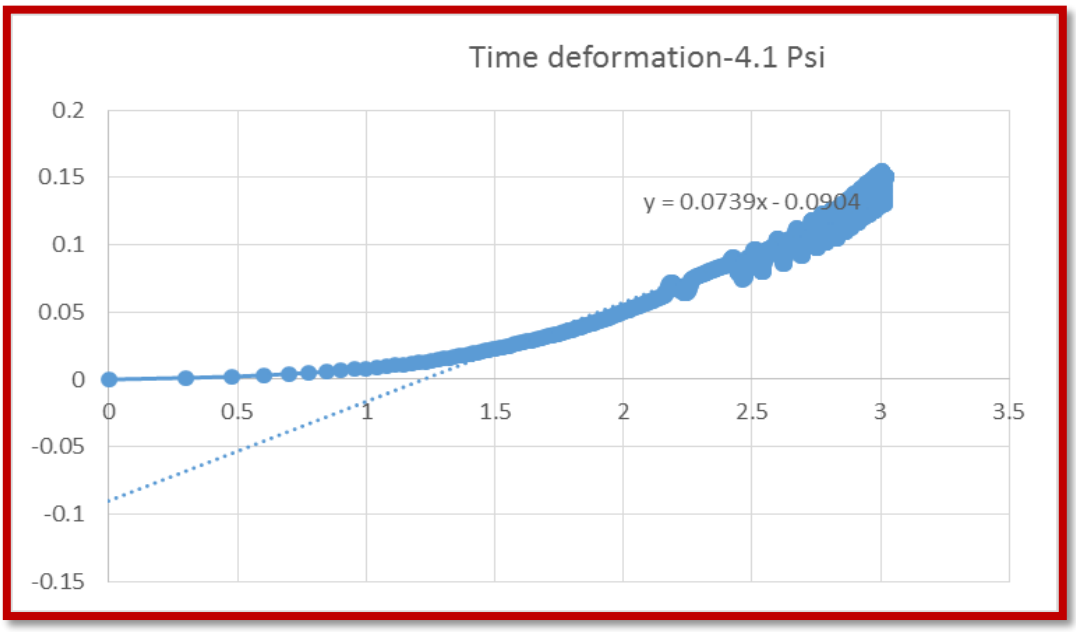

Figure 128 Strain time curve (log-log) at 4.1 psi of triaxial uu creep test at depth 12ft.

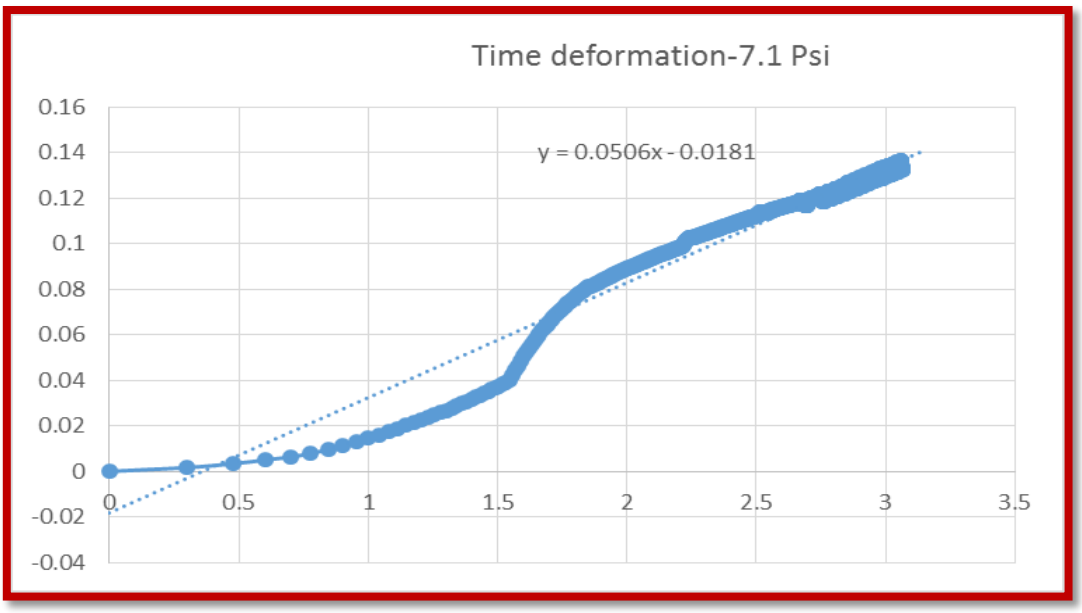

Figure 129 Strain time curve (log-log) at 7.1 psi of triaxial uu creep test at depth 12ft.

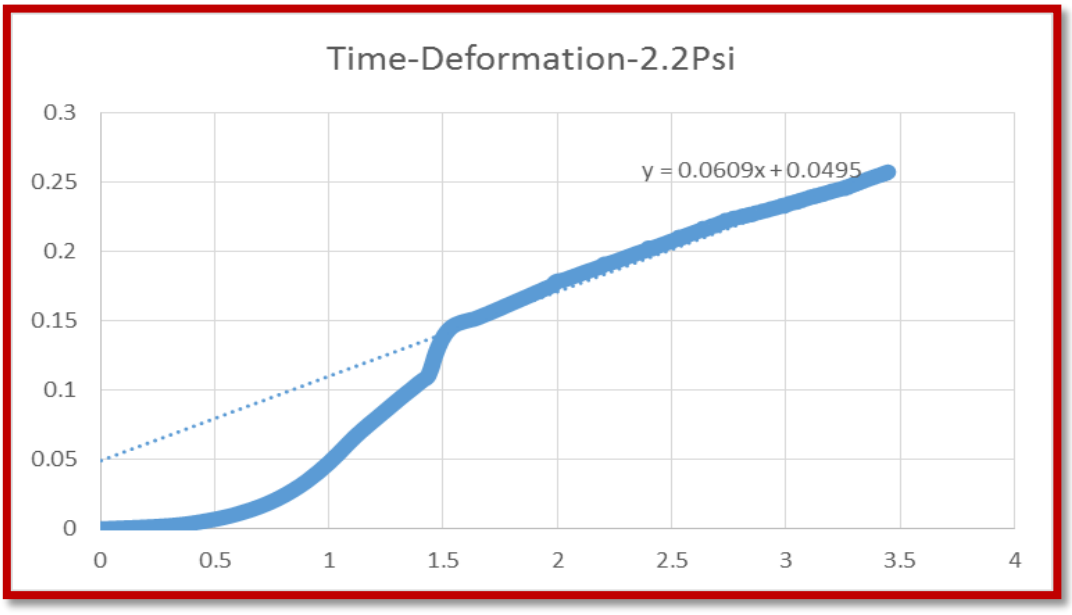

Figure 130 Strain time curve (log-log) at 2.2 psi of triaxial uu creep test at depth 22ft.

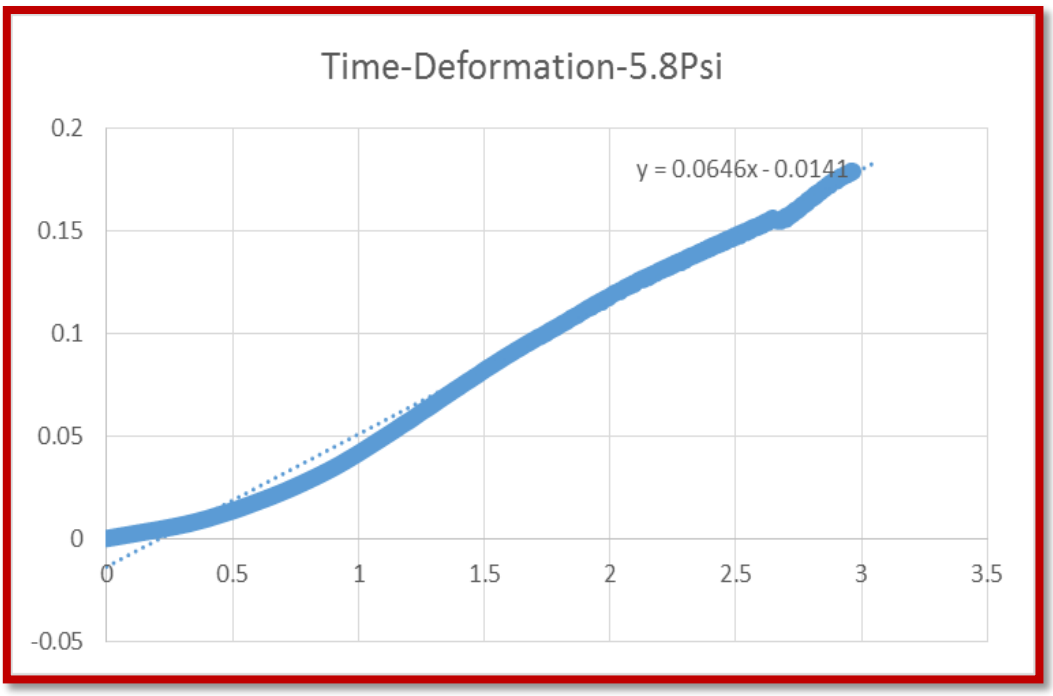

Figure 131 Strain time curve (log-log) at 5.8 psi of triaxial uu creep test at depth 22ft.